Coexistence between Heterogeneous Wireless Networks

by
Sneihil Gopal

Under the Supervision of Dr Sanjit Krishnan Kaul

Indraprastha Institute of Information Technology,
Delhi
December, 2020

Coexistence between Heterogeneous Wireless Networks

by
Sneihil Gopal

Submitted
in partial fulfillment of the requirements for the
degree of Doctor of Philosophy

to the

Indraprastha Institute of Information Technology,
Delhi
December, 2020

To my friends and family

"The first principle is that you must not fool yourself and you are the easiest person to fool."
–Richard P. Feynman

Abstract

The proliferation of data-intensive applications has led to an exponential growth in wireless data traffic over the last decade. Solutions to accommodate this increase in traffic demand include (a) improvements in technology, for example, using high-order modulation and coding schemes and multiple-input multiple-output (MIMO) systems, (b) network densification via deployment of small cell networks, and (c) efficient use of spectrum including spectrum refarming and spectrum sharing amongst different networks. While each solution has its own advantages and associated challenges, in this thesis we focus on spectrum sharing between networks.

Sharing spectrum bands, which are underutilized temporally or spatially, is a promising strategy to address the demand for spectrum. However, it introduces novel challenges that result from the networks having to coexist with each other. Coexistence could be challenging for several reasons, including disparity in spectrum access rights assigned to the networks by regulatory bodies and differences in technologies and utilities of the networks sharing the spectrum. For instance, in a paradigm shift in the US and Europe, the spectrum licensed to TV operators for exclusive use was opened for use by low power unlicensed devices, provided they did not impair the reception of TV broadcast at TV receivers. More recently, spectrum that was allocated for use by Intelligent Transportation Systems (ITS) was opened up by the Federal Communications Commission (FCC) for high throughput WiFi networks. This resulted in a coexistence scenario where while the networks have equal rights to the spectrum, they care for the different utilities of information timeliness and throughput, respectively. In this thesis, we address in detail the above two scenarios of coexistence for a CSMA/CA based access of the shared spectrum. Motivated by the distinct behavior of the network that cares for information timeliness and the growing interest in real-time monitoring applications, we conclude the thesis with novel insights on spectrum sharing amongst selfish nodes that care for timely delivery of information updates.

TV Whitespaces (TVWS) refers to the spectrum licensed for TV broadcast that was opened up by regulators for use by secondary (unlicensed) devices. We investigate the deployment of White-Fi networks of secondary devices, which coexist with TV networks, and the resulting throughputs. White-Fi networks use WiFi-like physical layer and medium access control (MAC) mechanisms. Unlike WiFi networks that operate in the 2.4 and 5 GHz bands and typically have a coverage of up to 100 m, outdoor White-Fi cells have much larger coverage of up to 5 km. As a result, nodes in a White-Fi cell see significant spatial heterogeneity in channel availability and link quality. We model the MAC throughput of a multi-cell city-wide White-Fi network. We formulate a throughput maximization problem for the White-Fi network under the constraint that its nodes' maximum aggregate interference at TV receivers is within acceptable limits. We propose a heuristic method and illustrate its efficacy over hypothetical deployments of White-Fi networks coexisting with real TV networks in the US cities of Columbus and Denver, which are good examples of heterogeneity in channel availability and link quality in TVWS. Our proposed framework provides useful insights. For instance, we show that while Columbus has higher channel availability than Denver, surprisingly, its network throughput is lower,

indicating that more channels may not result in increased throughput.

Next, we investigate the coexistence of two networks, one of which cares for information timeliness and the other for throughput. This is motivated by a recent ruling in which the FCC opened up the $5.85-5.925$ GHz ITS band, used for vehicular networking, for the unlicensed 802.11ac/802.11ax devices. While both networks have similar spectrum access rights, the incumbents of the ITS band, i.e., vehicular nodes, value timely delivery of information updates, and the sharers, i.e., the WiFi devices, desire high throughput. This novel spectrum sharing scenario raises an interesting question of whether such networks would cooperate or compete for spectrum access. We address this question using a game theoretic approach.

We capture the timeliness of information using the metric of age of information. We refer to the network that cares for timeliness as an age optimizing network (AON) and the other as a throughput optimizing network (TON). We study their coexistence under the assumption that both networks share the spectrum using a CSMA/CA based access mechanism and that the AON aims to minimize the age of updates while the TON seeks to maximize throughput. We employ a repeated game-theoretic approach that allows us to answer whether a simple coexistence etiquette that enables cooperation between networks is self-enforceable. Specifically, we introduce a coordination device, which is a randomized signaling device that allows the AON and the TON to access the spectrum in a non-interfering manner. The networks employ a grim trigger strategy when cooperating which ensures that networks would disobey the device only if competition were more beneficial than cooperation in the long run.

We apply the proposed etiquette to two distinct practical medium access settings: (a) when collision slots (more than one node accesses the spectrum leading to all transmissions received in error) are at least as large as successful transmission (interference-free) slots, and (b) collision slots are smaller than successful transmission slots. To exemplify, the former holds when networks use the basic access mechanism defined for the 802.11 MAC and the latter is true for networks employing the RTS/CTS based access mechanism. We show that for both medium access settings, while cooperation is self-enforceable when networks have a small number of nodes, networks prefer competition when they grow in size.

Our study of coexisting age and throughput optimizing networks shows that an age optimizing network behaves differently from a throughput optimizing one. This motivated us to consider the coexistence of nodes that care for timeliness of information and share the same spectrum. As before, we employ a game theoretic approach. We formulate a non-cooperative one-shot game with nodes as players and age of information as their utilities. We investigate nodes' equilibrium strategies in a CSMA/CA slot for the aforementioned medium access settings, i.e., when collisions are longer than successful transmissions and when collisions are shorter. For each setting, we provide insights into how competing nodes that value timeliness share the spectrum. We find that access settings exert strong incentive effects. Specifically, we show that under decentralized decision making by nodes, when collisions are shorter, transmit is a weakly dominant strategy, and when collisions are longer, no dominant strategy exists. For the latter case, we analytically derive the mixed strategy Nash equilibrium for when the ages at the beginning of the slot satisfy certain conditions.

Certificate

This is to certify that the thesis titled "Coexistence between Heterogeneous Wireless Networks" being submitted by Sneihil Gopal to the Indraprastha Institute of Information Technology Delhi, for the award of the degree of Doctor of Philosophy, is an original research work carried out by her under my supervision. In my opinion, the thesis has reached the standards fulfilling the requirements of the regulations relating to the degree.

The results contained in this thesis have not been submitted in part or full to any other university or institute for the award of any degree/diploma.

.....
Dr. Sanjit Krishnan Kaul
December, 2020

Indraprastha Institute of Information Technology Delhi
New Delhi 110 020

Acknowledgement

First and foremost, I would like to thank my advisor Dr. Sanjit Krishnan Kaul, for giving me this opportunity and for his guidance and generous support throughout my PhD. His advice and commitment to high-quality research have helped me develop as a researcher. I appreciate his spontaneity, enthusiasm, and attitude towards research and life in general. I would also like to express my gratitude towards my collaborator Dr. Rakesh Chaturvedi. This thesis would not have been possible without their profound knowledge, experience, and thoughtful discussions.

I would like to thank Professor Sumit Roy (University of Washington) for his valuable guidance on my research. His insights, knowledge on the subject matter, and research experience have helped me tremendously throughout my PhD. I am thankful to the monitoring committee, Dr. Vivek Ashok Bohara and Dr. Pravesh Biyani from the Indraprastha Institute of Information Technology Delhi (IIIT-Delhi), for their expert comments and feedback that helped me improve my work over the years. I would also like to extend my gratitude towards Dr. Abhinav Kumar from IIT Hyderabad and Dr. Gaurav Arora and Dr. Mukulika Maity from IIIT-Delhi for serving as examiners for my comprehensive exam. Their feedback helped in improving the quality of this dissertation.

I would like to thank all my colleagues at IIIT-Delhi, who have been a part of my PhD journey. I am also grateful to everyone in the Wireless Systems Lab for endless discussions, support, and making work pleasant. I also take the opportunity to thank the administration staff at IIIT-Delhi, especially Ms. Sheetu Ahuja and Ms. Priti Patel, for being kind enough to address all my queries throughout these years. Their efforts are well-acknowledged, and I am very grateful to them for all their help and support.

Words cannot express how lucky I am to have friends to share this journey. Apurv, Sakshi, and Monika thank you for all the support and laughs we had together. It has been a pleasure. A special thanks to my dear friend Anand for all the support and motivation throughout the years.

Lastly, I would like to thank my parents and my sister for the unconditional love, motivation, and support they have always provided me. I dedicate this thesis to them as a token of gratitude.

New Delhi, December 2020
Sneihil Gopal

Contents

List of Figures

List of Tables

List of Abbreviations

ACK	Acknowledgement
AoI	Age Of Information
AON	Age Optimizing Network
AP	Access Point
CDF	Cumulative Distribution Function
CDMA	Code-division Multiple Access
CSMA	Carrier-sense Multiple Access
CSMA/CA	Carrier-sense Multiple Access With Collision Avoidance
CTS	Clear-to-Send
DCF	Distributed Coordination Function
DIFS	DCF Interframe Space
DSRC	Dedicated Short Range Communication
ECC	Electronic Communications Committee
FCC	Federal Communications Commission
IoT	Internet-of-Things
ITS	Intelligent Transportation Systems
MAC	Medium Access Control
MIMO	Multiple-input Multiple-output
MSNE	Mixed Strategy Nash Equilibrium

Ofcom	Office Of Communications
OFDM	Orthogonal Frequency-division Multiplexing
PHY	Physical Layer
PMF	Probability Mass Function
QoS	Quality Of Service
RTS	Request-to-Send
RTS/CTS	Request To Send/Clear To Send
SINR	Signal-to-interference-and-noise-ratio
SPE	Subgame-perfect Equilibrium
TON	Throughput Optimizing Network
TVWS	TV White Spaces
UAVs	Unmanned Aerial Vehicles
VNI	Virtual Network Index
WCM	White-Fi Cell Map
WSM	White Space Map

Chapter 1
Introduction

The proliferation of data-intensive applications has led to a superlinear growth in wireless data traffic over the last decade. As per the virtual network index (VNI) report released by Cisco in 2018 [1], data traffic is anticipated to rise from 122 Exabytes per month in 2017 to 396 Exabytes per month in 2022 (see Figure 1.1). That is, nearly a threefold increase is expected. Solutions to accommodate this increase in data traffic rely on improvements in the three aspects of *technology*, *topology*, and *spectrum availability and usage*. Traditionally, the focus has been on improvement in technology, which includes using high-order modulation and coding schemes as well as multiple-input multiple-output (MIMO) systems [3, 4]. However, issues such as channel correlation, hardware implementations and impairments and interference management [5] have shifted the focus from improvement in technology to advancement in topology and efficient use of the spectrum [6].

Advancement in topology, which includes network densification and offloading via the deployment of small-cell networks [7–10] is a potential solution. However, it faces challenges such as providing mobility support as well as determining appropriate association between users and base stations across mutiple radio access technologies and requires careful planning and cost evaluation by mobile operators [11–14] to cater to the increasing traffic demands. Efficient spectrum utilization, on the other hand, is another promising strategy that includes *spectrum refarming* and *spectrum sharing* amongst different networks. Spectrum refarming involves re-visiting spectrum allocation across different access technologies and re-assigning frequencies allocated to legacy obsolete technologies to newer ones [15, 16]. For instance, in Europe, the 1800 MHz (resp. 2100 MHz) band, historically allocated to 2G (resp. 3G), has been re-assigned to 4G. Although allocating spectrum to more efficient new technologies allows processing more traffic within the same bands, it takes years to repurpose a

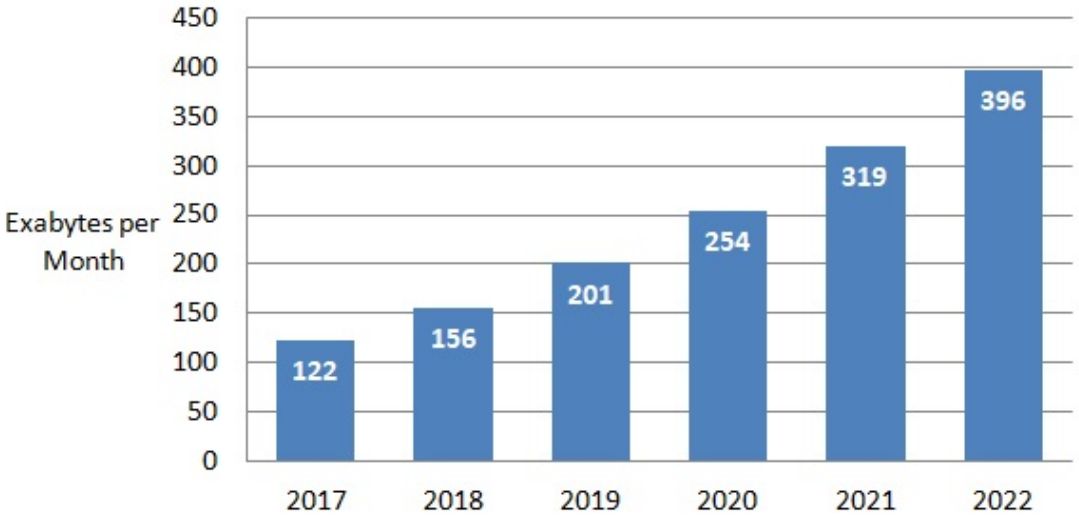

Figure 1.1: Data traffic growth prediction [1].

spectrum band for another use due to standardization.

Spectrum sharing, in contrast to spectrum refarming, aims to accommodate the data traffic growth by improving usage of existing spectrum bands that are temporally and spatially underutilized [17]. For instance, in the US and Europe, when analog TV channels switched to digital, new spectrum bands became available at different geographic locations. These spectrum bands, licensed to TV operators for exclusive use, in what was then a paradigm shift, were opened for use by low power unlicensed devices as long as they did not impair the reception of TV broadcast at TV receivers. The additional spectrum that became available as a result is often called the "TV White Spaces (TVWS)" and gave up to 300 MHz of bandwidth. It include bands of $54 - 698$ MHz in the United States [18] and $470 - 790$ MHz in Europe [19]. Similarly, in another ruling, the Federal Communications Commission (FCC) opened up 75 MHz of additional spectrum in the $5.85 - 5.925$ GHz Intelligent Transportation Systems (ITS) bands, used for vehicular networking, for unlicensed 802.11ac/802.11ax devices [20].

While spectrum sharing opens up more spectrum for use by data traffic, it also leads to the challenge of heterogeneous wireless networks having to coexist. The coexistence issue in the TV bands and other shared-access bands, such as the 2.4 GHz and 5 GHz band, is complex and challenging due to several reasons, including the disparity in spectrum access rights assigned to the networks by regulatory bodies and differences in technologies and utilities of the networks sharing the spectrum.

While each solution discussed above to accommodate the increase in data traffic

Solution	**Techniques Involved**	**Pros & Cons**
Improvement in technology	High-order modulation & coding schemes and MIMO	**Pros:** Increase in spectral efficiency (more bits/s/Hz), smoothed out channel responses and simple transmit/receive structures [3, 4]. **Cons:** Issue related to channel correlation, hardware implementations and impairments and interference management [5].
Advancement in topology	Network densification and offloading	**Pros:** Increase in area spectral efficiency (more nodes per unit area and Hz), spectrum reuse and reduction in the number of users competing for resources at each base station [7–10]. **Cons:** User association, handover and cost of installation, maintenance and backhaul [11–14].
Efficient spectrum utilization	Spectrum refarming and Spectrum sharing	**Pros:** Increase in bandwidth (more Hz) and better coverage. **Cons:** Need for effective management of spectrum resources, coexistence & interference issues, requirement of advancement in the areas of radio hardware, software, signal processing, protocols and access theory [15–17].

Table 1.1: Solutions to alleviate increasing data traffic and the associated advantages and challenges.

has its own advantages and associated challenges as shown in Table 1.1, in this thesis we only focus on spectrum sharing between networks. Specifically, we investigate two cases of practical interest in detail: (a) when unlicensed devices share spectrum with licensed TV users, and (b) when devices that aim to maintain the freshness of information share the unlicensed spectrum with bandwidth-hungry devices. While the former exemplifies the coexistence of networks with disparate spectrum access rights, the latter captures spectrum sharing between networks with different objectives. Also, the latter brings to light the distinct behaviour of devices that value information timeliness. This alongwith the growing interest in real-time applications motivated us to further study the coexistence of devices that care about timely delivery of their information updates and share spectrum for the same.

Next, we discuss each case briefly along with our contributions.

Coexistence of Licensed TV Users and Unlicensed WiFi Devices: TVWS, as mentioned above, are spectrum licensed for TV broadcast that spectrum regulators, for example, FCC [18] in the US and Ofcom [19] in Europe, have opened for unlicensed secondary devices, under the constraint that the incumbent TV network is protected from interference by the secondaries.

The network of secondary devices, also known as White-Fi, uses IEEE 802.11 (WiFi) like physical layer (PHY) and medium access control (MAC) mechanisms.

White-Fi cells may be deployed indoors, with coverage of a few 100 meters, and outdoors, with coverage as large as 5 km. Large cells may be used to provide internet access in sparsely populated areas. They may also be desirable when the white space channels available at a location are limited and do not allow for channelization and small cells. However, unlike its ISM band counterparts, White-Fi must obey requirements that protect TV reception. As a result, optimization of citywide White-Fi networks faces the challenge of spatial heterogeneity in channel availability and link quality. The former is because, at any location, channels in use by TV networks are not available for use by White-Fi. The latter is because the link quality at a White-Fi receiver is determined by not only its link gain to its transmitter but also by its link gains to TV transmitters, and its transmitter's link gains to TV receivers.

We investigate the deployment of White-Fi networks which coexist with TV networks and their resulting throughputs [21, 22]. Several studies including [23–26] and [27, 28] have proposed approaches for assessment of TVWS capacity under FCC and Electronic Communications Committee (ECC) regulations, respectively. Contrary to [23–26], [29] advocated that FCC regulations are stringent and must be replaced by spatially-aware rules for better utilization of TVWS. Motivated by [29], we leverage heterogeneity in channel availability and link quality both. Starting with optimizing the distributed coordination function (DCF) throughput of a single cell White-Fi network under aggregate interference and power constraints, while leveraging heterogeneity in link quality in [21], we study the throughput optimization of a multi-cell White-Fi network [22]. Specifically, we model and optimize the MAC throughput of a multi-cell city-wide White-Fi network operating in the spectrum licensed to TV operators. We propose a throughput maximization problem for the White-Fi network under the constraint that White-Fi nodes' maximum aggregate interference at the TV receivers is within acceptable limits. Aggregate interference at a TV receiver from a secondary network has also been studied in [30–35].

We propose a heuristic algorithm that is cognizant of spatial heterogeneity in channel availability and link quality, which, as mentioned above, are attributes specific to White-Fi networks operating in TVWS. While prior works assess the Shannon capacity of secondary links [36], we study the secondary network's MAC throughput. We demonstrate the efficacy of our proposed method over hypothetical deployments of White-Fi networks coexisting with real TV networks in the US cities of Columbus and Denver, which are good examples of heterogeneous channel availability and link quality in TVWS. Our proposed framework provides useful insights, such as, more channels may not result in increased throughput as observed in the case of Columbus

which has higher channel availability but lower network throughput than Denver. We also provide a discussion on how our proposed approach can leverage the architecture proposed in 802.11af to enable the use of white spaces by secondary devices. While there exist several studies on maximization of secondary network throughput under aggregate interference [30–35, 37–42], our work considers maximizing the throughput of a carrier-sense multiple access with collision avoidance (CSMA/CA) based citywide White-Fi network in which the secondaries can communicate over long distances.

Coexistence of Age and Throughput Optimizing Networks: The ubiquity of Internet-of-Things (IoT) devices has led to the emergence of applications that require these devices to sense and communicate information (status updates) to a monitoring facility or share with other devices in a timely manner. These applications include real-time monitoring systems such as disaster management, environmental monitoring, and surveillance [43, references therein], which require timely-delivery of information updates to a common ground station for better system performance, to networked control systems like vehicular networks, where each vehicle broadcasts status (position, velocity, steering angle, etc.) to nearby vehicles in real-time for safety and collision avoidance [44].

Such networks may share the wireless spectrum with WiFi networks. For instance, as mentioned earlier, the FCC in the US opened up 195 MHz of additional spectrum for unlicensed devices in the $5.35 - 5.47$ GHz and $5.85 - 5.925$ GHz bands. The regulation prescribed sharing the latter, that is, the $5.85 - 5.925$ GHz ITS band, used for vehicular networking, with high throughput WiFi (802.11ac/802.11ax) devices, leading to the possibility of coexistence between WiFi and vehicular networks [20]. Similarly, IoT devices like Unmanned Aerial Vehicles (UAVs), equipped with 802.11 a/b/g/n technology, operate in the 2.4 and 5 GHz bands in use by WiFi networks. While the coexisting networks have the same spectrum access rights, the vehicular nodes in the ITS band and the UAVs operating in the 2.4 and 5 GHz bands value information timeliness, whereas, the WiFi devices desire high throughputs. This novel spectrum sharing scenario raises an interesting question of whether such networks would prefer to cooperate or compete for spectrum access. In this part of the thesis, we address this question using a game-theoretic approach.

We quantify freshness using the metric of age of information [45] and refer to the network that cares about information timeliness as an age optimizing network (AON) and to the network that desires high throughput as a throughput optimizing network (TON). We use a game-theoretic approach to investigate the coexistence of

an AON and a TON when both networks use a WiFi like CSMA/CA based medium access, from a MAC layer perspective [46–48]. Several studies [49–53] have employed game theory to study the behavior of nodes in wireless networks. However, these studies have throughput as the payoff function. In contrast to throughput, age as a payoff function has recently garnered attention [54–60]. In addition, [61–63] employed repeated games in the context of coexistence, where the coexisting networks had similar objectives. We use a repeated game-theoretic approach that model networks as selfish players that aim to optimize their different utilities in the long run. While the AON aims to minimize the average age of updates, a TON seeks to maximize its throughput. We use the repeated game model to answer whether a simple coexistence etiquette that enables cooperation between an AON and a TON is self-enforceable. Specifically, we introduce a coordination device, which is a randomized signaling device that allows the AON and the TON to access the spectrum in a non-overlapping manner, that is, one at a time. The networks employ a grim trigger strategy when cooperating, which has both the networks *compete* in all stages following a stage in which a network disobeys the device. This ensures that the networks would disobey the device only if competition were more beneficial than cooperation in the long run.

We employ the proposed etiquette to two practical medium access settings: (a) collision slots are at least as large as successful transmission slots, which is, for example true when networks use the basic access mechanism defined for the 802.11 MAC [64], and (b) collision slots are smaller than successful transmission slots, which, for example holds for networks employing the Request To Send/Clear To Send (RTS/CTS) based access mechanism [64]. Our analysis reveals that for both medium access settings, while cooperation is self-enforceable when networks have a small number of nodes, networks prefer competition when they grow in size.

Coexistence of Selfish Age Optimizing Nodes: Motivated by the distinct behavior of age optimizing networks observed in the above study of the coexistence of age and throughput optimizing networks and the growing interest in real-time applications such as vehicular networking, where each vehicle desires to have timely status information (position, velocity, etc.) about other vehicles in the network, we consider spectrum sharing between nodes that care about the information timeliness. We investigate the coexistence of such nodes from a MAC layer perspective. We assume that each node accesses the spectrum using a slotted CSMA/CA based access mechanism and would like to minimize the average age of its status information at the other nodes. Age has previously been investigated for networks with multiple users sharing a slotted system in [65–70]. Also, as mentioned earlier, [46–48, 54, 55]

studied games with age as the payoff function. However, none of these works consider competing nodes that value information timeliness and share the spectrum using a slotted CSMA/CA based medium access. Specifically, we model the competition between nodes for the shared spectrum as a non-cooperative one-shot multiple access game parameterized by the age of every node and the medium access settings [71]. While the interaction for spectrum access is most realistically modeled as a repeated game [72], it is important to understand the one-shot game and its equilibria first before analyzing the repeated game. Therefore, we study the one-shot game played by the nodes in a CSMA/CA slot.

We investigate the nodes' equilibrium strategies when (a) collisions are longer than successful transmissions, and (b) collision are shorter. For each setting, we discuss how competing nodes that value timeliness share the spectrum and show that access settings exert strong incentive effects. Specifically, our analysis reveals that under decentralized decision making by nodes, while transmit is a weakly dominant strategy when collisions are shorter, no dominant strategy exists when collisions are longer. Also, for the latter we analytically derive the mixed strategy Nash equilibrium (MSNE) for when the ages at the beginning of the slot satisfy certain conditions.

The rest of the thesis is organized as follows. In Chapter 2, we discuss in detail the coexistence of White-Fi networks and licensed TV users in TV white spaces. We formulate the optimization problem, propose a heuristic algorithm, and illustrate our approach's efficacy over hypothetical deployments of White-Fi networks coexisting with real TV networks. Next, in Chapter 3, we study the coexistence of age and throughput optimizing networks. Specifically, we investigate a game-theoretic approach to AON-TON coexistence, formulate the repeated game model with the AON and the TON as players, propose a coexistence etiquette and explore the possibility of cooperation between the networks under the proposed etiquette. Note that since we investigate coexistence from a MAC layer perspective, we use MAC throughput and throughput interchangeably througout the thesis. Lastly, in Chapter 4, we study the coexistence of selfish age optimizing nodes that care about information timeliness, formulate a non-cooperative multiple access game with nodes as players, and investigate their equilibrium strategies for different medium access settings. We conclude with a summary of our work in Chapter 5 and list the publications that capture our contributions in Chapter 6.

Chapter 2
Coexistence of Licensed TV Users and Unlicensed WiFi Devices

2.1 Problem Overview and Motivation

TVWS are spectrum licensed for TV broadcast that spectrum regulators, for example, FCC [18] in the US and Ofcom [19] in Europe, have opened for use by unlicensed secondary devices, with approaches prescribed to protect the incumbent TV network from interference by the secondaries. TVWS include bands of $54 - 698$ MHz in the United States and $470 - 790$ MHz in Europe.

White-Fi and Super-WiFi are used to refer to a network of secondary devices that use IEEE 802.11 (WiFi) like PHY and MAC mechanisms. White-Fi cells may be deployed indoors, with coverage of a few 100 meters, and outdoors, with coverage as large as 5 km. Large cells may be used to provide internet access in sparsely populated areas. They may also be desirable when the white space channels available at a location are limited and do not allow for channelization and small cells.

In this chapter, we consider a citywide White-Fi network. Figure 2.1 provides an illustration. The geographical region covered by the network is tessellated by White-Fi cells. There are also multiple TV transmitters and receivers, with the transmitters servicing locations in and around the White-Fi network. Transmissions due to White-Fi nodes must not impair reception of TV broadcasts at TV receivers. This requirement, as we explain next, leads to fluctuation in *channel availability* and *achievable White-Fi link quality* as a function of location in a White-Fi network, and makes the optimization of such networks distinct from that of traditional WiFi networks operating in the 2.4 and 5 GHz unlicensed bands, which see homogeneity in channel availability and achievable link quality.

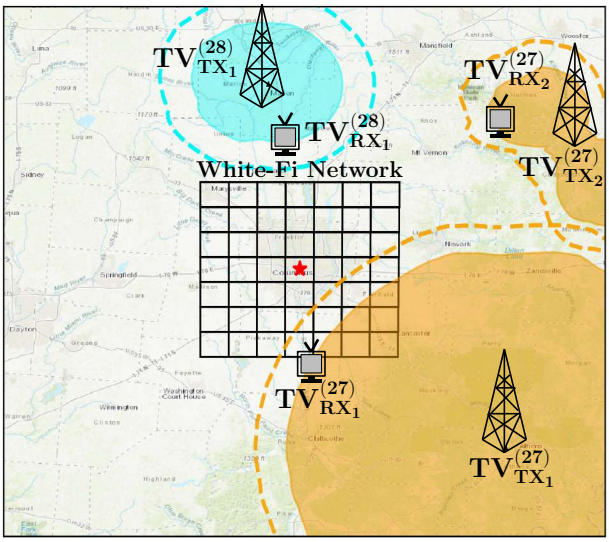

Figure 2.1: Illustration of a city-wide White-Fi network deployed in Columbus, Ohio, USA. Three TV networks, operating on channels 27 and 28, are shown. For each TV network we show the TV transmitter and a TV receiver. For example, on channel 28 we have $TV_{TX_1}^{(28)}$ and $TV_{RX_1}^{(28)}$. Around each TV transmitter we show its region of service (solid colored). The boundary of this region is the service contour of the transmitter. We also show the so-called protection contour (dashed line) for each transmitter. It encloses a safety zone in addition to the region of service of the transmitter. The contours were obtained from a database [2] created using information from the FCC.

Heterogeneity in channel availability: The region serviced by a TV transmitter, illustrated in Figure 2.1, is enclosed by its *service contour*. TV transmitters are allocated channels such that they don't create interference within each other's service contours. These channels are known a priori and may be obtained, for example, from [73], which has US related data. In addition, to protect TV receivers from interference due to transmissions by secondary devices, regulatory bodies disallow a secondary from transmitting over channels being used by TV transmitters if the secondary is within a certain geographic proximity of the TV transmitters. This results in heterogeneous channel availability across locations in a city-wide White-Fi network.

To exemplify, FCC [74] restricts transmissions over the so-called *protected region* around a TV transmitter i.e. a TV channel is available for transmission by secondary nodes at a location only if the location is outside the protected region of each TV transmitter operating on that channel. The protected region, shown with a dashed line in Figure 2.1, includes the region within the service contour and an additional

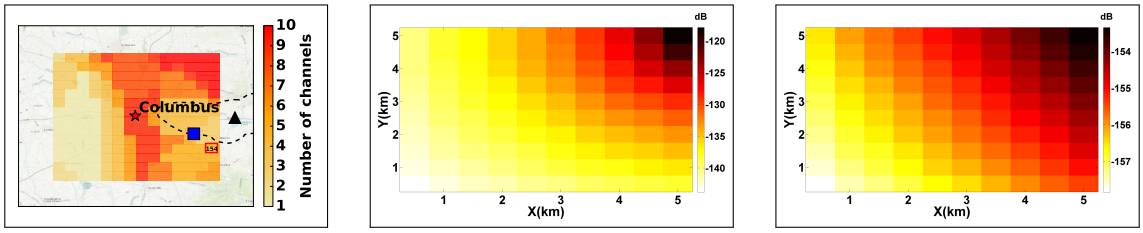

(a) (b) (c)

Figure 2.2: (a) Channel availability in the city of Columbus in Ohio, USA over a White-Fi network spread over an area of 4900 km^2. Each pixel in the White-Fi network represents a White-Fi cell covering an area of 25km^2. Channel availability is computed for a scenario where a channel is deemed available for a White-Fi cell if the cell lies outside the service contour of every TV transmitter operating on that channel. (b) Link gains from locations in the White-Fi cell (indexed 154 in (a)) to the TV receiver (solid blue square in (a)) located about 1 km away. (c) Link gains to locations in the White-Fi cell 154 from the TV transmitter (solid black triangle in (a)) located at a distance of 15.7 km. All link gain calculations assume a path loss model with an exponent of 3.

buffer to protect the TV receivers from secondary interference. Figure 2.2a shows the resulting number of channels available, for transmissions by secondary nodes, over an area of 4900 km^2 in the city of Columbus, Ohio, USA. The availability varies over a large range of $1 - 10$ channels.

Heterogeneity in achievable link quality: The link quality, specifically the signal-to-interference-and-noise-ratio (SINR), of a White-Fi link is impacted by the TV network in a two-fold manner. (a) Link SINR suffers due to interference from TV transmitters operating on the same/interfering channel as that of the link. Specifically, the larger the link gain between a TV transmitter and a White-Fi receiver, the smaller is the SINR of the corresponding White-Fi link. (b) The larger the link gain between a White-Fi transmitter and a TV receiver, the smaller the power the transmitter is allowed to use on its link without unduly impacting reception at the TV receiver.

Since White-Fi cells can be large in size, different locations within the same cell may see very different link gains to TV transmitters and receivers. Figure 2.2b shows the link gains from locations in a White-Fi cell of size 5 km $\times$ 5 km to a TV receiver located at a distance of about 1 km. A spread of about 25 dB is observed. Figure 2.2c shows link gains from a TV transmitter located at a distance of about 16 km from the cell. We observe a spread of about 5 dB in gains. This heterogeneity in gains, within a cell, to and from the TV network does not exist when the nodes are spread over a very small region as is the case in traditional WiFi.

The optimization problem: We investigate optimizing the MAC saturation (every node always has a packet to send) throughput of a citywide White-Fi network. Similar to traditional WiFi, nodes in a White-Fi cell use the DCF [64], which is a CSMA/CA based MAC to gain access to the medium. We want to maximize the MAC saturation throughput of the network under the constraint that reception at TV receivers is not impaired. Specifically, we enforce that the maximum aggregate interference that nodes in the White-Fi network create at any TV receiver is within allowed limits. We optimize over assignments of channel, transmit power, and medium access probability to nodes in the network. This allows us to adapt to the aforementioned heterogeneities.

As a result of optimization, a node may be assigned one or more channel. In this work, we assume that each node maintains a separate queue (in saturation condition) for each assigned channel. A node contends with other nodes in the White-Fi cell for each channel independently of the other assigned channels. However, the transmit power allocated to a channel is not independent of the allocation to other channels assigned to it. Specifically, each node in a White-Fi cell has a total power budget which it splits across the assigned channels. This allows for a better allocation of the available power budget, at every node, across assigned channels, given constraints on interference that may be created at the TV receivers and interference from the TV transmitters. In practice, this will require nodes to be able to use multiple orthogonal channels simultaneously, say, using multiple radios or an SDR that can operate on the assigned channels simultaneously.

Unlike our model, FCC regulations propose a simpler model of coexistence with the TV network in which any secondary node outside the protected region can transmit at its full power, as allowed for its device category [18]. Despite being conservative, the regulations do not guarantee protection of the TV network from excess *aggregate* interference that results from more than one node transmitting using the allowed power. Unlike the FCC, Office of Communications (Ofcom), the communications regulatory authority in Europe [19], requires secondary transmit power to be a function of location. This requirement is implicit in our constraint on aggregate interference at a TV receiver. The aggregate interference is a function of the transmit powers of the White-Fi nodes and their link gains to the TV receiver, where the gains are a function of the locations of the TV receiver and the White-Fi nodes. In fact, the White-Fi nodes that are assigned the same channel as the TV receiver may be located across different cells. As a consequence, the aggregate interference budget at the TV receiver is shared between nodes in different White-Fi cells.

Authors in [24] assess the Shannon capacity of secondary links whereas we study the DCF throughput of the White-Fi network. Also, there are prior studies such as [36, 39, 75–79] that propose maximization of secondary network throughput under aggregate interference and transmit power budget constraints. However, to the best of our knowledge, this work is the first attempt to model and optimize the DCF throughput of a multi-cell city-wide White-Fi network.

Our specific contributions are listed next.

- We formulate the problem of maximizing the DCF throughput of a multi-cell White-Fi network under the constraint that the maximum aggregate interference that White-Fi nodes create at TV receivers is within acceptable limits.
- We rework the saturation throughput model proposed by Bianchi in [64] to incorporate per node transmit power and data payload rates, per node access probabilities, and an overhead rate used to communicate control packets that is not fixed but results from the optimization of the White-Fi network.
- The throughput maximization is a non-linear optimization problem. We propose a two-phase heuristic solution. In the first phase, we assign TV white space channels to cells in the White-Fi network. In the second phase, we assign nodes in the cells their payload transmission rates/transmit powers and access probabilities, over each assigned channel.
- We demonstrate the efficacy of the proposed heuristic algorithm over hypothetical deployments of White-Fi networks coexisting with real TV networks in the US cities of Columbus, Ohio and Denver, Colorado. Together, these cities provide good examples of heterogeneity in channel availability and link quality in the white spaces. Surprisingly, while Columbus has higher channel availability as compared to Denver, its network throughput is lower.
- Further, we compare our approach to a baseline that adheres to restrictions on aggregate interference but allocates the same power and access probabilities to all nodes in a cell, which makes it easier to implement in practice.
- Last but not the least, we quantify the reduction in the availability of white spaces that may result from the use of FCC-like regulations when restrictions on aggregate interference from White-Fi nodes must be enforced.

The rest of the chapter is organized as follows. Section 2.2 describes related works. The network and the saturation throughput model are described in Section 2.3. This

is followed by the optimization problem in Section 2.4. The solution methodology is described in Section 2.5. The setup of the hypothetical White-Fi networks and results are respectively in Sections 2.6 and 2.7. Section 2.8 provides a discussion on how our proposals can leverage the architecture proposed in 802.11af to enable use of white spaces by secondaries. We conclude in Section 2.9.

2.2 Related Work

In preliminary work [21], we investigated optimization of DCF throughput of a single White-Fi cell flanked by two TV networks. Authors in [23–26] and [27, 28] have proposed approaches for assessment of TVWS capacity under FCC and ECC regulations, respectively. Contrary to [23–26], the authors in [29] advocate that FCC regulations are stringent and must be replaced by spatially-aware rules for better utilization of TVWS. Motivated by [29], this work focuses on leveraging heterogeneity in white space availability and link quality to maximize the throughput of a citywide White-Fi network. Also, while authors in [24–27] provide assessment of TVWS capacity at any location (very short range communication), in this work we are interested in the capacity of an outdoor White-Fi network comprising of long-range links.

In [21] we optimize the DCF throughput of a single cell White-Fi network under aggregate interference and power constraint while leveraging heterogeneity in white space signal quality only. In this work, we extend our previous work to study the throughput optimization of a multi-cell White-Fi network. Our current approach allow us to leverage heterogeneity in white space availability and quality both. The proposed throughput maximization problem is cognizant of aggregate interference constraint at the TV receivers. Modelling aggregate interference at a TV receiver from a secondary network has been previously studied in [30–35]. In [37, 38, 80] authors propose an approach for determining permissible transmit powers for secondary networks under aggregate interference constraints. Authors in [37] quantify the capacity available to a secondary system under constraints on interference at the TV receiver. In [81], authors propose to maximize the sum capacity of a secondary network by setting the power limits for each white space device while limiting the probability of harmful interference created at the primary network. While the aforementioned works, [30–35, 37, 38], study cellular-like secondary systems, in this work, we consider a WiFi-like secondary system.

Similar to this work, authors in [39–42] consider power control and channel al-

location in networks operating in TV white spaces. Authors in [39] propose fair spectrum allocation and capacity maximization for infrastructure-based secondary networks operating in TVWS. They consider an overlay secondary system and determine channel allocation and transmit powers according to licensed user activity. Contrary to [39], we consider an underlay approach while ensuring the licensed user (TV) is protected.

Authors in [40] propose an approach that maximizes the throughput of a cellular secondary network while maintaining a required SINR for all TV receivers and requires cooperation between secondary devices and TV networks. Authors in [41] use the Nash bargaining solution to allocate power and channel to nodes of a secondary network. Their network operates like an infrastructure mode WiFi network (clients communicate via an access point). However, they don't model WiFi throughput. Also, they do not take into consideration the interference to/from the TV networks. Authors in [42] propose a channel allocation/power control algorithm to maximize the spectrum utilization of a cellular secondary network while protecting the licensed users and ensuring a minimum SINR for each user in the secondary network. Authors propose a dynamic interference graph based approach to attain the objective. Authors in [82] propose a joint power and subcarrier allocation algorithm for sum capacity maximization under a peak power constraint. Authors in [83] propose a resource allocation scheme for Orthogonal frequency-division multiplexing (OFDM)-based secondary network which includes power allocation, bit loading and sub-carrier bandwidth sizing with the objective of maximizing secondary network throughput.

Authors in [36] propose throughput maximization of a WiFi like network in TVWS under aggregate interference. Similar to this work they allow variable transmit powers. However, they do not model the CSMA/CA based mechanism of the DCF. Instead, they model WiFi link rates to be their Shannon rates. Authors in [84] propose a white space wide area wireless network that extends WiFi like spectrum sharing to TVWS. Unlike this work, they assume that nodes can transmit at their maximum transmit powers. As a result they do not optimize the interplay between the secondary users and the TV network.

Authors in [75] propose a learning algorithm for dynamic rate and channel selection to maximize the throughput of a wireless system in white spaces. Authors in [76] and [77], propose channel assignment techniques for maximizing throughput of secondary networks in TVWS. Similar to this work, authors in [75–77] propose throughput maximization of secondary networks in TVWS, however, they do not consider the impact of aggregate interference from secondary users on TV receivers.

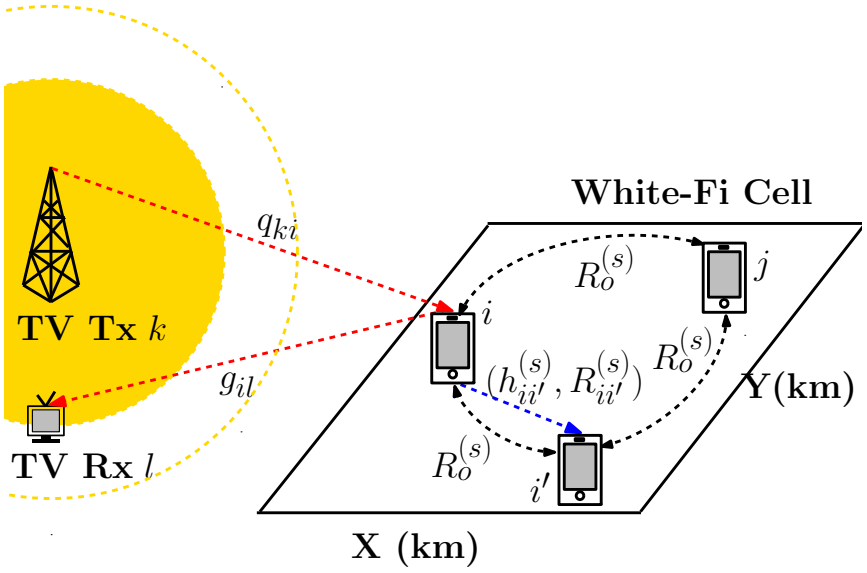

Figure 2.3: We summarize the different link gains and rates. A White-Fi cell with nodes i, i', and j is shown. The TV network consists of a transmitter (large tower) TV TX k and a receiver TV RX l (assumed to be operating in channel s). The gains g_{il} from node i to the TV receiver and q_{ki} from the TV transmitter to node i, are shown over the corresponding links. Also, we show the link gain $h_{ii'}^{(s)}$ between nodes i and i', over the channel s. All nodes broadcast control overheads on channel s at rate $R_o^{(s)}$ defined in (2.4). Node i sends its data payload to node i' at rate $R_{ii'}^{(s)}$ defined in (2.3).

Also, authors in [78] propose an admission control algorithm for Code-division multiple access (CDMA) networks which ensures Quality of Service (QoS) for underlay secondary networks and protects TV receivers. While the constraints are similar to this work, the objective of [78] is to ensure proportional and max-min fairness for a CDMA network, whereas we focus on maximizing the DCF throughput of a CSMA/CA based WiFi network.

In summary, while there exist several studies on maximization of secondary network throughput under aggregate interference and power budget constraints, to the best of our knowledge, this work is the first attempt to maximize throughput of a CSMA/CA based citywide White-Fi network in which the secondaries can communicate over long distances.

2.3 Network Model

Let $\mathcal{S}$ be the set of white space channels. Our TV network, illustrated in Figure 2.1, consists of TV transmitters and receivers that operate on channels in $\mathcal{S}$. Let $\text{TV}_{\text{TX}}^{(s)}$

and $\text{TV}_{\text{RX}}^{(s)}$ respectively be the set of TV transmitters and TV receivers operating on channel s. A TV transmitter k has a known transmit power P_k^{TV}. Our White-Fi network operates over a geographical region that is tessellated by a set $\mathcal{M}$ of White-Fi cells indexed $1, \ldots, M$. We define $\mathcal{N}$ to be the set of all White-Fi nodes and $\mathcal{N}_m$ to be the set of nodes in cell m. It follows that $\mathcal{N} = \cup_{m=1}^{M} \mathcal{N}_m$. Also, a node must belong to exactly one cell.

White-Fi nodes operating on a channel s will create interference at TV receivers in $\text{TV}_{\text{RX}}^{(s)}$ and will suffer interference from the TV transmitters in $\text{TV}_{\text{TX}}^{(s)}$. These interference powers are a function of the link gains, respectively, between the TV receivers and nodes, and the TV transmitters and nodes. Let q_{ki} be the link gain between TV transmitter k and a White-Fi node i. Further, let g_{il} be the link gain between node i and TV receiver l. These gains are illustrated in Figure 2.3. In practice, the knowledge of locations of the TV transmitters, receivers, and the White-Fi nodes, together with a suitable path loss model, can be used to estimate them.

Let $S_m \subset \mathcal{S}$ be the set of white space channels available in the geographical region covered by cell m. Further let $\overline{S}_m \subset S_m$ be the channels that are assigned for use in the cell. While S_m is known a priori, for example from [73], $\overline{S}_m$ is obtained as a result of the proposed throughput optimization. Let $T_m^{(s)}$ be the MAC throughput of cell m on a channel s assigned to it. We define the MAC throughput T_m of the cell m to be the sum of its throughputs on each channel assigned to it. The throughput T of the White-Fi network is simply the sum of the throughputs of its M cells. We have

$$T_m = \sum_{s \in \overline{S}_m} T_m^{(s)}, \tag{2.1}$$

$$T = \sum_{m=1}^{M} T_m. \tag{2.2}$$

Next we detail the calculation of the throughput $T_m^{(s)}$ of cell m on an assigned channel s.

Throughput of a cell on an assigned channel: A node in a cell will transmit data payloads over all channels assigned to the cell. Let $P_i^{(s)}$ be the power with which such a node i transmits its unicast data payload over channel s. Without loss of generality, assume that a certain other node i' in the cell is the destination for i's payload. Let the gain of the link between i and i' over channel s be $h_{ii'}^{(s)}$ (see Figure 2.3). Note that i and i' can communicate using all channels in the set $\overline{S}_m$ and

the link gain $h_{ii'}^{(s)}$ is a function of the channel $s \in \overline{S}_m$ under consideration. The data payload rate $R_{ii'}^{(s)}$ that may be achieved between i and i', for a channel bandwidth of B Hz and thermal noise of spectral intensity N_0 Watts/Hz, is the Shannon rate of the link and is given by

$$R_{ii'}^{(s)} = B \log_2(1 + \text{SINR}_{ii'}) \text{ bits/sec}, \tag{2.3}$$
$$\text{where SINR}_{ii'} = \frac{h_{ii'}^{(s)} P_i^{(s)}}{BN_0 + \sum_{k \in \text{TV}_{\text{TX}}^{(s)}} q_{ki'} P_k^{\text{TV}}}.$$

The numerator of $\text{SINR}_{ii'}$ is the power received at node i' from i. The denominator is the sum of receiver noise power at i' and the sum of interference powers received from TV transmitters on the channel s. For any TV transmitter k on the channel, the interference power is the product of its transmit power P_k^{TV} and its link gain $q_{ki'}$ to the White-Fi receiver i'. Node i achieves the data payload rate $R_{ii'}^{(s)}$ only for the fraction of time it gets successful access to the medium.

All White-Fi nodes in a cell (set $\mathcal{N}_m$ for cell m) follow the IEEE 802.11 DCF for medium access. We will enforce that all nodes in a cell can decode messages that help regulate access to the medium, for example, Request-to-Send (RTS), Clear-to-Send (CTS), and Acknowledgement (ACK), sent from any other node in the cell. We will refer to such messages as overheads. So while a data payload sent by i to i' at rate $R_{ii'}^{(s)}$ may not be correctly decoded by a node other than i', all overhead messages sent by i must be correctly decoded by all nodes.

These overheads transmitted by node i can be correctly decoded by any other node in the cell if they are sent at a rate not greater than $B \log_2(1+\min_{j \in \mathcal{N}_m, j \neq i} \text{SINR}_{ij})$. In this work, for simplicity of exposition, we will assume that all nodes within a cell m, use the same rate $R_o^{(s)}$ to send overheads. Note that this underestimates the achievable throughput of the cell. The overhead rate is given by

$$R_o^{(s)} = \min_{i \in \mathcal{N}_m} B \log_2(1 + \min_{\substack{j \neq i \\ j \in \mathcal{N}_m}} \text{SINR}_{ij}). \tag{2.4}$$

Next we will leverage the model for DCF proposed by Bianchi in [64] to calculate the MAC saturation throughput $T_m^{(s)}$ of the network of nodes $\mathcal{N}_m$ in a cell. Nodes are assumed to always have a packet to transmit.

A DCF slot during which no transmission takes place is called an idle slot. A slot in which exactly one node transmits sees a successful transmission. A slot in which more than one node transmits sees a collision and none of the transmitted

packets are decoded successfully. Let $\tau_i^{(s)}$ be the steady state probability with which White-Fi node i accesses the wireless medium during a DCF slot for transmitting its data payload, over channel s. The probability $p_{\text{succ,i}}^{(s)}$ that a transmission by i is successful and the probability $p_{\text{idle}}^{(s)}$ that a slot is idle are, respectively,

$$p_{\text{succ,i}}^{(s)} = \tau_i^{(s)} \prod_{\substack{j \in \mathcal{N}_m \\ j \neq i}} (1 - \tau_j^{(s)}) \text{ and } p_{\text{idle}}^{(s)} = \prod_{j \in \mathcal{N}_m} (1 - \tau_j^{(s)}). \tag{2.5}$$

Let idle slots be of duration σ. In practice, this is specified by the 802.11 standard. Let L bits be the size of data payload in a packet transmitted by any White-Fi node i. A slot that sees a successful transmission consists of the data payload, overhead bits including packet headers, RTS/CTS, ACK, and overheads due to inter frame spacings like DCF Interframe Space (DIFS). Let O_{bits} be the number of overhead bits. They are transmitted at the overhead rate $R_o^{(s)}$ defined in (2.4). The data payload is transmitted by node i to its destination node i' at rate $R_{ii'}^{(s)}$ defined in (2.3). Let O_{sec} denote the frame spacing related overheads. Therefore, the total duration of a successful transmission slot of node i is given by $T_{\text{succ,i}} = O_{\text{sec}} + O_{\text{bits}}/R_o^{(s)} + L/R_{ii'}^{(s)}$.

Finally, a slot that sees a collision has L_{col} bits and L_{colsec} time overheads. The duration of a collision is given by $T_{\text{col}} = L_{\text{col}}/R_o^{(s)} + L_{\text{colsec}}$. On use of RTS/CTS, which we assume in this work*, only RTS packets may collide. As a result, T_{col} is the same irrespective of which nodes' transmissions were involved in a collision. Following the analysis in [64], we can now calculate the time interval $\sigma_{\text{avg}}^{(s)}$ of an average DCF slot in our cell, over channel s, as

$$\sigma_{\text{avg}}^{(s)} = p_{\text{idle}}^{(s)}\sigma + \sum_{i \in \mathcal{N}_m} p_{\text{succ,i}}^{(s)} T_{\text{succ,i}} + (1 - p_{\text{idle}}^{(s)} - p_{\text{succ}}^{(s)}) T_{\text{col}},$$
$$\text{where } p_{\text{succ}}^{(s)} = \sum_{i \in \mathcal{N}_m} p_{\text{succ,i}}^{(s)}.$$

Note that $p_{\text{succ}}^{(s)}$ is simply the probability that a DCF slot sees a successful transmission. We have an average of $p_{\text{succ}}^{(s)} L$ payload bits transmitted successfully in the network over an average slot of length $\sigma_{\text{avg}}^{(s)}$. The throughput $T_m^{(s)}$ bits/sec can thus

*The case when the network does not use RTS/CTS introduces variable length collisions, where the length is a function of the data payload rates of the colliding transmissions. While, this can be incorporated in the model, the resulting expression for the length of the collision slot becomes unwieldy. Also, as is shown in [64], under saturation conditions the maximum throughput with or without RTS/CTS is the same. In fact, using RTS/CTS is more desirable as it makes the throughput less sensitive to small changes in access probability.

be obtained as

$$T_m^{(s)} = \frac{p_{\text{succ}}^{(s)} L}{\sigma_{\text{avg}}^{(s)}}.$$

On the DCF model: The model proposed by Bianchi [64] assumes that all nodes can decode control messages such as RTS, CTS, and ACK, sent from any other node in the cell. This precludes the possibility of hidden nodes in the network. There are many works that extend [64] to model the throughput in the presence of hidden nodes. It is noteworthy that the extension in [85] uses the same basic form of throughput as in [64] and is amenable to per node data payload rates and access probabilities, and optimizable overhead rates. That said, the extension to hidden nodes is non-trivial and we defer it to the future. Among other things, not all nodes in the cell see the same set of hidden nodes. Importantly, the basic interplay between the White-Fi network and the primary, which involves interference created by TV transmitters at White-Fi nodes and the interference created by the nodes at TV receivers, and the impact of interference on data payload and overhead rates in the network, is captured well by the White-Fi network model we consider in this work.

2.4 Optimization Problem

We want to optimize the network throughput T, defined in (2.2). However, transmissions by nodes in the White-Fi network must not impair TV reception. Specifically, we will impose limits on the aggregate interference that White-Fi nodes may create at TV receivers. In addition, we also impose (a) adjacent White-Fi cells must be assigned orthogonal channels, (b) a finite power budget per node in the White-Fi network, and (c) time fairness amongst White-Fi links in a cell.

Limits on aggregate interference: Recall that $\text{TV}_{\text{RX}}^{(s)}$ is the set of TV receivers operating in channel s. Let l be a receiver in the set. A White-Fi node i transmits in a DCF slot, over channel s, with probability $\tau_i^{(s)}$. As a result, the interference I_{il} that the node i creates at l in any DCF slot is a Bernoulli random variable

$$I_{il} = \begin{cases} g_{il} P_i^{(s)} & \text{w.p. } \tau_i^{(s)}, \\ 0 & \text{otherwise.} \end{cases} \tag{2.6}$$

Recall that g_{il} is the link gain between node i and TV receiver l and $P_i^{(s)}$ is the power

used by i on channel s. The receiver l will suffer interference from all nodes that are transmitting over channel s. These are the nodes that belong to cells that have been assigned the channel s. The aggregate interference I_l at l is

$$I_l = \sum_{m:s\in\overline{S}_m} \sum_{i\in\mathcal{N}_m} I_{il}.$$

In our earlier work on a single White-Fi cell [21], we had considered, separately, limits on the maximum of the random variable I_l and its expectation $E[I_l]$. Since the resulting qualitative insights were similar, in this work, we restrict our investigation to limits on the maximum of I_l. Let the desired limit on maximum aggregate interference at TV receiver l be IMAX_l. We require that the maximum aggregate interference created by White-Fi nodes at any TV receiver l, operating on a channel s assigned to any cell in the White-Fi network, not exceed IMAX_l. Observe from (2.6) that $\max(I_{il}) = g_{il}P_i^{(s)}$. Our desired constraint is given by the following system of inequalities, one for each TV receiver.

$$\max(I_l) = \sum_{m:s\in\overline{S}_m} \sum_{i\in\mathcal{N}_m} g_{il}P_i^{(s)} \leq \text{IMAX}_l, \quad \forall l \in \text{TV}_{\text{RX}}^{(s)}, \forall s \in \cup_{m=1}^{M}\overline{S}_m. \tag{2.7}$$

Observe that the aggregate interference at a TV receiver results from nodes in one or more White-Fi cells that are assigned the white space channel on which the TV receiver operates. As a result, nodes in a cell cannot be assigned transmit powers on a given channel independently of nodes in other cells that have been assigned the same channel.

Channel assignment constraint: Let the $M \times M$ matrix $[A] = \{a_{ij}\}$ be the adjacency matrix of the cells in the White-Fi network. For any two cells $m_1, m_2 \in \mathcal{M}$, we have $a_{m_1m_2} = 1$ if m_1 and m_2 are adjacent[†], otherwise, $a_{m_1m_2} = 0$. Nodes in cells that are adjacent can interfere with each other's transmissions. We require adjacent cells to be assigned orthogonal channels. That is

$$\overline{S}_{m_1} \cap \overline{S}_{m_2} = \phi \qquad \forall m_1, m_2 \text{ s.t. } a_{m_1m_2} = 1. \tag{2.8}$$

Power budget constraint: We assume that every White-Fi node has a total power

[†]Any two cells $m_1, m_2 \in \mathcal{M}$ are adjacent if the distance between the cells is $\leq d$, where, d is the distance at which the received power is 3 dB less than the noise floor. For a path loss exponent of 3, $d = 2.59$ km.

budget of P_T. The node may split this power over one or more assigned channels. We require

$$\sum_{s \in \overline{S}_m} P_i^{(s)} \leq P_T \qquad \forall i \in \mathcal{N}_m, \forall m \in \mathcal{M}. \tag{2.9}$$

Time fairness constraint: Finally, we enforce time fairness across links on each channel within a cell. That is, on an average, every link i in a cell spends the same fraction of time transmitting a data payload successfully to its destination on an assigned channel s. This constraint is essential to ensure that links with high link quality don't dominate access to the medium. Recall that the data payload is L bits. The average fraction of time spent by a node i transmitting its data payload successfully to a node i' over an average slot $\sigma_{\text{avg}}^{(s)}$ is given by $(p_{\text{succ,i}}^{(s)} L / R_{ii'}^{(s)})/\sigma_{\text{avg}}^{(s)}$. Given another node j transmitting to j', to satisfy time fairness, we must satisfy the conditions

$$\frac{(1-\tau_i^{(s)})}{\tau_i^{(s)}} R_{ii'}^{(s)} = \frac{(1-\tau_j^{(s)})}{\tau_j^{(s)}} R_{jj'}^{(s)}, \quad \forall i, i', j, j' \in \mathcal{N}_m, \forall s \in \overline{S}_m, \forall m \in \mathcal{M}. \tag{2.10}$$

We want to maximize the throughput T of the White-Fi network, which is given by equation (2.2), under the above defined constraints. Our optimization problem is

$$\text{Maximize: } T, \quad \text{subject to: } (2.7), (2.8), (2.9), (2.10). \tag{2.11}$$

Our variables of optimization are the sets $\overline{S}_m$ of channels assigned to cells $m \in \mathcal{M}$, the powers $P_i^{(s)}$ and medium access probabilities $\tau_i^{(s)}$ assigned to any node i on any channel s that is assigned to the node's cell. This throughput maximization is a non-linear optimization problem that is non-convex in the variables.

2.5 Solution Methodology

We propose a heuristic algorithm that carries out *Channel Assignment* followed by *Power and Access Probability Assignment.*

- *Channel Assignment:* For each White-Fi cell, assign a set of channels from those available to the cell such that adjacent cells are assigned orthogonal channels (constraint Equation (2.8)).
- *Power and Access Probability Assignment:* Assign transmit power and access prob-

Algorithm 1 Channel Assignment

Data: $\mathcal{M}, [A], S_m, \forall m \in \mathcal{M}$;
Result: $\overline{S}_m, \forall m \in \mathcal{M}$;
Set $m_1, m_2, \ldots, m_M$ such that $d(m_1) \leq d(m_2) \ldots \leq d(m_M)$, where $m_1, \ldots, m_M \in \mathcal{M}$;
while $\bigcup_{m \in \mathcal{M}} S_m \neq \phi$ **do**
  for $m = m_1, \ldots, m_M$ **do**
    if $S_m \neq \phi$ **then**
      $s^* \leftarrow \arg\max_{s \in S_m} \gamma_s$;
      $\overline{S}_m \leftarrow \overline{S}_m \cup s^*$; ▷ assign selected channel to cell
      $S_m \leftarrow S_m \setminus \{s^*\}$; ▷ remove assigned channel from list of available channels
      UpdateChannelList$(()s^*, m)$;
    end if
  end for
end while
function UpdateChannelList(s, m)
  $A_m \leftarrow \{m' \in \mathcal{M} : a_{mm'} = 1\}$; ▷ get neighboring cells of cell m
  $A'_m \leftarrow \{m' \in A_m : s \in S_{m'}\}$; ▷ get those neighboring cells with channel s in available channel list
  $S_{m'} \leftarrow S_{m'} \setminus \{s\}, \forall m' \in A'_m$;
end function

ability to every node in the White-Fi network, for each channel assigned to it, such that constraints (2.7), (2.9), and (2.10) are satisfied.

2.5.1 Channel Assignment

The channel assignment problem can be modeled as a *graph coloring problem* [86]. We abstract the White-Fi network as an undirected graph $G = (V, E)$ with set V of vertices and E of edges. The White-Fi cells in the network are the vertices of the graph and an edge exists between any two adjacent cells. We have, the set of vertices $V = \mathcal{M}$. Also, if $a_{m_1 m_2} = 1$ for cells $m_1, m_2 \in \mathcal{M}$, then an edge between them is in set E. White-Fi channels (colors) must be assigned to the cells such that no two adjacent cells are assigned the same channel (color).

We would like to exploit the fact that the presence of the TV network causes the link quality that may be achieved by nodes in cell m to differ over the set S_m of available channels. To this end, given IMAX_l is the limit on interference at TV receiver l, we quantify the achievable link quality when using channel s available in cell m as

$$\gamma_m^{(s)} = \min_{i \in \mathcal{N}_m, l \in \text{TV}_{\text{RX}}^{(s)}} \frac{\text{IMAX}_l / g_{il}}{(BN_0 + \sum_{k \in \text{TV}_{\text{TX}}^{(s)}} q_{ki} P_k^{\text{TV}})}. \tag{2.12}$$

where, the numerator IMAX_l/g_{il} is the maximum transmit power that node i in cell m can use without exceeding the limit IMAX_l on interference at l. Typically, since other nodes may transmit over the channel, the transmit power that i will be able to use will be smaller. The denominator consists of the sum of interference powers received from all TV transmitters at node i together with the receiver noise at i. Thus the ratio is the maximum SINR that node i can achieve in channel s, given TV receiver l. The channel quality $\gamma_m^{(s)}$ is therefore the smallest SINR achieved by any node on channel s in cell m, over all $l \in \text{TV}_{\text{RX}}^{(s)}$.

Solving the graph coloring problem optimally is known to be NP-complete [87]. We propose a heuristic approach that is summarized in Algorithm 1. The algorithm takes as input the set of cells $\mathcal{M}$, the adjacency matrix $[A]$, and the set of available channels S_m for each cell m. It returns the set of assigned channels for each cell. Channel assignment is performed in multiple rounds. In every round (lines 3-10), we assign channels to cells in ascending order of their degree[‡]. The degree $d(m)$ of cell m is the number of cells adjacent to it. That is $d(m) = \sum_{j \in \mathcal{M}, j \neq m} a_{mj}$. In a round, cell m is assigned a channel that has the largest $\gamma_m^{(s)}$ in the set S_m of channels available in m. The chosen channel s^* is added to the set of assigned channels $\overline{S}_m$ and removed from S_m. It is also removed from the sets of available channels of all adjacent cells of m (function UpdateChannelList in Algorithm 1). The algorithm repeats the above in the next round in case there is at least one available channel in any cell in the network (see condition in line 2).

2.5.2 Power and Access Probability Assignment

For every assigned channel s, we now assign transmit powers $P_i^{(s)}$ and access probabilities $\tau_i^{(s)}$ to all nodes i in cells that were assigned s. Let the vector of transmit powers and access probabilities be $\mathbf{P}$ and $\mathbf{\Psi}$, respectively. The elements of $\mathbf{P}$ are $P_i^{(s)}$, for any node i in $\mathcal{N}$ and channel s in $\mathcal{S}$. Likewise, the elements of $\mathbf{\Psi}$ are the $\tau_i^{(s)}$. If channel s is not assigned to a cell m, then for all nodes i in the cell $P_i^{(s)} = 0$ and $\tau_i^{(s)} = 0$. Further, $T(\mathbf{\Psi}, \mathbf{P})$ is the throughput (2.2) of the network when the access probability and transmit power vectors are $\mathbf{\Psi}$ and $\mathbf{P}$, respectively.

We split this assignment problem into the sub-problems of *Power Initialization*, *Solve for Access*, and *Solve for Power*. *Power Initialization* gives us an initial power allocation $\mathbf{P}_0$ that satisfies (2.7) and (2.9). *Solve for Access* finds the $\mathbf{\Psi}$ that solves

[‡]This method is similar to that in [88], in which the nodes obtain different *rewards* on different channels, and would like to choose channels to optimize their rewards.

Algorithm 2 Power and Access Probability Assignment

Result: $\mathbf{\Psi}^*, \mathbf{P}^*$;
1: $iter \leftarrow 0$;
2: Throughput($iter$) $\leftarrow 0$;
3: $\mathbf{P}_0 \leftarrow$ *Power Initialization*; ▷ Problem (2.13)-(2.14)
4: $\mathbf{P}^* \leftarrow \mathbf{P}_0$;
5: **while** true **do**
6: $iter \leftarrow iter + 1$;
7: $\mathbf{\Psi}^* \leftarrow$ *Solve for Access* ($\mathbf{P}^*$); ▷ Problem (2.15)
8: $\mathbf{P}^* \leftarrow$ *Solve for Power* ($\mathbf{\Psi}^*$); ▷ Problem (2.18)
9: Throughput($iter$) $\leftarrow T(\mathbf{\Psi}^*, \mathbf{P}^*)$;
10: **if** $|\text{Throughput}(iter) - \text{Throughput}(iter-1)| < \epsilon$ **then**
11: break;
12: **end if**
13: **end while**

the throughput optimization problem (2.11), for a power allocation $\mathbf{P}^*$ that satisfies (2.7) and (2.9). *Solve for Power* finds a power allocation $\mathbf{P}$ that solves (2.11), for an access probability assignment $\mathbf{\Psi}^*$ obtained from *Solve for Access*. Having found an initial power assignment, we iterate over *Solve for Access*, and *Solve for Power* till the obtained throughput (2.2) is judged (empirically) to have converged. Algorithm 2 summarizes the approach. We next describe the sub-problems.

2.5.2.1 Power Initialization

We want to initialize the vector of transmit powers such that (2.7) and (2.9) are satisfied. We formulate a simplified problem to do the same. We proceed by assuming that nodes in a cell take turns to transmit their data payloads. Further, during its turn a node i in cell m transmits the data payload of L bits *simultaneously using all* assigned channels. The resulting data payload rate is $\sum_{s\in\overline{S}_m} R_{ii'}^{(s)}$. It also transmits header and other overhead information at a rate $\overline{R}$ that is the smallest rate between any two nodes in the cell. For cell m, we have $\overline{R} = \min_{s\in\overline{S}_m, i,i'\in\mathcal{N}_m} R_{ii'}^{(s)}$, where $R_{ii'}^{(s)}$ was defined in (2.3). We will include all the time (O_{sec}) and bit (O_{bit}) overheads that were included for a node when calculating the White-Fi cell throughput T_m defined in (2.1). The time t_i taken by node i's unicast transmission (data payload and overheads) to i' is $t_i = L\left(\sum_{s\in\overline{S}_m} R_{ii'}^{(s)}\right)^{-1} + \frac{O_{bits}}{\overline{R}} + O_{sec}$. Node i transmits a data payload of L over a time of $\sum_{i\in\mathcal{N}_m} t_i$, which is the time that is required for all nodes in m to take their turn. Thus, the throughput of node i is $L/\sum_{i\in\mathcal{N}_m} t_i$ and that of cell m is $|\mathcal{N}_m|L/\sum_{i\in\mathcal{N}_m} t_i$.

The network throughput is $\sum_{m\in\mathcal{M}} |\mathcal{N}_m|L/\sum_{i\in\mathcal{N}_m} t_i$. We want to solve for the power vector that maximizes the network throughput under the sum power constraint given by (2.9), and the constraint (2.7) that limits the maximum aggregate interference. The resulting convex optimization problem is given by

$$\text{Maximize: } \sum_{m\in\mathcal{M}} |\mathcal{N}_m|L\left(\sum_{i\in\mathcal{N}_m} t_i\right)^{-1}, \tag{2.13}$$

$$\text{subject to: } (2.7),\ (2.9). \tag{2.14}$$

The optimizer is the initial estimate $\mathbf{P}_0$.

2.5.2.2 Solve for Access

We solve for a vector of access probabilities $\mathbf{\Psi}$ that maximizes the White-Fi network throughput T defined in (2.2), for a given transmit power vector $\mathbf{P}^*$ that is obtained from either *Power Initialization* or *Solve for Power*. Such power vectors satisfy constraints (2.7) and (2.9) for any $\mathbf{\Psi}$. However, the time fairness constraint (2.10) must be enforced. The optimization problem is

$$\text{Maximize: } T(\mathbf{\Psi}, \mathbf{P}^*), \quad \text{subject to: } (2.10). \tag{2.15}$$

Since the power vector is given, the problem (2.15) can be separated into maximizing throughputs $T_m^{(s)}$ for each selection of cell m and channel s, where s is a channel in the set of channels assigned to m. For every such selection of m and s, we must choose access probabilities $\tau_i^{(s)}$, for every node i in cell m, such that $T_m^{(s)}$ is maximized. For a selection of m and s, the maximization problem can be reduced to the following minimization.

$$\text{Minimize:} \frac{1-\tau_j^{(s)}}{\tau_j^{(s)}}\sigma + \left(\prod_{k=1}^{\mathcal{N}_m}\left(\frac{R_{kk'}^{(s)}}{R_{jj'}^{(s)}} + \frac{1-\tau_j^{(s)}}{\tau_j^{(s)}}\right) - \frac{1-\tau_j^{(s)}}{\tau_j^{(s)}}\right) T_{\text{col}}, \tag{2.16}$$

$$\text{subject to: } 0 \le \tau_i^{(s)} \le 1. \tag{2.17}$$

The reduction can be obtained by using the fairness constraint (2.10) to rewrite the throughput $T_m^{(s)}$ of cell m on channel s in terms of the access probability $\tau_j^{(s)}$ of node j in the cell that has the smallest data payload rate $R_{jj'}^{(s)}$ on s amongst all nodes in the cell. The problem (2.16)-(2.17) is one of convex optimization. See Appendix A for details. Solving the problem gives us the access probability $\tau_j^{(s)}$ for the chosen

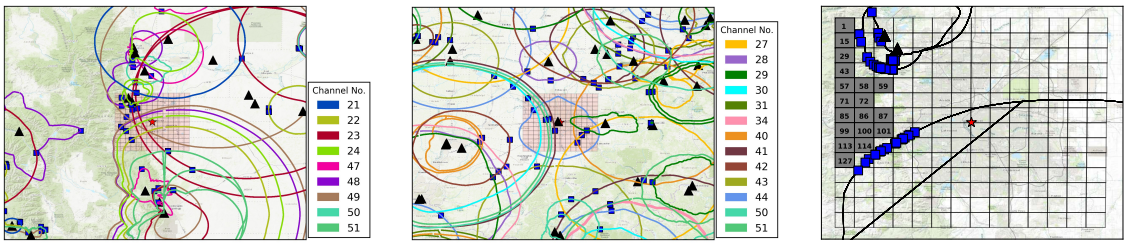

(a) (b) (c)

Figure 2.4: Illustration of White-Fi networks deployed over an area of 4900 km^2 in the cities of (a) Denver and (b) Columbus. City centers are marked by a solid star. Each White-Fi network comprises of 196 cells where each cell is spread over an area of 25 km^2. TV networks operating on different available channels are also shown. Each TV network comprises of a TV tower (solid triangle) surrounded by service contour. For each tower, we show a TV receiver (solid square) located on its service contour. The diagonal of the shown maps is of length 800 km. (c) Illustration of afflicted TV receiver (solid blue squares) locations on the service contour of TV transmitters operating on channel 24 in the city of Denver. The solid black triangles are the TV transmitters (only two are seen in the figure). Cells colored grey are the ones at which channel 24 is available. Each cell covers an area of 25 km^2.

node j. This probability together with the fairness constraint (2.10) can be used to calculate the corresponding access probabilities for all other nodes in the cell.

2.5.2.3 Solve for Power

Given a vector $\mathbf{\Psi}^*$ that solves (2.15), we solve for a vector of transmit powers that optimizes the network throughput. The optimization problem is

$$\text{Maximize: } T(\mathbf{\Psi}^*, \mathbf{P}), \quad \text{subject to: (2.7), (2.9), (2.10).} \tag{2.18}$$

The problem is non-convex in $\mathbf{P}$. To show this, observe that the equality constraint (2.10) is non-linear in $\mathbf{P}$.

2.6 Evaluation Methodology

We describe the White-Fi and TV networks that we used to evaluate our approach.

We considered hypothetical deployments of White-Fi networks over the cities of Denver and Columbus in the United States. Each White-Fi network was deployed over a square region of area 4900 km^2 that covers the city. The region was tessellated

by squares. Each square was considered to be a separate White-Fi cell. For the sake of evaluation, we considered networks tessellated by cells of areas 12.25 (square of length 3.5 km), 25, and 100 km^2. These areas correspond to, respectively, 400, 196, and 49 White-Fi cells in the White-Fi network. White-Fi networks tessellated by cells of area 25 km^2 and superimposed on the maps of the cities are shown in Figure 2.4. For a given channel availability and White-Fi node power budget, one would expect throughput to deteriorate as the cell size increases. In practice, however, large cell sizes may be desirable in sparsely populated areas with limited access to wired backhaul connectivity to the Internet.

We simulated a total of 4900 White-Fi nodes that were split equally amongst all cells. Nodes in each cell were distributed uniformly and independently of other nodes. For every node in a cell, another node in the cell was chosen randomly as the receiver of its data payload. Each node was assigned a total power budget $P_T = 0.1$ W. This is also the maximum transmit power that FCC allows personal/portable nodes operating outside the protected region of a TV transmitter. As we will show later, nodes in cells close to TV networks operating on their assigned channels are often unable to exhaust this assigned power budget. For the chosen cell sizes and power budget, cells are adjacent if and only if they are physically adjacent (have a common edge).

All cells use a bandwidth of 6 MHz centered around each assigned channel. For this bandwidth, the 802.11 timing parameters were obtained by scaling, by a factor of about 3, the parameters used in [64] for a WiFi network that uses 20 MHz of bandwidth. The length of data payload was set to $L = 8184$ bits. All link gains were calculated using a path loss propagation model with a path loss exponent of 3.

We obtained information about the TV networks in and around the region covered by the White-Fi networks from [73], [89], and [90]. Information such as TV transmitter locations, their operating channel, and transmit powers, were obtained from the FCC database [73]. Service contours were obtained from [89]. We used them to create the protected region for every TV TX by following the guidelines in [90]. We have compiled a database [2] that includes all the above information for all TV transmitters in the US. Figures 2.4a and 2.4b show the resulting TV transmitters, their service contours, and the channels in which they operate, for the cities of Denver and Columbus, respectively.

We considered only TV channels in the set $\{21, \ldots, 51\} \setminus \{37\}$ for assignment to White-Fi nodes. This is as per the FCC regulations for personal/portable devices. These channels occupy the spectrum in the $512 - 698$ MHz range. We evaluated our

approach for the following two ways of calculating channels available in a White-Fi cell.

1. *Exact* FCC: A channel may be accessed by a node only if it lies outside the protection region of all TV transmitters that operate on the channel.

2. *Relaxed*: A node may be inside the protection region. It must, however, be outside the service contour of all TV transmitters on the channel.

While location information is available for TV transmitters, it is not available for TV receivers. As a workaround, for each TV transmitter and White-Fi cell assigned the channel on which the transmitter broadcasts, we placed a TV receiver at a location deemed to be most afflicted by interference from nodes in the cell. At such a location, the constraint (2.7) on aggregate interference is binding, for a fixed limit IMAX_l for all receiver locations l.

Given the path loss propagation model, this *most afflicted* receiver must lie on the service contour of the TV transmitter. Further, we approximated the most afflicted location by calculating for each vertex of the cell the point on the contour that is closest to it. Among the four obtained points, we picked the point that has the smallest distance from its corresponding vertex as the location of the *most afflicted* receiver. The resulting locations of receivers operating on channel 24 in the city of Denver are shown in Figure 2.4c.

In all evaluation, we assumed a limit on maximum interference $\text{IMAX}_l = -140$ dB, $\forall l$. This was obtained by assuming that the TV receiver is tolerant to about 3 dB increase in its noise floor [29]. In the following section, we compare our *Proposed* approach detailed in Section 2.5 with a *Baseline* that doesn't leverage the heterogeneity in available link quality, due to the presence of the TV network, within a cell. Specifically, the *Baseline* allocates the same power and access probabilities to all nodes in a cell on an assigned channel. This allocation may, however, vary over channels assigned to the cell and over different cells. Both *Baseline* and *Proposed* use the same channel assignment.

2.7 Results

We use our proposed approach to compare the White-Fi throughput obtained in the cities of Denver and Columbus. We show how greater channel availability, i.e., a larger number of channels available over area covered by the White-Fi network, in

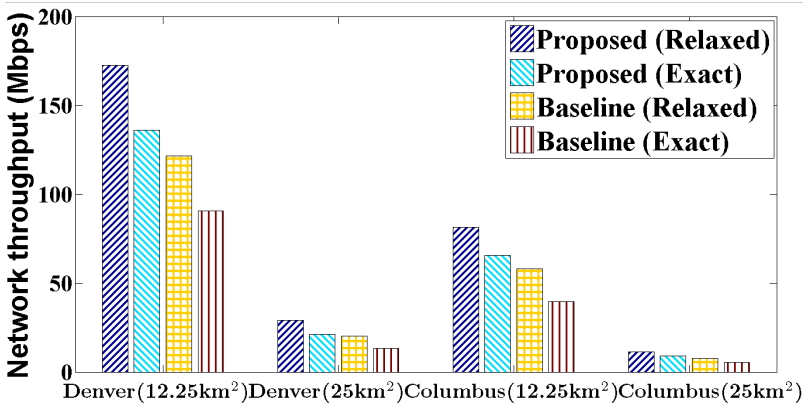

Figure 2.5: Network throughputs obtained by the *Proposed* method and the *Baseline* for the hypothetical White-Fi deployments in Denver and Columbus shown in Figure 2.4. We show throughputs for cell size choices of 12.25 and 25 km^2, and channel availability calculated using *Exact* FCC and *Relaxed*. The corresponding throughputs (kbps) for a cell size of 100 km^2 are 815, 644, 530, and 362 for Denver and 260, 197, 197, and 124 for Columbus.

Columbus than in Denver doesn't translate into larger throughput in Columbus due to a much larger presence of TV transmitters in the city. We also show the throughput achieved by the *Baseline* that makes power and access probability allocation within a cell homogeneous and hence a lot simpler in practice. We end this section with an estimate of loss of White-Fi coverage when White-Fi access is allowed by rules akin to FCC regulations, wherein *all* nodes outside a certain region around a TV transmitter are allowed to transmit using their full power budget of 100 mW.

2.7.1 Observations on Network Throughput

As a Function of Cell Size: Figure 2.5 shows the network throughputs (2.2), obtained using the *Proposed* approach and the *Baseline*, for the cities of Denver and Columbus. For both approaches and cities, the throughput reduces with increasing cell size. This is because in larger cells, White-Fi nodes are typically farther apart and see smaller link gains than in smaller cells. While the median link gains for a cell size of 12.25 km^2 are about -90 dB, they are 10 dB less for a cell size of 100 km^2. Note that, as we will see later, channel assignment is not impacted by choice of cell size.

Baseline vs. Proposed: In both the cities, for different cell sizes, and the approaches of *Exact* FCC and *Relaxed*, the *Proposed* approach leads to large throughput gains in the range of $40 - 70\%$ over *Baseline*.

Exact FCC *vs. Relaxed:* Now compare the throughputs obtained when using *Ex-*

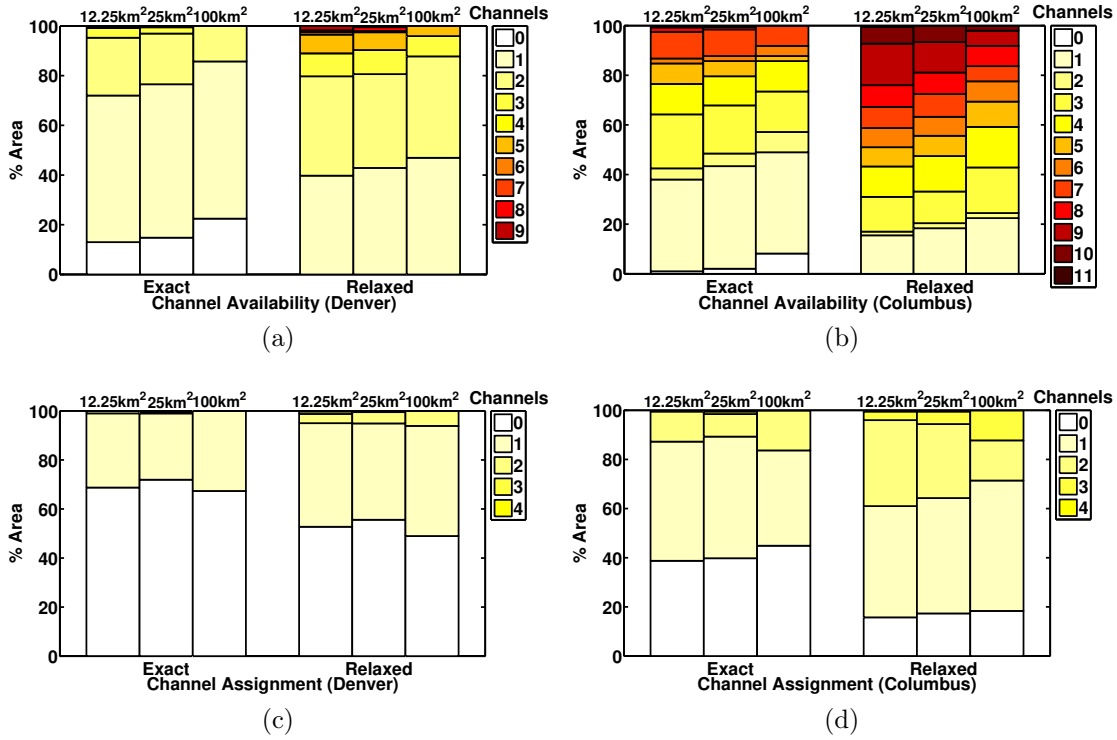

Figure 2.6: Distribution of the number of available ((a) and (b)) and assigned ((c) and (d)) channels over the White-Fi networks in Denver and Columbus.

act FCC and *Relaxed*. The choice of *Relaxed* always leads to larger throughputs. For a cell size of 12.25 km^2 and the city of Denver, *Relaxed* leads to gains in throughput of about 27% over the throughput obtained using *Exact* FCC. For Columbus, the corresponding gains are about 36%. Similar gains in throughput are seen for larger cell sizes too. In fact, even the *Baseline* approach leads to similar gains on using *Relaxed*. Recall that *Relaxed* allows White-Fi nodes to utilize a channel as long as the nodes are outside the service contour of the TV transmitter using the channel. *Exact* requires nodes to be outside the protection region. That is the channel cannot be used over a larger region. This impacts channel availability and, hence, channel assignment to White-Fi cells, and explains the observed reduction in network throughput.

Channel Availability and Assignment: Figures 2.6a and 2.6b show for the cities of Denver and Columbus, respectively, the distribution of the number of available channels over area covered by the White-Fi network. For example, for a cell size of 12.25 km^2 and the city of Columbus, when using *Relaxed*, about 20% of the area has exactly one available channel and about 60% has greater than 4 available channels. Both Denver and Columbus have a larger average number of channels

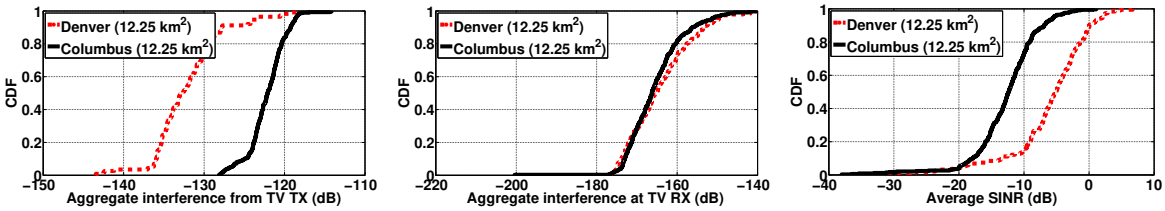

(a) (b) (c)

Figure 2.7: Empirical CDFs of (a) average aggregate interference from TV transmitters at White-Fi nodes in a cell (b) aggregate interference at afflicted TV receivers from White-Fi nodes in a cell (c) average SINR(dB) of nodes in a cell.

available per unit area when using *Relaxed*. Specifically, when using *Relaxed*, on an average Columbus has 5 available channels as opposed to 3 when using *Exact* FCC. The corresponding numbers for Denver are 2 and 1. This results in a larger number of *assigned* channels, when using *Relaxed*, as shown in Figures 2.6c and 2.6d.

In Denver, more than 50% of the area under the White-Fi network, for both *Relaxed* and *Exact* FCC, is not assigned any channel. Most cells in the remaining area are assigned a single channel. This is explained by the fact that most cells in the network have either channel 21 or 51 available and the channel assignment constraint (2.8) must be satisfied. In Columbus, a smaller region suffers from outage. Especially under *Relaxed*, greater than 80% of the region is assigned at least one channel and about 40% (for a cell size of 12.25 km^2) is assigned two or more channels. Again, the numbers of assigned channels are much smaller than the corresponding numbers of available channels. Given the assignment constraint (2.8), this is explained by the fact that the total number of unique available channels is just 12 and, as is seen in Figure 2.2a, cells with large numbers of available channels are clustered together in space.

Network Throughput of Columbus is Smaller than that of Denver: As observed above, when compared to Denver, a much smaller area of Columbus is starved of white space channels and a larger percentage of area is assigned more than one channel. However, Columbus has a network throughput (see Figure 2.5) much smaller than Denver. For example, for a cell size of 12.25 km^2 and using *Relaxed*, the throughput of Columbus, using *Proposed*, is about half that of Denver.

It turns out that while Columbus has more assigned channels on an average, it also suffers significantly more due to a high density of TV networks (see Figures 2.4a and 2.4b). Figures 2.7a-2.7c compare the impact of the TV networks on the White-Fi networks in Denver and Columbus.

Figure 2.7a shows the empirical cumulative distribution function (CDF) of aggregate interference from TV transmitters averaged over White-Fi nodes in a cell, for each of the two cities. For a cell that is assigned more than one channel, the aggregate is chosen for an assigned channel on which it is the minimum. Nodes in Columbus see aggregate interference that, on an average, is about 10 dB larger than that seen by nodes in Denver.

Figure 2.7b shows the CDF of the aggregate interference created by White-Fi nodes at afflicted TV receivers operating on the assigned channels that were selected for Figure 2.7a. The CDF(s) for both the cities are similar, which says that the TV receivers are as much of a constraint in Denver as in Columbus. This makes us believe that the reduced throughput seen by Columbus is because of excessive interference from TV transmitters. The impact of the TV transmitters and receivers is summarized in Figure 2.7c that shows the CDF of SINR of White-Fi links, for each of the two cities. Links in Columbus see SINR that is on an average about 7 dB smaller than SINR of links in Denver.

We end our observations on throughput by noting that channel availability reduces slightly with increasing cell size in Figures 2.6a and 2.6b. This is because a channel is said to be available in a cell only if it is available in all of the area of the cell. If assigned, such a channel may be used by any node in the cell. Our method of calculating availability, however, has little or no impact on assignment. In fact, the reduction in throughout with cell size is, as explained above, simply a result of smaller link gains in larger cell sizes.

2.7.2 Insights into Gains from Using the Proposed Approach

We show how the *Proposed* approach adapts to heterogeneity in link quality because of the TV network. We do so using cells that are assigned channel 21 in Denver by Algorithm 1. The cells are of size 100 km^2. Our observations remain the same qualitatively, over other cell sizes and also Columbus.

Figure 2.8b shows the aggregate interference, from each of the cells assigned channel 21, at the afflicted TV receiver in Figure 2.8a. Cells that are closer to the TV receiver are responsible for larger aggregate interference and exhaust a significant share of the interference budget that is available at the TV receiver without violation of constraint (2.7). To exemplify, the aggregate interference seen from cell 36 at the TV receiver is about -159 dB, while the interference from nodes in cell 2 is an aggregate of -143 dB.

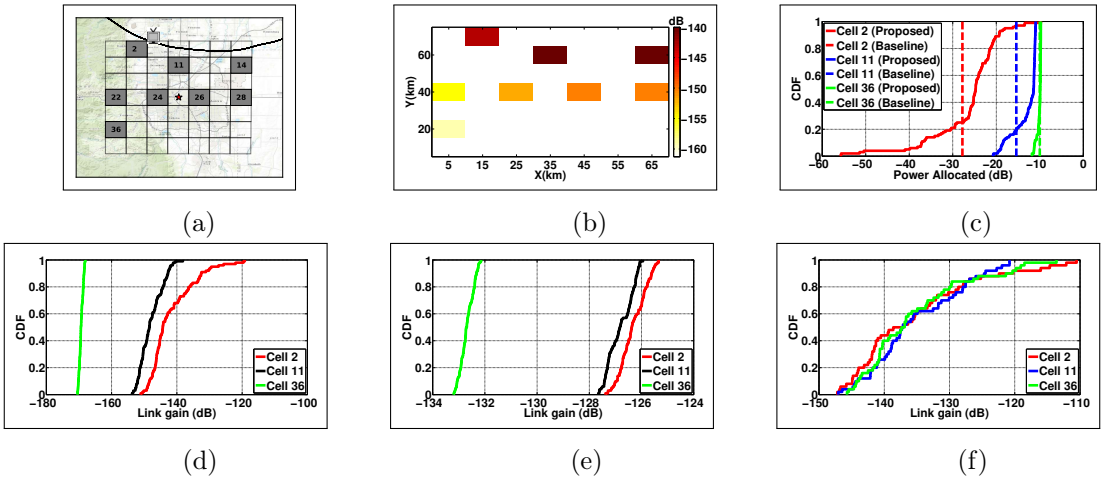

Figure 2.8: (a) We show the cells (numbered) that are assigned channel 21 in Denver. Each cell covers an area of 100km^2. An afflicted TV receiver is shown adjacent to cell 2. (b) Aggregate sum interference created at the TV receiver by each of the numbered cells. (c) CDF of the power allocated to White-Fi nodes for three cells. CDF(s) are shown for the *Proposed* method and the *Baseline*. (d) CDF of link gains between the White-Fi nodes and the TV receiver for the three cells. (e) CDF of link gains between the White-Fi nodes and the TV transmitter broadcasting on channel 21. The transmitter's service contour (black curve) is partly shown in (a). It is also the blue contour in Figure 2.4a. (f) CDF(s) of the link gains between White-Fi nodes for the three cells.

Consider the cells numbered 2, 11, and 36, in Figure 2.8a. Cell 2 is very close to the afflicted TV receiver and the service contour of the corresponding transmitter, cell 11 is farther than 2, and cell 36 is the farthest. As shown in Figure 2.8d, this results in larger link gains between the TV receiver and the White-Fi nodes in cell 2, than for nodes in cells 11 and 36. The proximity of nodes in 2 also leads to the nodes see a larger spread (greater heterogeneity) of these link gains.

Figure 2.8e shows the distribution of link gains between the White-Fi nodes and the TV transmitter. Given the large service region of the TV transmitter (radius of 70.82 km), these link gains show a limited spread of about 2 dB for each of the three cells. While the heterogeneity in gains within a cell is limited, the three cells see different gains from the transmitter. Specifically, cell 36 sees gains on an average about 6 dB smaller than cells 2 and 11. Finally, as shown in Figure 2.8f, the link gains between White-Fi nodes in the cells, as one would expect, are similarly distributed.

The varied impact of the TV network on the cells is well adapted to by the *Proposed* approach. Compare the distributions (Figure 2.8c) of power allocated to nodes in the cells by the *Proposed* and the *Baseline*. As shown earlier, nodes in cell 2 have a large spread of link gains to the TV receiver. This leads to *Proposed* allocate a

wide spread of transmit powers to them. The *Baseline*, on the other hand, allocates all the nodes in the cell the same power. Nodes in cell 11 too see a spread in power allocation on using *Proposed*. However, nodes in cell 36 are assigned powers very similar to that assigned by *Baseline*. Their being far from the TV network leads all nodes to see similar link gains to the TV receivers and also the transmitters.

This ability of *Proposed*, which we illustrated using the cells 2, 11, and 36, to adapt power allocation to link gains between nodes in a cell and between nodes and the receivers and transmitters of the TV network, explains the gains in throughput achieved by *Proposed* over *Baseline*.

2.7.3 FCC Like Regulations

Since *Proposed* and *Baseline* allocate transmit power to nodes in a manner such that interference constraints at TV receivers are not violated, nodes of a White-Fi cell can use a TV channel as long as they are outside the service contour of any TV transmitter broadcasting over the channel. FCC, instead, allows all nodes to use their full transmit power budget of 100 mW as long as they are outside the protection contour. That is FCC regulations protect the TV receiver by simply ensuring that a separation distance is maintained between the afflicted receivers and the White-Fi nodes. While this method is simple as it doesn't require per node (*Relaxed*) or per cell (*Baseline*) power allocation, it reduces the region over which white space channels may be accessed by the White-Fi nodes. Also, a fixed separation distance can't ensure that the interference constraint at the TV receivers is satisfied for different White-Fi node densities.

Figure 2.9 shows the separation distance (from the service contour) that must be maintained for the constraints on maximum interference to be satisfied at the TV receivers while all nodes in the network use a fixed power of 100 mW, as suggested by FCC regulations. Note that the protection contour provides for a separation distance of 11.1 km [90], which is not large enough for node densities larger than 1 node/km^2 for Denver and for all chosen densities for the city of Columbus. Since aggregate interference is only a function of the number of nodes in the White-Fi network, the separation distance doesn't change with cell size. In summary, the separation distance, and hence the loss of coverage in white spaces, increases with increasing node density. Also, this distance is significantly large.

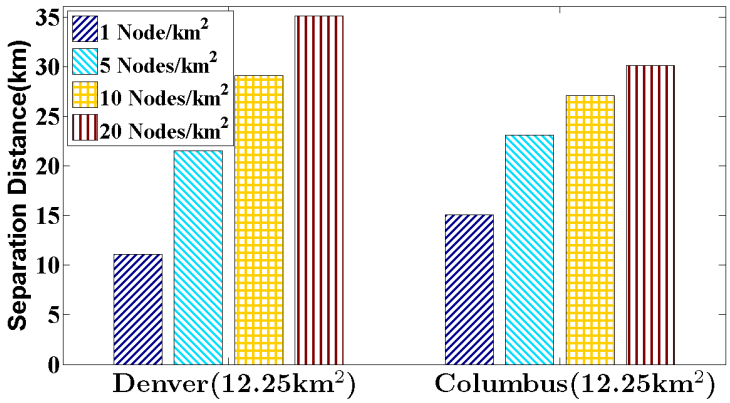

Figure 2.9: Minimum desired separation distance from the service contour for varying node densities and a cell size of 12.25 km^2. The distance for each density is an average calculated over multiple White-Fi node placements generated for the density.

2.7.4 Comments on Fairness and Overhead Rate

Impact of the time fairness constraint: We illustrate the impact of time fairness constraint (2.10) in Figure 2.10 by comparing (a) *Proposed*, (b) *Baseline*, and (c) *Proposed* without the time fairness constraint being enforced. For each cell we define fairness in time share and fairness in throughput, obtained by links within the cell. We use Jain's fairness index [91] to quantify fairness. The Jain's fairness index is defined as, $\mathcal{J} = \frac{\left(\sum_{i=1}^{n} x_i\right)^2}{n\sum_{i=1}^{n} x_i^2}$, where, n is the number of links in a cell. For computation of fairness in time share, x_i is the fraction of time $\frac{p^{(s)}_{\text{succ,i}} L/R^{(s)}_{ii'}}{\sigma^{(s)}_{\text{avg}}}$ that the i^{th} link spends on a successful transmission over channel s. For fairness in throughput, x_i is the throughput $\frac{p^{(s)}_{\text{succ,i}} L}{\sigma^{(s)}_{\text{avg}}}$ of the i^{th} link.

As shown in Figure 2.10a, the throughput obtained per cell for *Proposed* without time fairness is the largest. However, as shown in Figure 2.10b and Figure 2.10c, this approach is highly unfair both in time share and throughput. This is because in the absence of time fairness only the link with the highest link quality in a cell accesses the medium while other links are starved. For the *Baseline*, as shown in Figure 2.10a, it has the smallest per cell throughput and as shown in Figure 2.10b an average time fairness of 0.55 (obtained by averaging the fairness indices across cells on the same channel). However, as shown in Figure 2.10c, it is highly throughput fair. The high throughput fairness in *Baseline* is because it assigns the same transmit power and access probabilities to all nodes in a cell. Lastly, as shown in Figure 2.10b, the *Proposed* approach has high time fairness, but has an average throughput fairness of

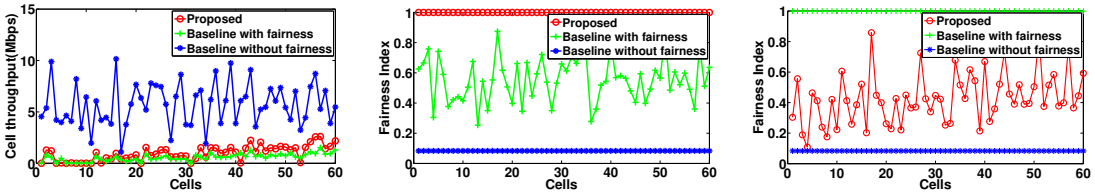

(a) (b) (c)

Figure 2.10: (a) Per cell throughput. (b) Per cell time fairness. (c) Per cell throughput fairness. Figure 2.10a-2.10b correspond to cells assigned channel 21 in the White-Fi network in Denver with each cell covering an area of 12.25 km^2. Results are shown for (i) *Proposed* (ii) *Baseline*, and (iii) *Proposed* without fairness when using *Relaxed*.

0.43 across cells on the same channel (see Figure 2.10c).

Rate allocation and access probability assignment under fairness constraint: Figures 2.11c and 2.11d respectively show the rate and access probability assignment for White-Fi nodes in cell 2. Nodes assigned larger data payload rates (because of larger SINR) have larger access probabilities. This is because we optimize under the constraint (2.10) of time fairness. For the case when all nodes have White-Fi links with the same SINR to their destinations, we confirm that all nodes transmit at the same rates and use the same access probability per channel. In fact, the access probabilities are the same as those shown via simulation and approximate analysis in [64].

Impact of Overhead Rate On Power Allocation: Recall from Section 2.3 that White-Fi nodes transmit overheads at a rate that all nodes in their cell can decode. Figure 2.11a shows the power allocation to nodes in the White-Fi cell marked 2 in Figure 2.8a. Each node in the cell is colored in accordance with power allocated to it. While the high power allocation to nodes that are far from the TV receiver (nodes closer to $(0, 0)$ in Figure 2.11a) is as per expectation given that such nodes have smaller link gains to the TV receiver and transmitter, the high power allocation to nodes that are closest to the TV receiver (nodes closer to $(10, 10)$) is explained by the requirement of the overhead rate.

This rate is determined by the nodes in the White-Fi cell that are farthest from each other. Allocating a small power to nodes that are close to TV receiver will make the rate very small, which in turn will adversely affect the throughputs of all nodes in the cell. Power allocation of the kind seen in Figure 2.11a is seen in cells in which nodes are unable to use their entire power budget because of the constraint (2.7) on aggregate interference.

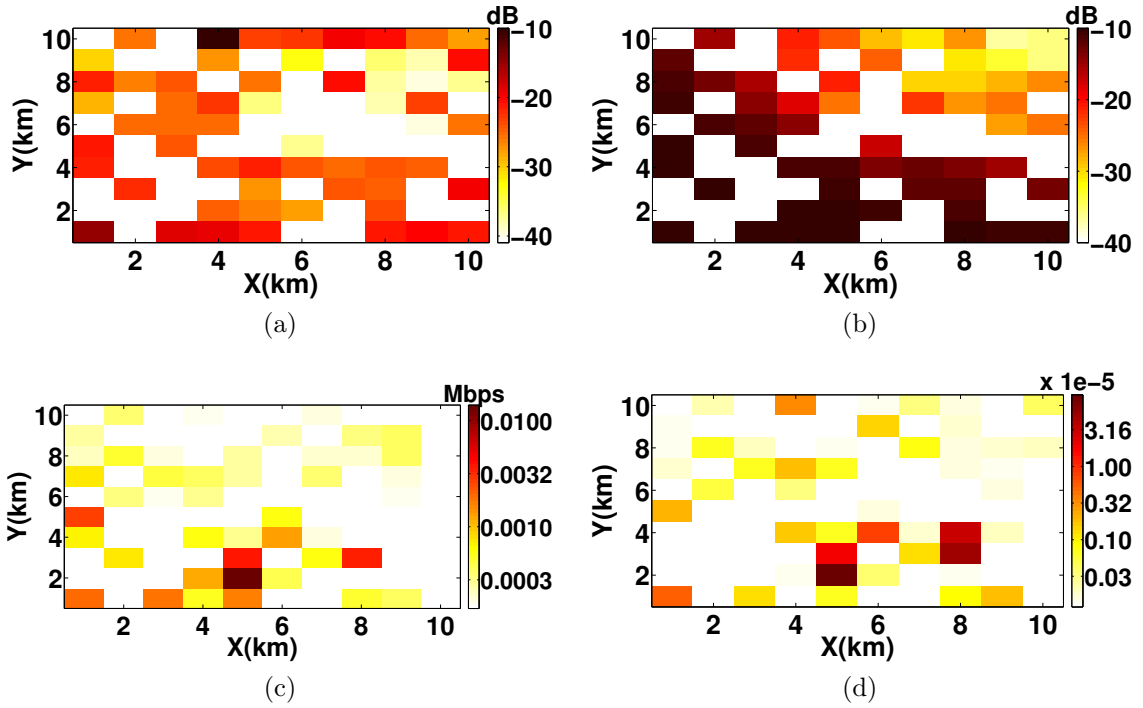

Figure 2.11: (a) Power allocated to White-Fi nodes, by the *Proposed* approach, in cell 2 of the White-Fi network shown in Figure 2.8a. (b) Power allocated as in (a), however, in the absence of overheads defined in Section 2.3. (c) Rates allocated to the nodes in cell 2, corresponding to the power allocated in (a). (d) Access probabilities assigned to the nodes in cell 2.

Figure 2.11b shows the power allocation for the cell 2 when the number of overhead bits is forced to zero. The lack of overhead bits makes the overhead rate inconsequential. The resulting power allocation follows the familiar pattern [29] of the allocation being larger at nodes that are farther from the TV receiver.

2.8 Discussion

The IEEE 802.11af standard [92] proposes an architecture that enables operation of secondary networks in compliance with a multitude of regulatory mechanisms designed to protect the TV network. Figure 2.12 shows the essential components of the architecture and how the architecture can be leveraged to execute the proposed algorithms. Each cell in the White-Fi network has a geolocation database-dependent enabling (GDD-enabling [92]) access point (AP). While the AP is like any node in the cell, unlike others, it has access to the geolocation database, which keeps updated information about the TV network. The AP of every cell in the network sends

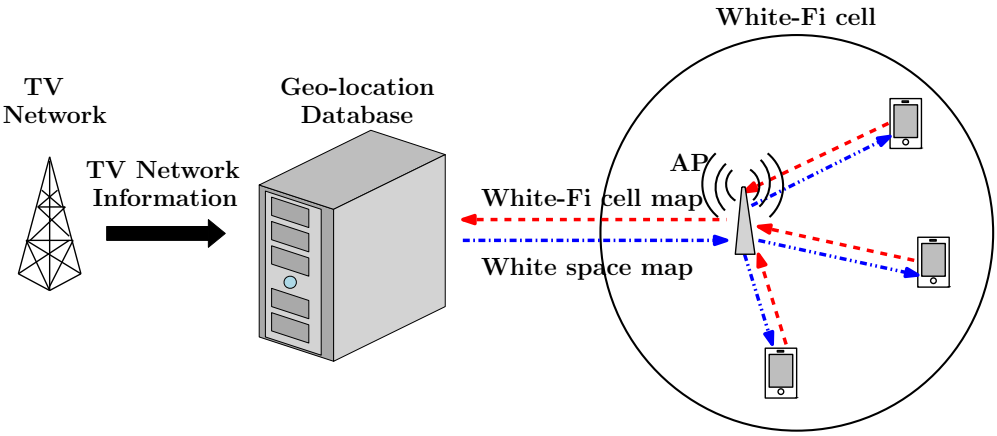

Figure 2.12: Architecture, similar to the one proposed in 802.11af , that enables a White-Fi network to use the white spaces. Each cell in the White-Fi network has an access point (AP) that facilitates communication between other nodes in the network and a geolocation database.

the *White-Fi cell map (WCM)*, which consists of the locations of all nodes in the cell, to the geolocation database. The database uses the TV network information and the location information of the nodes as an input to the proposed algorithms. The resulting channel, power, and access allocations are communicated to the access points as the *white space map (WSM)* [92], which then communicate the same to nodes in their respective cells. The time granularity at which the above exchange of messages between the geolocation database and the nodes in the White-Fi cells can take place will determine limits on mobility of the nodes in the cells and the ability of the White-Fi network to adapt to changes in the TV network.

2.9 Conclusions

We modeled the saturation throughput of a multi-cell city-wide White-Fi network, which is a WiFi like network that uses TV white spaces. Transmissions by nodes in the White-Fi network must not impair reception at TV receivers. We captured this requirement via limits on the aggregate interference that may be created by the White-Fi network at the TV receivers. We proposed a method to optimize the saturation throughput of the White-Fi network that was able to effectively leverage the heterogeneity in channel availability and quality in the white spaces. We demonstrated the efficacy of our method using hypothetical deployments of White-Fi networks amongst real TV networks in the cities of Denver and Columbus. We

compared the proposed approach with a simpler to implement baseline and also FCC-like mechanisms. Last but not the least, we outlined how the architecture proposed by 802.11af could be used to execute the proposed approach.

Chapter 3
Coexistence of Age and Throughput Optimizing Networks

3.1 Problem Overview and Motivation

The emerging IoT will require large number of (non-traditional) devices to sense and communicate information (either their own status or that of their proximate environment) to a network coordinator/aggregator or other devices. Applications include real-time monitoring for disaster management, environmental monitoring, industrial control and surveillance [43, references therein], which require timely delivery of updates to a central station. Another set of popular applications include vehicular networking for future autonomous operations where each vehicular node broadcasts a vector (e.g. position, velocity and other status information) to enable applications like collision avoidance and vehicle coordination like platooning [44].

In many scenarios, such new IoT networks will use existing (and potentially newly allocated) unlicensed bands, and hence be required to share the spectrum with incumbent networks. For instance, the U.S. FCC recently opened up the $5.85-5.925$ GHz band, previously reserved for vehicular dedicated short range communication (DSRC) for use by high throughput WiFi, leading to the need for spectrum sharing between WiFi and vehicular networks [20]. Figure 3.1 provides an illustration in which a WiFi access point communicates with its client in the vicinity of a DSRC-based vehicular network. Similarly, UAVs [43] equipped with WiFi technology used for (wide-area) environmental monitoring will need to share spectrum with regular terrestrial WiFi networks.

Networks of such IoT devices would like to optimize *freshness of status*. In our work, we measure freshness using the age of information (AoI) [45] metric. AoI is a

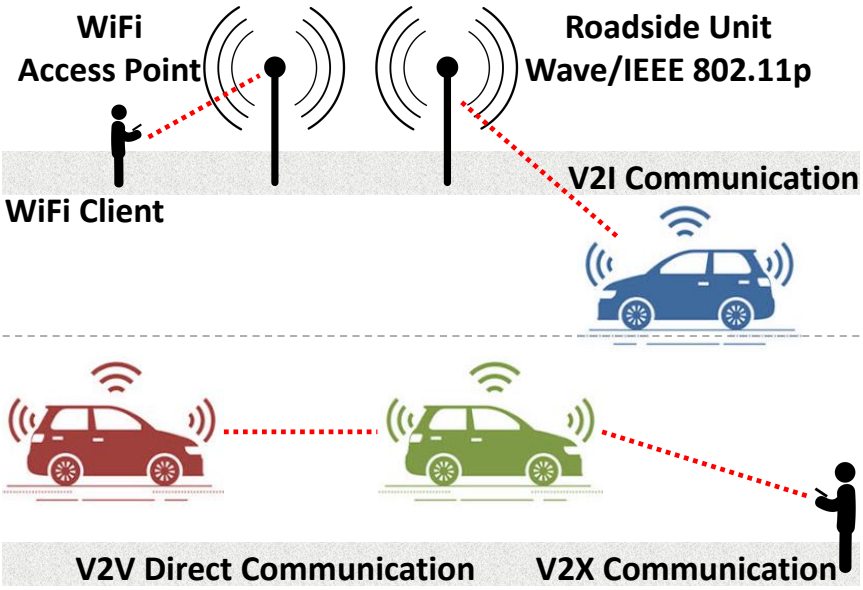

Figure 3.1: Example spectrum sharing scenario where a WiFi AP-client link shares the 5.85−5.925 GHz band with a DSRC-based vehicular network. The band previously reserved for vehicular communication was recently opened by the FCC in the US for use by WiFi (802.11ac/802.11ax) devices.

newly introduced metric that measures the time elapsed since the last update received at the destination was generated at the source [45]. It is, therefore, a destination-centric metric, and is suitable for networks that care about timely delivery of updates. A typical example is the DSRC-based vehicular network shown in Figure 3.1, where, each vehicle desires fresh status updates (position, velocity etc.) from other vehicles, to enable applications such as collision avoidance, platooning, etc. Such networks, hereafter referred to as AON will need to co-exist with traditional data networks such as WiFi designed to provide high throughput for its users, hereafter, TON. This work explores strategies for their coexistence using a repeated game theoretic approach. For symmetry, we assume that both networks use a WiFi-like CSMA/CA based medium access protocol. Each CSMA/CA slot represents a stage game whereby all networks are assumed to be selfish players that optimize their own long-run utility. While an AON wants to minimize the discounted sum average age of updates of its nodes (at a monitor), a TON wants to maximize the discounted sum average throughput.

We consider two modes of coexistence namely *competition* and *cooperation*. When *competing*, as shown in Figure 3.2a, nodes in the networks probabilistically interfere

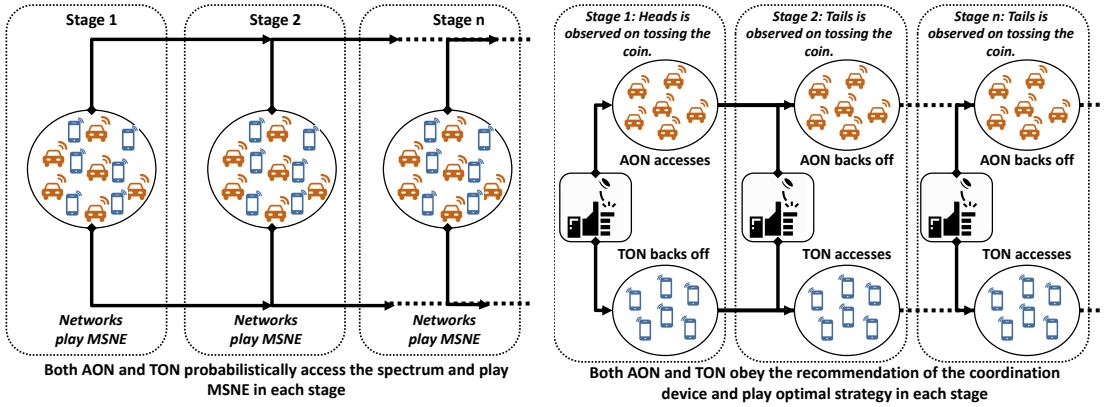

(a) Competitive Mode of Coexistence (b) Cooperative Mode of Coexistence

Figure 3.2: Illustration of different modes of coexistence. (a) Networks compete and probabilistically access the shared spectrum in every stage of the repeated game. (b) Networks cooperate and cooperation is enabled using a coordination device which tosses a coin in every stage of the repeated game and recommends the AON (resp. the TON) to access the shared spectrum when heads (resp. tails) is observed on tossing the coin and the TON (resp. the AON) to backoff.

with those of the other as they access the shared medium. We model the interaction between an AON and a TON in each CSMA/CA slot as a non-cooperative stage game and derive its MSNE. We study the evolution of the equilibrium strategy over time, when players play the MSNE in each stage of the repeated game, and the resulting utilities of the networks.

When cooperating, as shown in Figure 3.2b, a coordination device schedules the networks to access the medium such that nodes belonging to different networks don't interfere with each other. The coordination device uses a coin toss in every stage to recommend who between the AON and TON must access the medium during the slot. Similar to the competitive mode, we define the stage game and derive the optimal strategy that networks would play in a stage, if chosen by the device to access the medium.

Next, we check whether networks prefer cooperation to competition over the long run. To do so, we propose a coexistence etiquette, where, if in any stage a network doesn't follow the device's recommendation, networks revert to using the MSNE forever. In other words, if a network doesn't cooperate in any stage, networks stop cooperating and start competing in the stages thereafter. Such a strategy is commonly referred to as *grim trigger* [93] because it includes a trigger: once a network deviates from the device's recommendation, this is the trigger that causes the networks to revert their behavior to playing the MSNE forever. Figure 3.3 illustrates an

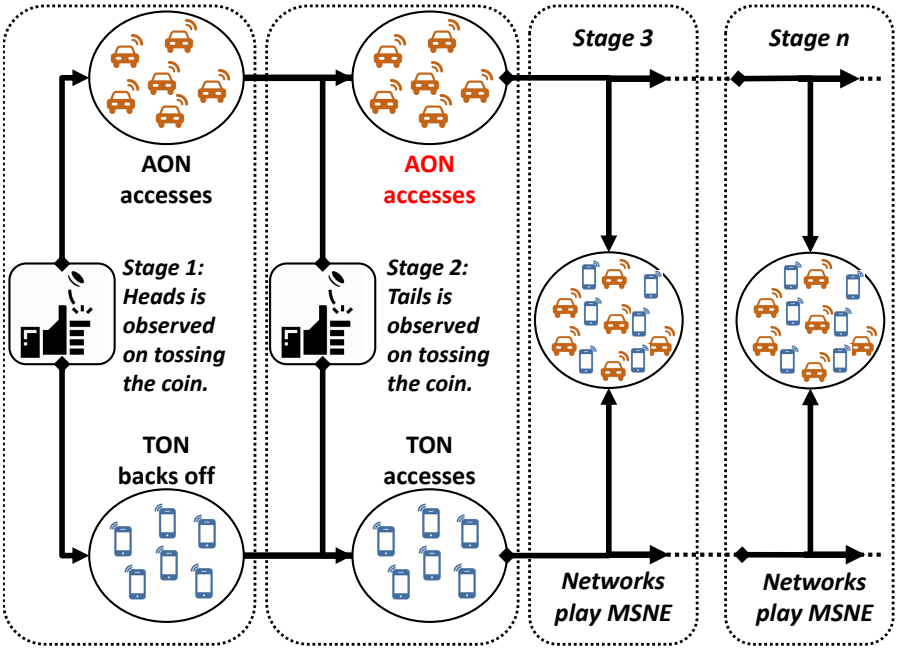

Figure 3.3: Illustration of the proposed coexistence etiquette, where, the AON disobeys the recommendation of the device in stage 2 such that the grim trigger comes into play, and the networks revert to using the MSNE from stage 3 onward.

example scenario where the coexistence etiquette is employed. The AON disobeys the recommendation of the device in stage 2 such that the grim trigger comes into play, and networks revert to using the MSNE forever from stage 3 onward. One would expect that grim trigger will have networks always obey the device if in fact they preferred cooperation to competition in the long run. We identify when networks prefer cooperation by checking if the strategy profile that results by obeying the device forms a subgame-perfect equilibrium (SPE) [93].

Further, we employ the proposed coexistence etiquette to two cases of practical interest (a) when collision slots (more than one node accesses the channel leading to all transmissions received in error) are at least as large as slots that see a successful (interference free) data transmission by exactly one node, and (b) collision slots are smaller than a successful data transmission slot. To exemplify, while the former holds when networks use the basic access mechanism defined for the 802.11 MAC [64], the latter is true for networks employing the RTS/CTS* based access mechanism [64].

We show that in both cases networks prefer cooperation when they have a small

*In RTS/CTS based access mechanism, under the assumption of perfect channel sensing, collisions occur only when RTS frames are transmitted, which are much smaller than data payload frames, and hence a collision slot is smaller than a successful transmission slot.

number of nodes. However, for large numbers of nodes, networks end up competing, as disobeying the coordination device benefits one of them. Specifically, when collision slots are at least as large as successful transmission slots, the TON finds competition more favorable, i.e., sees higher throughput, and the AON finds cooperation more beneficial, i.e., sees smaller age, whereas, when collision slots are smaller than successful transmission slot, the TON prefers cooperation and the AON competition. Our analysis shows that in the former, occasionally the AON refrains from transmitting during a slot. If competing, such slots allow the TON interference free access to the medium. If cooperating, such slots are not available to the TON. Thus, competing improves TON's payoff. In contrast, in the latter, the AON sees benefit in accessing the medium aggressively. Competition improves the AON payoff.

Next, in Section 3.2, we give an overview of related works. In Section 3.3 we describe the network model. This is followed by Section 3.4 in which we discuss the formulation of the non-cooperative stage game, derive the MSNE and analyze the repeated game with competition. In Section 3.5 we discuss the stage game with cooperation, derive the optimal strategies that networks would play and analyze the repeated game. We describe the proposed coexistence etiquette in detail in Section 3.6. Computational analysis is carried out in Section 3.7 where we describe the evaluation setup and also state our main results. We conclude in Section 3.8.

3.2 Related Work

Recent works such as [20, 94–96] studied the coexistence of DSRC based vehicular networks and WiFi. In these earlier works authors provided an in-depth study of the inherent differences between the two technologies, the coexistence challenges and proposed solutions to improve coexistence. However, the aforementioned works looked at the coexistence of DSRC and WiFi as the coexistence of two CSMA/CA based networks, with different MAC parameters, where the packets of the DSRC network took precedence over that of the WiFi network. Also, in [20, 94–96] authors proposed tweaking the MAC parameters of the WiFi network in order to protect the DSRC network. In contrast to [20, 94–96], in this work, we look at the coexistence problem as that of coexistence of networks which have equal access rights to the spectrum, use similar access mechanisms but have different objectives. While the WiFi network (TON) aims to maximize throughput and the DSRC network (AON) desires to minimize age.

In [49–53] authors employed game theory to study the behavior of nodes in wireless networks. In [49] authors studied the behavior of competing users sharing a channel using Aloha and showed the existence of equilibrium that could be reached by the users for given throughput demands. In [50] authors studied the selfish behavior of nodes in CSMA/CA networks and proposed a distributed protocol to guide multiple selfish nodes to operate at a Pareto-optimal Nash equilibrium. In [51] authors studied user behavior under a generalized slotted-Aloha protocol, identified throughput bounds for a system of cooperative users and explored the trade-off between user throughput and short-term fairness. In [52] authors analyzed Nash equilibria in multiple access with selfish nodes and in [53] authors developed a game-theoretic model called random access game for contention control and proposed a novel medium access method derived from CSMA/CA that could stabilize the network around a steady state that achieves optimal throughput.

While throughput as the payoff function has been extensively studied from the game theoretic point of view (see [49–53]), age as a payoff function has not garnered much attention yet. In [97], the authors investigated minimizing the age of status updates sent by vehicles over a carrier-sense multiple access (CSMA) network. The concept was further investigated in the context of wireless networks in [98–101]. In [46,47,54–60,71] authors studied games with age as the payoff function. In [54–57], authors studied an adversarial setting where one player aims to maintain the freshness of information updates while the other player aims to prevent this. In [58], authors formulated a two-player game to model the interaction between two transmitter-receiver pairs over an interference channel in a time-critical system. The transmitters desire freshness of their updates at their receivers and can choose their transmit power levels. The Nash and Stackelberg strategies are derived and it is shown that the Stackelberg strategy dominates the Nash strategy.

In [71] and [59], authors studied the coexistence of nodes that value timeliness of their information at others and provided insights into how competing nodes would coexist. In [71], authors proposed a one-shot multiple access game with nodes as players, where each node shares the spectrum using a CSMA/CA based access mechanism. Authors investigated the equilibrium strategies of nodes in each CSMA/CA slot when collision slots are shorter than successful transmissions, and when they are longer. They showed that when collisions are shorter, transmit is a weakly dominant strategy and when collisions are longer, no weakly dominant strategy exists and they derived a mixed strategy Nash equilibrium. In [59], authors considered a distributed competition mode where each node wants to minimize a function of its age and

transmission cost and where network information such as the number of nodes in the network and strategies is not available. Authors proposed a learning strategy for each node that determines its transmit probability in each slot and depends on the current empirical average of age and transmission cost. They showed that for a certain set of parameters the proposed strategy converges to an equilibrium that is identified as the Nash equilibrium for a suitable virtual game. In [60], authors proposed a Stackelberg game between an access point and its helpers for a wireless powered network where the helpers contribute toward charging a sensor via wireless power transfer. The access point would like to minimize a utility that includes the age of information from the sensor, the power transferred by it to charge the sensor, and the payments it makes to the helpers. The helpers benefit from the payments and bear costs that result form transferring power. In [102], authors designed a mobile edge computing enabled 5G health monitoring system for the Internet of Medical Things (IoMT) to minimize the system-wide cost, which depends on medical criticality, age of information, and energy consumption of health monitoring packets. The authors divided the IoMT into two sub-networks, i.e., intra-WBANs and beyond-WBANs. For the intra-WBANs, the authors formulated a cooperative game to minimize the cost per patient. For the beyond-WBANs, where patients can choose to analyze the information either at local devices or at edge servers, the authors formulated a non-cooperative game and analyzed the Nash equilibrium.

In earlier work [46], we proposed a game theoretic approach to study the coexistence of DSRC and WiFi, where the DSRC network desires to minimize the time-average age of information and the WiFi network aims to maximize the average throughput. We studied the one-shot game and evaluated the Nash and Stackelberg equilibrium strategies. However, the model in [46] did not capture well the interaction of networks, evolution of their respective strategies and payoffs over time, which the repeated game model allowed us to capture in [47]. In [47], via the repeated game model we were able to shed better light on the AON-TON interaction and how their different utilities distinguish their coexistence from the coexistence of utility maximizing CSMA/CA based networks. In this part of the thesis, starting with modeling the interaction between an AON and a TON using a repeated game model, we explore the possibility of cooperation between the networks.

In [103–105], authors considered the economic issues related to age in content centric networks. In [103], authors studied the economic issues related to managing age by taking sampling cost and competition between content platforms for updates into consideration and modeled the interactions between selfish platforms

as a non-cooperative game under various information scenarios. In [104], authors studied the pricing mechanism design for fresh data and proposed a time-dependent and a quantity-based pricing scheme. Authors showed that on an average optimal quantity-based pricing is more profitable and incurs less social cost than optimal time-dependent pricing. In [105], authors studied dynamic pricing that minimized the discounted age and payment over time for the content provider.

Works such as [61–63] employed repeated games in the context of coexistence. Since repeated games might foster cooperation, authors in [61] studied a punishment-based repeated game to model cooperation between multiple networks in an unlicensed band and illustrated that under certain conditions selfish behavior incur negligible losses and whether the systems cooperate or not does not have much influence on the performance. Similar to [61], authors in [62] studied a punishment-based repeated game to incorporate cooperation, however, they also proposed mechanisms to ensure user honesty. Contrary to the above works, where coexisting networks have similar objectives and the equilibrium strategies are static in each stage, networks in our work have different objectives and the equilibrium strategy of the AON, as we show later, is dynamic and evolves over stages.

3.3 Network Model

Let $\mathcal{N}_{\mathrm{A}} = \{1, 2, \ldots, \mathrm{N_A}\}$ and $\mathcal{N}_{\mathrm{T}} = \{1, 2, \ldots, \mathrm{N_T}\}$ denote the set of nodes in the AON and the TON, respectively, that contend for access to the shared wireless medium. Both AON and TON nodes use a CSMA/CA based access mechanism. For the purposes of this section, *network* represents a group of nodes that contend for the medium without reference to whether the nodes belong to the AON or the TON. Contention for the shared wireless medium results in interference between nodes which may cause transmitted packets to be decoded in error. The impact of interference is often captured either by employing the SINR model [106] or by using a collision channel model [50,53,64]. In this work, we employ a collision channel model. Specifically, we assume that all nodes can sense each other's packet transmissions and model the CSMA/CA mechanism as a slotted access mechanism. A slot in which no transmission is observed is an idle slot.In case exactly one node transmits a packet in a slot, the transmission is always successfully decoded. If more than one node transmits, none of the transmissions in the slot are successfully decoded and we say that a collision slot occurred. We assume a generate-at-will model [107,108], wherein

an AON node is able to generate a fresh update at will. The consequence of this assumption is that a node that transmits a packet always sends a freshly generated update (age 0 at the beginning of the transmission) in it.

Let p_{I} be the probability of an idle slot, which is a slot in which no node transmits. Let $p_{\mathrm{S}}^{(i)}$ be the probability of a successful transmission by node i in a slot and let p_{S} be the probability of a successful transmission in a slot. We say that node i sees a busy slot if in the slot node i doesn't transmit and exactly one other node transmits. Let $p_{\mathrm{B}}^{(i)}$ be the probability that a busy slot is seen by node i. Let p_{C} be the probability that a collision occurs in a slot. Let σ_I, σ_S and σ_C denote the lengths of an idle, successful, and collision slot, respectively.

Next, we define the throughput of a TON node and the age of an AON node, respectively, in terms of the above probabilities and slot lengths. We will detail the calculation of these probabilities for the competitive and the cooperative mode in Section 3.4 and Section 3.5, respectively.

3.3.1 Throughput of a TON node over a slot

Let the rate of transmission be fixed to r bits/sec in any slot. Define the throughput Γ_i of any TON node $i \in \mathcal{N}_{\mathrm{T}}$, in a slot as the number of bits transmitted successfully in the slot. This is a random variable with probability mass function (PMF)

$$P[\Gamma_i = \gamma] = \begin{cases} p_{\mathrm{S}}^{(i)} & \gamma = \sigma_{\mathrm{S}} r, \\ 1 - p_{\mathrm{S}}^{(i)} & \gamma = 0, \\ 0 & \text{otherwise.} \end{cases} \tag{3.1}$$

Thus the throughput $\widetilde{\Gamma}_i$ of node i is

$$\widetilde{\Gamma}_i = p_{\mathrm{S}}^{(i)} \sigma_{\mathrm{S}} r. \tag{3.2}$$

The network throughput of the TON in a slot is

$$\widetilde{\Gamma} = \frac{1}{\mathrm{N_T}} \sum_{i=1}^{\mathrm{N_T}} \widetilde{\Gamma}_i. \tag{3.3}$$

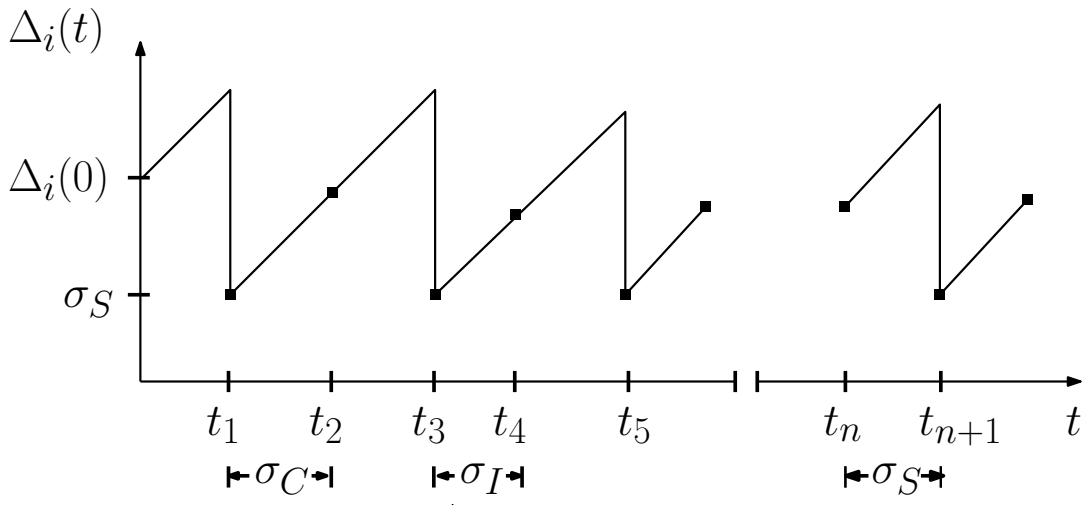

Figure 3.4: Sample path of age $\Delta_i(t)$ of AON node i's update at other AON nodes. $\Delta_i(0)$ is the initial age. A successful transmission by node i resets its age to σ_{S}. Otherwise its age increases either by σ_{S}, σ_{C} or σ_{I} depending on whether the slot is a busy slot, a collision slot or an idle slot. The time instants t_n, where, $n \in \{1, 2, \dots\}$, show the slot boundaries. In the figure, a collision slot starts at t_1, an idle slot at t_3, and a slot in which the node i transmits successfully starts at t_n. Note that while the age $\Delta_i(t)$ evolves in continuous time, stage payoffs (3.8), (3.9), (3.15), (3.16) are calculated only at slot (stage) boundaries.

We assume that the throughput in a slot is independent of that in the previous slots[†].

3.3.2 Age of an AON node over a slot

Let $u_i(t)$ be the timestamp of the most recent status update of any AON node $i \in \mathcal{N}_{\mathrm{A}}$, at other nodes in the AON at time t. The status update age of node i at AON node $j \in \mathcal{N}_{\mathrm{A}} \setminus i$ at time t is the stochastic process $\Delta_i(t) = t - u_i(t)$. Given the generate-at-will model, node i's age at any other node j either resets to σ_{S} if a successful transmission occurs or increases by σ_{I}, σ_{C} or σ_{S} at all other nodes in the AON, respectively, when an idle slot, collision slot or a busy slot occurs. Figure 3.4 shows an example sample path of the age $\Delta_i(t)$. In what follows we will drop the explicit mention of time t and let Δ_i be the age of node i's update at the end and Δ_i^- be the age at the beginning of a given slot.

The age Δ_i at the end of a slot is thus a random variable with PMF conditioned

[†]Our assumption is based on the analysis in [64], where the author assumes that at each transmission attempt, regardless of the number of retransmissions suffered, the probability of a collision seen by a packet being transmitted is constant and independent.

on age at the beginning of a slot, given by

$$P[\Delta_i = \delta_i | \Delta_i^- = \delta_i^-] = \begin{cases} p_{\mathrm{I}} & \delta_i = \delta_i^- + \sigma_{\mathrm{I}}, \\ p_{\mathrm{C}} & \delta_i = \delta_i^- + \sigma_{\mathrm{C}}, \\ p_{\mathrm{B}}^{(i)} & \delta_i = \delta_i^- + \sigma_{\mathrm{S}}, \\ p_{\mathrm{S}}^{(i)} & \delta_i = \sigma_{\mathrm{S}}, \\ 0 & \text{otherwise.} \end{cases} \tag{3.4}$$

Using (3.4), we define the conditional expected age of AON node i as

$$\begin{aligned} \widetilde{\Delta}_i &\triangleq E[\Delta_i | \Delta_i^- = \delta_i^-]. \\ &= (1 - p_{\mathrm{S}}^{(i)})\delta_i^- + (p_{\mathrm{I}}\sigma_{\mathrm{I}} + p_{\mathrm{S}}\sigma_{\mathrm{S}} + p_{\mathrm{C}}\sigma_{\mathrm{C}}). \end{aligned} \tag{3.5}$$

The network age of AON at the end of the slot, is

$$\widetilde{\Delta} = \frac{1}{\mathrm{N_A}} \sum_{i=1}^{\mathrm{N_A}} \widetilde{\Delta}_i. \tag{3.6}$$

3.4 Competition between an AON and a TON

We define a repeated game to model the competition between an AON and a TON. In every CSMA/CA slot, networks must contend for access with the goal of maximizing their expected payoff over an infinite horizon (a countably infinite number of slots). We capture the interaction in a slot as a non-cooperative stage game $G_{\mathbb{NC}}$, where $\mathbb{NC}$ stands for non-cooperation or competition and derive it's MSNE. The interaction over the infinite horizon is modeled as the stage game $G_{\mathbb{NC}}$ played repeatedly in every slot and is denoted by $G_{\mathbb{NC}}^{\infty}$. Next, we discuss the games $G_{\mathbb{NC}}$ and $G_{\mathbb{NC}}^{\infty}$ in detail.

3.4.1 Stage game

We define a parameterized strategic one-shot game [72] $G_{\mathbb{NC}} = (\mathcal{N}, (\mathcal{S}_k)_{k\in\mathcal{N}}, (u_k)_{k\in\mathcal{N}}, \widetilde{\Delta}^-)$, where $\mathcal{N}$ is the set of players, $\mathcal{S}_k$ is the set of pure strategies of player k, u_k is the payoff of player k and $\widetilde{\Delta}^-$ is the additional parameter input to the game $G_{\mathbb{NC}}$ given by $\widetilde{\Delta}^- = (1/\mathrm{N_A}) \sum_{i=1}^{\mathrm{N_A}} \Delta_i^-$.

- **Players:** The AON and the TON are the players. We denote the former by A and the latter by T. We have $\mathcal{N} = \{\mathrm{A}, \mathrm{T}\}$.

- **Strategy:** Let $\mathcal{T}$ denote transmit and $\mathcal{I}$ denote idle. For an AON comprising of $\mathrm{N_A}$ nodes, the set of pure strategies is $\mathcal{S}_\mathrm{A} \triangleq \mathbb{S}_1 \times \mathbb{S}_2 \times \cdots \times \mathbb{S}_{\mathrm{N_A}}$, where $\mathbb{S}_i = \{\mathcal{T}, \mathcal{I}\}$, $\forall i$, is the set from which an action must be assigned to node i in the AON. That is a pure strategy requires the AON to select for each node in the set $\mathcal{N}_\mathrm{A}$ either transmit or idle. Similarly, for a TON comprising of $\mathrm{N_T}$ nodes, the set of pure strategies is $\mathcal{S}_\mathrm{T} \triangleq \mathbb{S}_1 \times \mathbb{S}_2 \times \cdots \times \mathbb{S}_{\mathrm{N_T}}$.

  We allow networks to play mixed strategies. For the strategic game $G_{\mathbb{N}\mathbb{C}}$ define $\mathbf{\Phi}_k$ as the set of probability distributions over the set of strategies $\mathcal{S}_k$ of player $k \in \mathcal{N}$. A mixed strategy for player k is an element $\phi_k \in \mathbf{\Phi}_k$, where ϕ_k is a probability distribution over $\mathcal{S}_k$. For example, for an AON with $\mathrm{N_A} = 2$, the set of pure strategies is $\mathcal{S}_\mathrm{A} = \mathbb{S}_1 \times \mathbb{S}_2 = \{(\mathcal{T}, \mathcal{T}), (\mathcal{T}, \mathcal{I}), (\mathcal{I}, \mathcal{T}), (\mathcal{I}, \mathcal{I})\}$ and the probability distribution over $\mathcal{S}_\mathrm{A}$ is ϕ_A, such that $\phi_\mathrm{A}(s_\mathrm{A}) \geq 0$ for all $s_\mathrm{A} \in \mathcal{S}_\mathrm{A}$ and $\sum_{s_\mathrm{A} \in \mathcal{S}_\mathrm{A}} \phi_\mathrm{A}(s_\mathrm{A}) = 1$.

  Note that the size of the set of pure strategies increases exponentially in the number of nodes in the networks. In general, a PMF would assign probabilities to each pure strategy in the set. That is the number of probabilities that a PMF must capture increases exponentially in the number of nodes in the network. Given this seemingly intractable space of PMF(s), in this work, we restrict ourselves to the space of PMF(s) such that the mixed strategies of the AON are a function of τ_A and that of the TON are a function of τ_T, where τ_A and τ_T, are the probabilities with which nodes in an AON and a TON, respectively, attempt transmission in a slot[‡]. As a result, the probability distribution for an AON with $\mathrm{N_A} = 2$, parameterized by τ_A, is $\phi_\mathrm{A}(\tau_\mathrm{A}) = \{\tau_\mathrm{A}^2, \tau_\mathrm{A}(1-\tau_\mathrm{A}), (1-\tau_\mathrm{A})\tau_\mathrm{A}, (1-\tau_\mathrm{A})^2\}$. Similarly, for a TON with $\mathrm{N_T} = 2$, the probability distribution parameterized by τ_T, is $\phi_\mathrm{T}(\tau_\mathrm{T}) = \{\tau_\mathrm{T}^2, \tau_\mathrm{T}(1-\tau_\mathrm{T}), (1-\tau_\mathrm{T})\tau_\mathrm{T}, (1-\tau_\mathrm{T})^2\}$.

- **Payoffs:** We have $\mathrm{N_T}$ throughput optimizing nodes that attempt transmission with probability τ_T and $\mathrm{N_A}$ age optimizing nodes that attempt transmission with probability τ_A. As defined in Section 3.3, for the non-cooperative game $G_{\mathbb{N}\mathbb{C}}$, let $p_{\mathrm{I},\mathbb{N}\mathbb{C}}$ be the probability of an idle slot, $p_{\mathrm{S},\mathbb{N}\mathbb{C}}$ be the probability of a successful

[‡]This forces all nodes in a given network to have the same probability of access. We believe that this is not too restrictive, given that nodes in a network have no intrinsic reason (they all can sense each other's transmissions and those of nodes in the other network, and contribute equally to the network payoff) to experience a different access to the shared spectrum.

transmission in a slot, $p^{(i)}_{\mathrm{S},\mathbb{NC}}$ be the probability of a successful transmission by node i, $p^{(i)}_{\mathrm{B},\mathbb{NC}}$ be the probability of a busy slot seen by node i and $p_{\mathrm{C},\mathbb{NC}}$ be the probability of collision. We have

$$p_{\mathrm{I},\mathbb{NC}} = (1-\tau_{\mathrm{A}})^{\mathrm{N_A}}(1-\tau_{\mathrm{T}})^{\mathrm{N_T}}, \tag{3.7a}$$

$$p_{\mathrm{S},\mathbb{NC}} = \mathrm{N_A}\tau_{\mathrm{A}}(1-\tau_{\mathrm{A}})^{(\mathrm{N_A}-1)}(1-\tau_{\mathrm{T}})^{\mathrm{N_T}} + \mathrm{N_T}\tau_{\mathrm{T}}(1-\tau_{\mathrm{T}})^{(\mathrm{N_T}-1)}(1-\tau_{\mathrm{A}})^{\mathrm{N_A}}, \tag{3.7b}$$

$$p^{(i)}_{\mathrm{S},\mathbb{NC}} = \begin{cases} \tau_{\mathrm{A}}(1-\tau_{\mathrm{A}})^{(\mathrm{N_A}-1)}(1-\tau_{\mathrm{T}})^{\mathrm{N_T}}, & \forall i \in \mathcal{N}_{\mathrm{A}}, \\ \tau_{\mathrm{T}}(1-\tau_{\mathrm{T}})^{(\mathrm{N_T}-1)}(1-\tau_{\mathrm{A}})^{\mathrm{N_A}}, & \forall i \in \mathcal{N}_{\mathrm{T}}, \end{cases} \tag{3.7c}$$

$$p^{(i)}_{\mathrm{B},\mathbb{NC}} = \begin{cases} (\mathrm{N_A}-1)\tau_{\mathrm{A}}(1-\tau_{\mathrm{A}})^{(\mathrm{N_A}-1)}(1-\tau_{\mathrm{T}})^{\mathrm{N_T}} \\ \quad + \mathrm{N_T}\tau_{\mathrm{T}}(1-\tau_{\mathrm{T}})^{(\mathrm{N_T}-1)}(1-\tau_{\mathrm{A}})^{\mathrm{N_A}}, & \forall i \in \mathcal{N}_{\mathrm{A}}, \\ (\mathrm{N_T}-1)\tau_{\mathrm{T}}(1-\tau_{\mathrm{T}})^{(\mathrm{N_T}-1)}(1-\tau_{\mathrm{A}})^{\mathrm{N_A}} \\ \quad + \mathrm{N_A}\tau_{\mathrm{A}}(1-\tau_{\mathrm{A}})^{(\mathrm{N_A}-1)}(1-\tau_{\mathrm{T}})^{\mathrm{N_T}}, & \forall i \in \mathcal{N}_{\mathrm{T}}, \end{cases} \tag{3.7d}$$

$$p_{\mathrm{C},\mathbb{NC}} = 1 - p_{\mathrm{S},\mathbb{NC}} - p_{\mathrm{I},\mathbb{NC}}. \tag{3.7e}$$

Note that the probabilities (3.7a)-(3.7e) are independent of the specific node i being considered. This is expected given the mixed strategies we are considering. The probabilities (3.7a)-(3.7e) can be substituted in (3.1)-(3.2) and (3.4)-(3.5), respectively, to calculate the network throughput (3.3) and age (3.6). We use these to obtain the stage payoffs $u^{\mathrm{T}}_{\mathbb{NC}}$ and $u^{\mathrm{A}}_{\mathbb{NC}}$ of the TON and the AON. They are

$$u^{\mathrm{T}}_{\mathbb{NC}}(\tau_{\mathrm{A}},\tau_{\mathrm{T}}) = \widetilde{\Gamma}(\tau_{\mathrm{A}},\tau_{\mathrm{T}}), \tag{3.8}$$

$$u^{\mathrm{A}}_{\mathbb{NC}}(\tau_{\mathrm{A}},\tau_{\mathrm{T}}) = -\widetilde{\Delta}(\tau_{\mathrm{A}},\tau_{\mathrm{T}}). \tag{3.9}$$

The networks would like to maximize their payoffs.

3.4.2 Mixed Strategy Nash Equilibrium

Figure 3.5 shows the payoff matrix when each network consists of a single node. As stated in [109], every finite non-cooperative game has a MSNE. For the game $G_{\mathbb{NC}}$ defined in Section 3.4.1, a mixed-strategy profile $\phi^*(\tau^*_{\mathrm{A}},\tau^*_{\mathrm{T}}) = (\phi^*_{\mathrm{A}}(\tau^*_{\mathrm{A}}),\phi^*_{\mathrm{T}}(\tau^*_{\mathrm{T}}))$ is a Nash equilibrium [109], if $\phi^*_A(\tau^*_{\mathrm{A}})$ and $\phi^*_T(\tau^*_{\mathrm{T}})$ are the best responses of player A and

A(AON) \ T(TON)	$\mathcal{T}$	$\mathcal{I}$
$\mathcal{T}$	$-(\Delta_1(0)+\sigma_C), 0$	$-\sigma_S, 0$
$\mathcal{I}$	$-(\Delta_1(0)+\sigma_S), \sigma_S r$	$-(\Delta_1(0)+\sigma_I), 0$

(a)

A(AON) \ T(TON)	$\mathcal{T}$	$\mathcal{I}$
$\mathcal{T}$	$-2.02, 0$	$-1.01, 0$
$\mathcal{I}$	$-2.02, 1.01$	$-1.02, 0$

(b)

Figure 3.5: Payoff matrix for the game $G_{\mathbb{NC}}$ when the AON and the TON have one node each. We use negative payoffs for player A (AON), since it desires to minimize age. (a) Shows the payoff matrix with slot lengths and AoI value at the end of the stage 1. (b) Shows the payoff matrix obtained by substituting $\sigma_{\mathrm{S}} = \sigma_{\mathrm{C}} = 1+\beta$, $\sigma_{\mathrm{I}} = \beta$[§], $\Delta_1(0) = 1+\beta$ and $\beta = 0.01$. $(\mathcal{T},\mathcal{T})$, $(\mathcal{T},\mathcal{I})$ and $(\mathcal{I},\mathcal{T})$ are the pure strategy Nash equilibria.

player T, to their respective opponents' mixed strategy. We have

$$u^{\mathrm{T}}_{\mathbb{NC}}(\phi^*_A, \phi^*_T) \geq u^{\mathrm{T}}_{\mathbb{NC}}(\phi^*_A, \phi_T), \quad \forall \phi_T \in \mathbf{\Phi}_T,$$
$$u^{\mathrm{A}}_{\mathbb{NC}}(\phi^*_A, \phi^*_T) \geq u^{\mathrm{A}}_{\mathbb{NC}}(\phi_A, \phi^*_T), \quad \forall \phi_A \in \mathbf{\Phi}_A,$$

where, $\phi^*(\tau^*_{\mathrm{A}}, \tau^*_{\mathrm{T}}) \in \mathbf{\Phi}$ and $\mathbf{\Phi} = \mathbf{\Phi}_T \times \mathbf{\Phi}_A$ is the profile of mixed strategy. Recall that the probability distributions $\phi_{\mathrm{A}}(\tau_{\mathrm{A}})$ and $\phi_{\mathrm{T}}(\tau_{\mathrm{T}})$ are parameterized by τ_{A} and τ_{T}, respectively. Proposition 1 gives the MSNE.

Proposition 1. *The mixed strategy Nash equilibrium for the game $G_{\mathbb{NC}}$ is given by the probabilities τ^*_{A} and τ^*_{T}, where*

$$\tau^*_{\mathrm{A}} = \begin{cases} \dfrac{(1-\tau^*_{\mathrm{T}})(\widetilde{\Delta}^- - \mathrm{N_A}(\sigma_S - \sigma_I)) + \mathrm{N_A N_T}\tau^*_{\mathrm{T}}(\sigma_S - \sigma_C)}{(1-\tau^*_{\mathrm{T}})\mathrm{N_A}(\widetilde{\Delta}^- + (\sigma_I - \sigma_C) - \mathrm{N_A}(\sigma_S - \sigma_C)) + \mathrm{N_A N_T}\tau^*_{\mathrm{T}}(\sigma_S - \sigma_C)} & \widetilde{\Delta}^- > \Theta_{th}, \\ 1 & \widetilde{\Delta}^- \leq \Theta_{th} \ \& \ \Theta_{th} = \Theta_{th,1}, \\ 0 & \widetilde{\Delta}^- \leq \Theta_{th} \ \& \ \Theta_{th} = \Theta_{th,0}. \end{cases} \tag{3.10a}$$

$$\tau^*_{\mathrm{T}} = \frac{1}{\mathrm{N_T}}. \tag{3.10b}$$

where, $\Theta_{th} = \max\{\Theta_{th,0}, \Theta_{th,1}\}$, $\Theta_{th,0} = \mathrm{N_A}(\sigma_S - \sigma_I) - \frac{\mathrm{N_A N_T}\tau^*_{\mathrm{T}}(\sigma_S - \sigma_C)}{(1-\tau^*_{\mathrm{T}})}$ *and* $\Theta_{th,1} = \mathrm{N_A}(\sigma_S - \sigma_C)$.

Proof: The proof is given in Appendix B.1. ■

[§]We set the values of σ_{I}, σ_{S} and σ_{C} based on the analysis of CSMA slotted Aloha in [110], where the authors assume that idle slots have a duration β and all data packets have unit length. Nodes

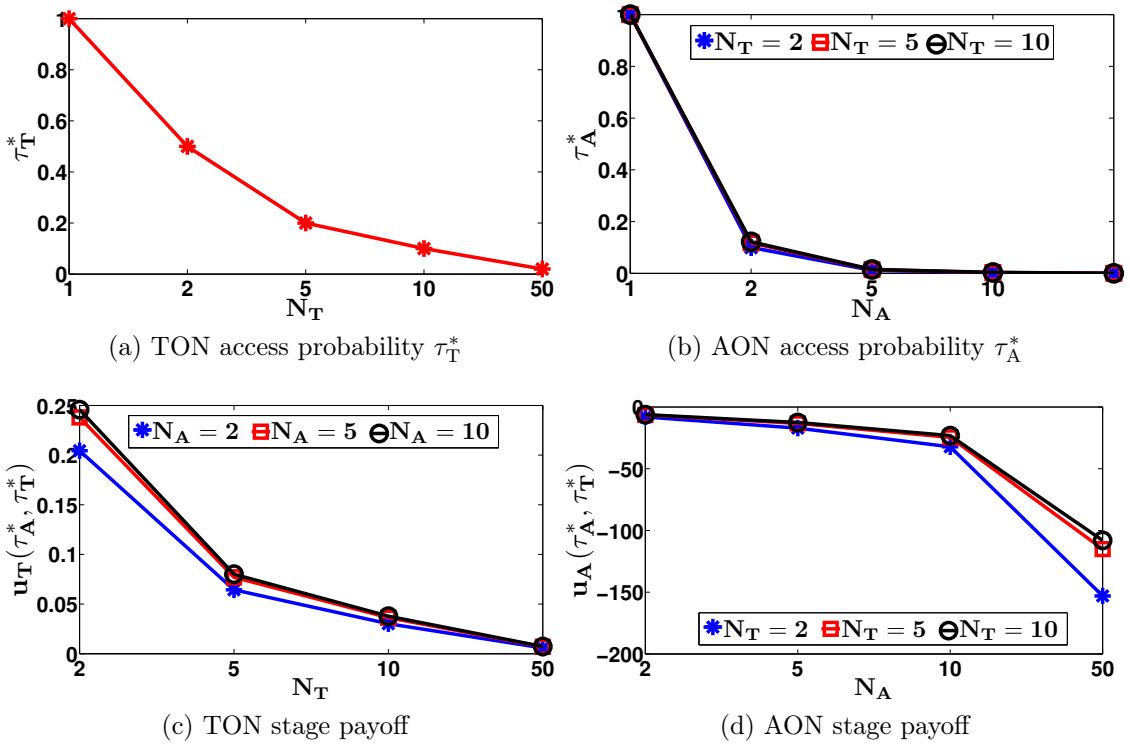

(a) TON access probability τ_{T}^*

(b) AON access probability τ_{A}^*

(c) TON stage payoff

(d) AON stage payoff

Figure 3.6: Access probabilities and stage payoff of the TON and the AON for different selections of $\mathrm{N_T}$ and $\mathrm{N_A}$ when networks choose to play the MSNE. The stage payoff corresponds to $\widetilde{\Delta}^- = \Theta_{\mathrm{th},0} + \sigma_{\mathrm{S}}$, $\sigma_{\mathrm{S}} = 1 + \beta$, $\sigma_{\mathrm{C}} = 2(1 + \beta)$, $\sigma_{\mathrm{I}} = \beta$ and $\beta = 0.01$.

Note in (3.10a) and (3.10b) that τ_{A}^* is a function of network age $\widetilde{\Delta}^-$ observed at the beginning of the slot and the number of nodes in both the networks, whereas, τ_{T}^* is only a function of number of nodes in the TON. The threshold value Θ_{th} can either take a value equal to $\Theta_{\mathrm{th},0}$ or $\Theta_{\mathrm{th},1}$. For instance, when $\mathrm{N_A} = 1$, $\mathrm{N_T} = 1$, and $\sigma_{\mathrm{S}} > \sigma_{\mathrm{C}}$, the threshold value Θ_{th} is equal to $\Theta_{\mathrm{th},1} = (\sigma_{\mathrm{S}} - \sigma_{\mathrm{C}})$ resulting in $\tau_{\mathrm{A}}^* = 1$. In contrast, when $\sigma_{\mathrm{S}} < \sigma_{\mathrm{C}}$ for $\mathrm{N_A} = 1$, $\mathrm{N_T} = 1$ the threshold value Θ_{th} is equal to $\Theta_{\mathrm{th},0} = \infty$, and since $\widetilde{\Delta}^- \leq \infty$, τ_{A}^* in this case is 0. Note that while the parameter τ_{T}^* corresponding to the TON is equal to 1, for all selections of σ_{C}, the AON chooses $\tau_{\mathrm{A}}^* = 1$ when $\sigma_{\mathrm{S}} > \sigma_{\mathrm{C}}$, and $\tau_{\mathrm{A}}^* = 0$ when $\sigma_{\mathrm{S}} < \sigma_{\mathrm{C}}$. This is because when $\sigma_{\mathrm{S}} < \sigma_{\mathrm{C}}$ the increase in age due to a successful transmission by the TON, which has $\tau_{\mathrm{T}}^* = 1$, is less than that due to a collision that would have happened if the AON chose $\tau_{\mathrm{A}} = 1$. We discuss this in detail in Section 3.4.3.

A distinct feature of the stage game is the effect of *self-contention* and *competition*

in CSMA are allowed to transmit only after detecting an idle slot, i.e., each successful transmission slot and collision slot is followed by an idle slot. Hence, $\sigma_{\mathrm{S}} = \sigma_{\mathrm{C}} = (1 + \beta)$.

on the network utilities[¶]. We define self-contention as the impact of nodes within one's own network and competition as the impact of nodes in the other network, respectively, on the network utilities. Figure 3.6 shows the affect of self-contention and competition on the access probabilities and stage payoffs. We choose $\widetilde{\Delta}^{-} = \Theta_{\text{th},0}+\sigma_{\text{S}}$ as it gives $\tau_{\text{A}}^{*} \in (0,1)$ (see (3.10a)). As shown in Figure 3.6a and Figure 3.6c, while the access probability τ_{T}^{*} for the TON is independent of the number of nodes in the AON, the payoff of the TON increases as the number of nodes in the AON increase. Intuitively, since increase in the number of AON nodes results in increase in competition, the payoff of the TON should decrease. However, the payoff of the TON increases. For example, for $\text{N}_{\text{T}} = 2$, as shown in Figure 3.6c, the payoff of the TON increases from 0.2044 to 0.2451 as N_{A} increases from 2 to 10. This increase is due to increase in self-contention within the AON which forces it to be conservative. Specifically, as shown in Figure 3.6b, the access probability τ_{A}^{*} decreases with increase in the number of nodes in the AON. For $\text{N}_{\text{T}} = 2$, τ_{A}^{*} decreases from 1 to 0.0001 as N_{A} increases from 1 to 50. This benefits the TON. Similarly as shown in Figure 3.6d, as the number of TON nodes increases the payoff of the AON improves, since the access probability of the TON decreases (see Figure 3.6a).

For the game $G_{\mathbb{NC}}$, when $\sigma_{\text{S}} = \sigma_{\text{C}}$, the access probabilities τ_{A}^{*} and τ_{T}^{*} are shown in Corollary 1. They are independent of the number of nodes in the other network and their access probability.

Corollary 1. *Proof.* The MSNE for the game $G_{\mathbb{NC}}$ when $\sigma_{\text{S}} = \sigma_{\text{C}}$ is obtained using (3.10a) and is given by

$$\tau_{\text{A}}^{*} = \begin{cases} \frac{\text{N}_{\text{A}}(\sigma_{\text{I}}-\sigma_{\text{S}})+\widetilde{\Delta}^{-}}{\text{N}_{\text{A}}(\sigma_{\text{I}}-\sigma_{\text{C}}+\widetilde{\Delta}^{-})} & \widetilde{\Delta}^{-} > \text{N}_{\text{A}}(\sigma_{\text{S}}-\sigma_{\text{I}}), \\ 0 & \text{otherwise .} \end{cases} \tag{3.11a}$$

$$\tau_{\text{T}}^{*} = \frac{1}{\text{N}_{\text{T}}}. \tag{3.11b}$$

This equilibrium strategy of each network is also its dominant strategy. ■

3.4.2.1 Discussion on Mixed Strategy Nash Equilibrium (MSNE)

The TON is indifferent to the presence of the AON. This can be explained via the stage payoff of the TON given in (3.8). Clearly, the τ_{T} that optimizes the stage payoff is independent of N_{A} and τ_{A}.

[¶]We had earlier observed self-contention and competition in [46] where we considered an alternate one-shot game and in [47] where we studied a repeated game with competing networks.

One may intuitively explain the indifference of the TON to the presence of the AON in the following manner. Recall that the TON has a node see a throughput greater than zero only when the node transmits successfully. Else, it sees a throughput of 0. We argue that there is no reason for the TON to choose an access probability, in the presence of the AON, that is larger than what it would choose in the absence of the AON. This is because a larger probability of access will simply increase the self-contention amongst the nodes in the TON resulting in a larger fraction of collision slots and a smaller throughput. In case, in the presence of the AON, the TON chooses a smaller probability of access than it would choose in the absence of the AON, its nodes will have fewer successful transmissions and will see more idle slots and slots with successful transmissions by nodes in the AON. In summary, choosing neither a larger nor a smaller probability of access than it would choose in the absence of the AON increases the throughput of the TON.

Now consider the AON. It sees an increase in age in an idle slot, in a slot that sees a successful transmission by the TON and a collision slot. A reduction occurs only if a node in the AON transmits successfully. The equilibrium access probability of the AON is impacted by the relative lengths of the collision and successful transmission slots. When collision slots are shorter than successful transmission slots, the AON picks larger probabilities of access and in fact may have its nodes transmit with probability 1 (see (3.10a)). On the other hand, when the successful transmission slots are smaller than collision slots, the AON picks relatively smaller probabilities of access and in fact may have its nodes access with probability 0 (3.10a).

The above choices by the AON capture the fact that when competing for spectrum, the AON adapts to the TON by pushing for either relatively more collision slots or more slots in which a node in the TON transmits successfully. For when the length of a collision slot is equal to that of a successful transmission slot, the AON is indifferent to any change in the balance between collision slots and slots in which a node in the TON transmits successfully that occurs due to the competing TON. The access probability of the AON becomes independent of $\mathrm{N_T}$ and τ_{T}.

3.4.3 Repeated game

We consider an infinitely repeated game, defined as $G^{\infty}_{\mathbb{N}\mathbb{C}}$, in which the one-shot game $G_{\mathbb{N}\mathbb{C}}$, where, players play the MSNE (3.10), is played in every stage (slot) $n \in \{1, 2, \dots\}$. We consider perfect monitoring [72], i.e., at the end of each stage,

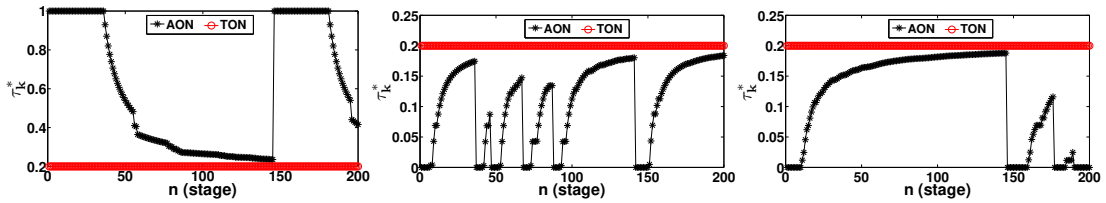

(a) (b) (c)

Figure 3.7: Illustration of per stage access probability τ_k^* ($k \in \{\mathrm{A}, \mathrm{T}\}$) of the AON and the TON when (a) $\sigma_{\mathrm{C}} = 0.1\sigma_{\mathrm{S}}$, (b) $\sigma_{\mathrm{C}} = \sigma_{\mathrm{S}}$, and (c) $\sigma_{\mathrm{C}} = 2\sigma_{\mathrm{S}}$. The results correspond to $\mathrm{N_A} = 5, \mathrm{N_T} = 5, \sigma_{\mathrm{S}} = 1 + \beta, \sigma_{\mathrm{I}} = \beta$ and $\beta = 0.01$.

all players observe the action profile chosen by every other player.[‖]

The essential components of a repeated game include the state variable, the constituent stage game, and the state transition function. For our repeated game $G^{\infty}_{\mathbb{NC}}$, the state at the beginning of stage n consists of the ages $\Delta_i^-(n)$, at the beginning of the stage, for all nodes i in the AON. The constituent stage game is the parameterized game $G_{\mathbb{NC}}$, defined in Section 3.4.1, where in the parameter at the beginning of stage n is $\widetilde{\Delta}^-(n)$, which, given the definition in Section 3.4.1, is $\widetilde{\Delta}^-(n) = (1/\mathrm{N_A}) \sum_{i=1}^{\mathrm{N_A}} \Delta_i^-(n)$. The ages $\Delta_i(n)$ at the end of a stage (which is also the beginning of the next stage), given $\Delta_i^-(n)$, for all nodes i in the AON, are governed by the conditional PMF given in Equation (3.4), with the probabilities of idle, successful transmission, busy, and collision in the equation, appropriately substituted by those corresponding to the stage game and given by (3.7a)-(3.7e).

Player k's average discounted payoff for the game $G^{\infty}_{\mathbb{NC}}$, where $k \in \mathcal{N}$ is

$$\mathrm{U}^k_{\mathbb{NC}} = E_{\phi}\left\{(1-\alpha)\sum_{n=1}^{\infty}\alpha^{n-1}u^{k,n}_{\mathbb{NC}}(\phi)\right\}, \tag{3.12}$$

where, the expectation is taken with respect to the strategy profile ϕ, $u^{k,n}_{\mathbb{NC}}(\phi)$ is player k's payoff in stage n and $0 < \alpha < 1$ is the discount factor. A discount factor α closer to 1 means that the player values not only the stage payoff but also the impact of its action on payoffs in the future, i.e., the player is far-sighted, whereas α closer to 0 means that the player is myopic and values more the payoffs in the short-term. By substituting (3.8) and (3.9) in (3.12), we can obtain the average discounted payoffs $\mathrm{U}^{\mathrm{T}}_{\mathbb{NC}}$ and $\mathrm{U}^{\mathrm{A}}_{\mathbb{NC}}$, of the TON and the AON, respectively.

[‖]We leave the study of more realistic assumptions of imperfect and private monitoring to future work.

Figure 3.7 shows the access probabilities of the TON and the AON for the repeated game $G^{\infty}_{\mathbb{N}\mathbb{C}}$ when (a) $\sigma_{\mathrm{S}} > \sigma_{\mathrm{C}}$ (see Figure 3.7a), and (b) $\sigma_{\mathrm{S}} \leq \sigma_{\mathrm{C}}$ (see Figure 3.7b for $\sigma_{\mathrm{S}} = \sigma_{\mathrm{C}}$ and Figure 3.7c for $\sigma_{\mathrm{S}} < \sigma_{\mathrm{C}}$). We set $\mathrm{N_A} = \mathrm{N_T} = 5$, $\sigma_{\mathrm{S}} = 1 + \beta$, $\sigma_{\mathrm{C}} = 0.1\sigma_{\mathrm{S}}$, $\sigma_{\mathrm{I}} = \beta$ and $\beta = 0.01$. As a result, the threshold values in (3.10a), i.e., $\Theta_{\mathrm{th},0}$ and $\Theta_{\mathrm{th},1}$, are -0.6812 and 4.5450, respectively, resulting in $\Theta_{\mathrm{th}} = \max\{\Theta_{\mathrm{th},0}, \Theta_{\mathrm{th},1}\} = 4.5450$. Since $\Theta_{\mathrm{th},0}$ and $\Theta_{\mathrm{th},1}$ are independent of $\widetilde{\Delta}^{-}$ (see Proposition 1), the resulting Θ_{th} is constant across all stages of the repeated game $G^{\infty}_{\mathbb{N}\mathbb{C}}$. As a result, as shown in Figure 3.7a, $\tau^{*}_{\mathrm{A}} = 1$ for $n \in \{1, \ldots, 36\}$ since $\widetilde{\Delta}^{-}(n) < 4.5450$. However, for $n = 37$, $\tau^{*}_{\mathrm{A}} = 0.9295$ as $\widetilde{\Delta}^{-}(37) = 4.6460$ exceeds the threshold value. Similarly, the threshold value in (3.11a), when $\sigma_{\mathrm{S}} = \sigma_{\mathrm{C}}$, is $\mathrm{N_A}(\sigma_{\mathrm{S}} - \sigma_{\mathrm{I}}) = 5$. As a result, as shown in Figure 3.7b, nodes in the AON access the medium with $\tau^{*}_{\mathrm{A}} \in (0, 1)$ in any stage n only if the network age in the $(n-1)^{th}$ stage exceeds the threshold value, i.e., $\widetilde{\Delta}^{-}(n) > 5$, otherwise $\tau^{*}_{\mathrm{A}} = 0$.

Note that when $\sigma_{\mathrm{S}} \leq \sigma_{\mathrm{C}}$, nodes in the AON as shown in Figure 3.7b and Figure 3.7c, occasionally refrain from transmission, i.e., choose $\tau^{*}_{\mathrm{A}} = 0$ during a stage. In contrast, when $\sigma_{\mathrm{S}} > \sigma_{\mathrm{C}}$, nodes in the AON as shown in Figure 3.7a, often access the medium aggressively, i.e., with $\tau^{*}_{\mathrm{A}} = 1$ during a stage. Such a behavior of nodes in the AON is due to the presence of the TON. As the length of the collision slot decreases, the impact of collision on the age of the AON reduces. If nodes in the AON choose to refrain from transmission, the network age of the AON will depend on the events – successful transmission, collision or idle slot, happening in the TON. Whereas if nodes in the AON choose to transmit aggressively with $\tau^{*}_{\mathrm{A}} = 1$, the network age of the AON would only be impacted by the collision slot. For instance, for a coexistence scenario with $\mathrm{N_A} = \mathrm{N_T} = 5$, $\sigma_{\mathrm{S}} = 1 + \beta$, $\sigma_{\mathrm{C}} = 0.1\sigma_{\mathrm{S}}$, $\sigma_{\mathrm{I}} = \beta$, $\beta = 0.01$ and $\widetilde{\Delta}^{-} = \sigma_{\mathrm{S}}$, if $\tau_{\mathrm{A}} = 0$, the network age in the stage computed using (3.6) is 1.4535, whereas, if $\tau_{\mathrm{A}} = 1$, the network age is 1.1110. As a result, due to reduced impact of collision, nodes in the AON choose to contend with the TON aggressively for the medium and transmit with $\tau^{*}_{\mathrm{A}} = 1$ during a stage.

3.5 Cooperation between an AON and a TON

Consider the 2-player one-shot game shown in Figure 3.5b. Figure 3.8 shows the convex hull of payoffs corresponding to it. The game has three pure strategy Nash Equilibria, i.e., $(\mathcal{T}, \mathcal{T})$, $(\mathcal{T}, \mathcal{I})$ and $(\mathcal{I}, \mathcal{T})$, which have, respectively either both the networks transmit or one of them transmit and the other idle. The corresponding

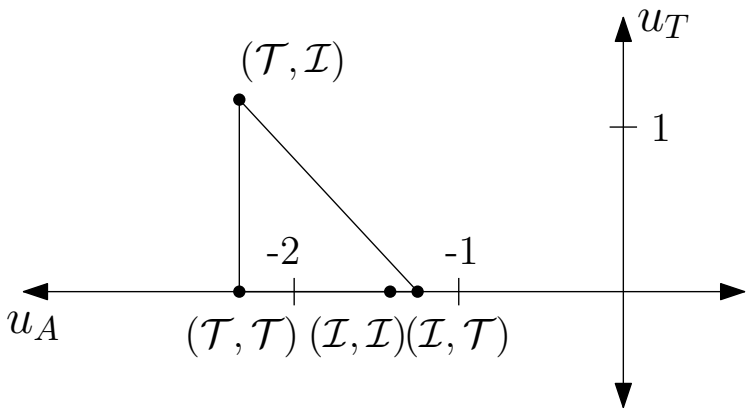

Figure 3.8: The convex hull of payoffs for the 2-player one-shot game (see Figure 3.5b).

MSNE is given by $\phi_A^* = \{1, 0\}$ and $\phi_T^* = \{1, 0\}$. Both networks transmit with probability 1.

Now suppose that the players cooperate and comply with the recommendation of a coordination device, which probabilistically chooses exactly one player to transmit in a stage while the other idles. Say, with probability 0.5, the device recommends that the AON transmit and the TON stays idle. The expected payoff of the AON is $(-1.01 \times \mathrm{P_R} - 2.02 \times (1 - \mathrm{P_R})) = -1.515$ and that of the TON is $(0 \times \mathrm{P_R} + 1.01 \times (1 - \mathrm{P_R})) = 0.505$, which is more than what the AON and the TON would get had they played the MSNE, i.e., payoffs of -2.02 and 0, respectively.

As exemplified above, players may achieve higher expected one-shot payoffs in case they cooperate instead of playing the MSNE (3.10). This motivates us to enable cooperation between an AON and a TON in the following manner. Consider a coordination device that picks one of the two networks to access ($\mathcal{A}$) the shared spectrum in a slot and the other to backoff ($\mathcal{B}$). To arrive at its recommendation, the device tosses a coin with the probability of obtaining heads ($\mathbb{H}$), $\mathrm{P}[\mathbb{H}] = \mathrm{P_R}$, and that of obtaining tails ($\mathbb{T}$), $\mathrm{P}[\mathbb{T}] = (1 - \mathrm{P_R})$. In case $\mathbb{H}$ (resp. $\mathbb{T}$) is observed on tossing the coin, the device picks the AON (resp. the TON) to access the medium and the TON (resp. the AON) to backoff.

Note that the recommendation of the device allows interference free access to the spectrum and eliminates the impact of competition, leaving the networks to deal with self-contention alone. We assume that the probabilities and the recommendations are common knowledge to players.

3.5.1 Stage game with cooperating networks

We begin by modifying the network model defined in Section 3.3 to incorporate the recommendation of the coordination device $\mathrm{P_R}$. The AON gets interference free access to the spectrum with probability $\mathrm{P_R}$. Let $\widehat{\tau}_A$ denote the optimal probability with which nodes in the AON must attempt transmission, given that the AON has access to the spectrum. Let $\widehat{\tau}_T$ be the corresponding probability for the TON.

Proposition 2. *The optimal strategy of the one-shot game $G_{\mathbb{C}}$ when networks cooperate is given by the probabilities $\widehat{\tau}_A$ and $\widehat{\tau}_T$. We have*

$$\widehat{\tau}_A = \begin{cases} \dfrac{\widetilde{\Delta}^- - \mathrm{N_A}(\sigma_S - \sigma_I)}{\mathrm{N_A}(\widetilde{\Delta}^- + (\sigma_I - \sigma_C) - \mathrm{N_A}(\sigma_S - \sigma_C))} & \widetilde{\Delta}^- > \Theta_{th}, \\ 1 & \widetilde{\Delta}^- \leq \Theta_{th} \ \& \ \Theta_{th} = \Theta_{th,1}, \\ 0 & \widetilde{\Delta}^- \leq \Theta_{th} \ \& \ \Theta_{th} = \Theta_{th,0}. \end{cases} \tag{3.13a}$$

$$\widehat{\tau}_T = \frac{1}{\mathrm{N_T}}. \tag{3.13b}$$

where, $\Theta_{th} = \max\{\Theta_{th,0}, \Theta_{th,1}\}$, $\Theta_{th,0} = \mathrm{N_A}(\sigma_S - \sigma_I)$ *and* $\Theta_{th,1} = \mathrm{N_A}(\sigma_S - \sigma_C)$.

Proof: The proof is given in Appendix B.2. ■

Similar to (3.10a), the optimal strategy $\widehat{\tau}_A$ (3.13a) of the AON in any slot is a function of $\widetilde{\Delta}^-$. However, in contrast to (3.10a), in the cooperative game $G_{\mathbb{C}}$, $\widehat{\tau}_A$ is a function of only the number of nodes in its own network, since the coordination device allows networks to access the medium one at a time. Similarly, the optimal strategy $\widehat{\tau}_T$ of the TON is a function of the number of nodes in its own network and is independent of the number of nodes in the AON. The threshold value Θ_{th} can either take a value equal to $\Theta_{\mathrm{th,0}}$ or $\Theta_{\mathrm{th,1}}$. For instance, when $\mathrm{N_A} = 1$, $\mathrm{N_T} = 1$ and $\sigma_{\mathrm{S}} = \sigma_{\mathrm{C}}$, Θ_{th} takes a value equal to $\Theta_{\mathrm{th,0}} = (\sigma_{\mathrm{S}} - \sigma_{\mathrm{I}})$, and the AON chooses $\widehat{\tau}_A = 1$.

As defined in Section 3.3, for the cooperative game $G_{\mathbb{C}}$, let $p_{\mathrm{I},\mathbb{C}}$ be the probability of an idle slot, $p_{\mathrm{S},\mathbb{C}}$ be the probability of a successful transmission in a slot, $p^{(i)}_{\mathrm{S},\mathbb{C}}$ be the probability of a successful transmission by node i, $p^{(i)}_{\mathrm{B},\mathbb{C}}$ be the probability of a

busy slot and $p_{\mathrm{C},\mathbb{C}}$ be the probability of collision. We have

$$p_{\mathrm{I},\mathbb{C}} = \mathrm{P_R}(1-\widehat{\tau}_A)^{\mathrm{N_A}} + (1-\mathrm{P_R})(1-\widehat{\tau}_T)^{\mathrm{N_T}}, \tag{3.14a}$$

$$p_{\mathrm{S},\mathbb{C}} = \mathrm{P_R N_A}\widehat{\tau}_A(1-\widehat{\tau}_A)^{(\mathrm{N_A}-1)} + (1-\mathrm{P_R})\mathrm{N_T}\widehat{\tau}_T(1-\widehat{\tau}_T)^{(\mathrm{N_T}-1)}, \tag{3.14b}$$

$$p^{(i)}_{\mathrm{S},\mathbb{C}} = \begin{cases} \mathrm{P_R}\widehat{\tau}_A(1-\widehat{\tau}_A)^{(\mathrm{N_A}-1)}, \ \ \forall i \in \mathcal{N}_{\mathrm{A}}, \\ (1-\mathrm{P_R})\widehat{\tau}_T(1-\widehat{\tau}_T)^{(\mathrm{N_T}-1)}, \ \ \forall i \in \mathcal{N}_{\mathrm{T}}, \end{cases} \tag{3.14c}$$

$$p^{(i)}_{\mathrm{B},\mathbb{C}} = \begin{cases} (1-\mathrm{P_R})\mathrm{N_T}\widehat{\tau}_T(1-\widehat{\tau}_T)^{(\mathrm{N_T}-1)} \\ \quad + \mathrm{P_R}(\mathrm{N_A}-1)\widehat{\tau}_A(1-\widehat{\tau}_A)^{(\mathrm{N_A}-1)}, \ \ \forall i \in \mathcal{N}_{\mathrm{A}}, \\ (1-\mathrm{P_R})(\mathrm{N_T}-1)\widehat{\tau}_T(1-\widehat{\tau}_T)^{(\mathrm{N_T}-1)} \\ \quad + \mathrm{P_R N_A}\widehat{\tau}_A(1-\widehat{\tau}_A)^{(\mathrm{N_A}-1)}, \ \ \forall i \in \mathcal{N}_{\mathrm{T}}, \end{cases} \tag{3.14d}$$

$$p_{\mathrm{C},\mathbb{C}} = 1 - p_{\mathrm{S},\mathbb{C}} - p_{\mathrm{I},\mathbb{C}}. \tag{3.14e}$$

By substituting (3.14a)-(3.14e) in (3.3) and (3.6), we can obtain the stage utility of the TON and the AON, defined in (3.8) and (3.9), respectively, when networks cooperate.

$$u^{\mathrm{T}}_{\mathbb{C}}(\widehat{\tau}_A, \widehat{\tau}_T) = \widetilde{\Gamma}(\widehat{\tau}_A, \widehat{\tau}_T), \tag{3.15}$$

$$u^{\mathrm{A}}_{\mathbb{C}}(\widehat{\tau}_A, \widehat{\tau}_T) = -\widetilde{\Delta}(\widehat{\tau}_A, \widehat{\tau}_T). \tag{3.16}$$

The networks would like to maximize their payoffs.

3.5.2 Cooperating vs. competing in a stage

We consider when both networks find cooperation to be beneficial over competition in a stage game. That is $u^{\mathrm{T}}_{\mathbb{C}}(\widehat{\tau}_A, \widehat{\tau}_T) \geq u^{\mathrm{T}}_{\mathbb{N}\mathbb{C}}(\tau^*_{\mathrm{A}}, \tau^*_{\mathrm{T}})$ and $u^{\mathrm{A}}_{\mathbb{C}}(\widehat{\tau}_A, \widehat{\tau}_T) \geq u^{\mathrm{A}}_{\mathbb{N}\mathbb{C}}(\tau^*_{\mathrm{A}}, \tau^*_{\mathrm{T}})$. Using these inequalities, we determine the range of $\mathrm{P_R}$, given in (3.17), over which networks prefer cooperation in the stage game.

$$\frac{\begin{array}{r}\widetilde{\Delta}^- p^{(i)}_{\mathrm{S},\mathbb{N}\mathbb{C}} - (\sigma_I - \sigma_C)(p_{\mathrm{I},\mathbb{N}\mathbb{C}} - (1-\widehat{\tau}_T)^{N_T}) \\ - (\sigma_S - \sigma_C)(p_{\mathrm{S},\mathbb{N}\mathbb{C}} - N_T\widehat{\tau}_T(1-\widehat{\tau}_T)^{N_T-1})\end{array}}{\begin{array}{l}\widetilde{\Delta}^-\widehat{\tau}_A(1-\widehat{\tau}_A)^{N_A-1} - (\sigma_I - \sigma_C)((1-\widehat{\tau}_A)^{N_A} - (1-\widehat{\tau}_T)^{N_T}) \\ \quad - (\sigma_S - \sigma_C)(N_A\widehat{\tau}_A(1-\widehat{\tau}_A)^{N_A-1} - N_T\widehat{\tau}_T(1-\widehat{\tau}_T)^{N_T-1})\end{array}} \leq P_R \leq 1 - (1-\tau^*_A)^{N_A} \tag{3.17}$$

Consider when $\mathrm{N_A} = 1$ and $\mathrm{N_T} = 1$. The range of $\mathrm{P_R}$ in (3.17) depends on the length σ_{C} of the collision slot. As discussed earlier in Section 3.4, when networks compete and $\sigma_{\mathrm{S}} \geq \sigma_{\mathrm{C}}$, $\tau^*_{\mathrm{A}} = \tau^*_{\mathrm{T}} = 1$, whereas, when $\sigma_{\mathrm{S}} < \sigma_{\mathrm{C}}$, $\tau^*_{\mathrm{A}} = 0$ and $\tau^*_{\mathrm{T}} = 1$. In

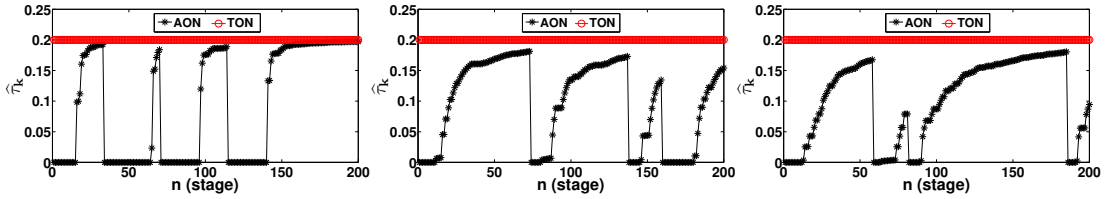

(a) (b) (c)

Figure 3.9: Illustration of per stage access probability $\widehat{\tau}_k$ ($k \in \{\mathrm{A}, \mathrm{T}\}$) of the AON and the TON, as a function of the stage, obtained from an independent run when (a) $\sigma_{\mathrm{C}} = 0.1\sigma_{\mathrm{S}}$, (b) $\sigma_{\mathrm{C}} = \sigma_{\mathrm{S}}$, and (c) $\sigma_{\mathrm{C}} = 2\sigma_{\mathrm{S}}$. The results correspond to $\mathrm{N_A} = 5, \mathrm{N_T} = 5, \sigma_{\mathrm{S}} = 1 + \beta, \sigma_{\mathrm{I}} = \beta, \beta = 0.01$ and $\mathrm{P_R} = 0.5$.

contrast, when $\mathrm{N_A} = 1$ and $\mathrm{N_T} = 1$, irrespective of the length of collision slot σ_{C}, when networks cooperate, $\widehat{\tau}_A = 1$ and $\widehat{\tau}_T = 1$. As a result, cooperation is beneficial for $\mathrm{P_R} \in [0, 1]$ when $\sigma_{\mathrm{S}} \geq \sigma_{\mathrm{C}}$, and only beneficial at $\mathrm{P_R} = 0$ when $\sigma_{\mathrm{S}} < \sigma_{\mathrm{C}}$. This is because when $\sigma_{\mathrm{S}} \geq \sigma_{\mathrm{C}}$, while networks see a collision when they compete, they see a successful transmission if they choose to cooperate. In contrast, when $\sigma_{\mathrm{S}} < \sigma_{\mathrm{C}}$, since the AON chooses not to access the medium when networks compete, the TON gets a competition free access to the medium and hence always sees a successful transmission. As a result, the TON suffers from cooperation unless the AON doesn't get a chance to access the medium, which is when $\mathrm{P_R} = 0$. Note that while the analysis for $\mathrm{N_A} = 1$ and $\mathrm{N_T} = 1$ as discussed above, is simple, (3.17) becomes intractable for $\mathrm{N_A} > 1$ and $\mathrm{N_T} > 1$. Hence, we resort to computational analysis and show that as the number of nodes increases, when $\sigma_{\mathrm{S}} \leq \sigma_{\mathrm{C}}$, cooperation is beneficial only at $\mathrm{P_R} = 0$, whereas, when $\sigma_{\mathrm{S}} > \sigma_{\mathrm{C}}$, it is beneficial only for higher values of $\mathrm{P_R}$, i.e., for $\mathrm{P_R}$ close to 1. We discuss this in detail in Section 3.7.

3.5.3 Repeated game with cooperating networks

We define an infinitely repeated game $G_{\mathbb{C}}^{\infty}$ given the coordination device $\mathrm{P_R}$. The course of action followed by the networks is: Players in the beginning of stage n receive a recommendation $\mathrm{R}_n \in \{\mathbb{H}, \mathbb{T}\}$ from the coordination device $\mathrm{P_R}$ and, following on the recommendation, the players either access ($\mathcal{A}$) the shared spectrum or backoff ($\mathcal{B}$). We define the strategy profile of players in stage n as

$$a_n = \begin{cases} (\mathcal{A}, \mathcal{B}) & \text{if } \mathrm{R}_n = \mathbb{H}, \\ (\mathcal{B}, \mathcal{A}) & \text{if } \mathrm{R}_n = \mathbb{T}. \end{cases} \tag{3.18}$$

The evolution of ages, as the players go from playing one stage to another in the repeated game, is governed by the conditional PMF given in Equation (3.4), with the probabilities of idle, successful transmission, busy, and collision in the equation, appropriately substituted by those corresponding to the cooperation stage game and given by (3.14a)-(3.14e).

We have player k's average discounted payoff for the game $G^{\infty}_{\mathbb{C}}$, where $k \in \mathcal{N}$ is

$$\mathrm{U}^{k}_{\mathbb{C}} = E_{\phi}\left\{(1-\alpha)\sum_{n=1}^{\infty}\alpha^{n-1}u^{k,n}_{\mathbb{C}}(\phi)\right\}, \tag{3.19}$$

where the expectation is taken with respect to the strategy profile ϕ, $u^{k,n}_{\mathbb{C}}(\phi)$ is player k's payoff in stage n and $0 < \alpha < 1$ is the discount factor. By substituting (3.15) and (3.16) in (3.19), we can obtain the average discounted payoffs $\mathrm{U}^{\mathrm{T}}_{\mathbb{C}}$ and $\mathrm{U}^{\mathrm{A}}_{\mathbb{C}}$, of the TON and the AON, respectively.

Figure 3.9 shows the access probabilities of TON and AON for the repeated game $G^{\infty}_{\mathbb{C}}$ when (a) $\sigma_{\mathrm{S}} > \sigma_{\mathrm{C}}$ (Figure 3.9a), and (b) when $\sigma_{\mathrm{S}} \leq \sigma_{\mathrm{C}}$ (Figure 3.9b corresponds to $\sigma_{\mathrm{S}} = \sigma_{\mathrm{C}}$ and Figure 3.9c corresponds to $\sigma_{\mathrm{S}} < \sigma_{\mathrm{C}}$) . The results correspond to AON-TON coexistence with $\mathrm{N_A} = \mathrm{N_T} = 5$ and $\mathrm{P_R} = 0.5$.

In contrast to the repeated game in Section 3.4.3 where nodes in the AON choose to occasionally access the medium aggressively when $\sigma_{\mathrm{S}} > \sigma_{\mathrm{C}}$, in the repeated game $G^{\infty}_{\mathbb{C}}$, nodes in the AON as shown in Figure 3.9, irrespective of the length of collision slot, never access the medium aggressively, i.e., do not choose $\widehat{\tau}_A = 1$, instead they occasionally refrain from transmission and choose $\widehat{\tau}_A = 0$ during a stage. This is due to the absence of competition from the TON when networks obey the recommendation of the coordination device. In the absence of competition from the TON when the coordination device chooses the AON to access and the TON to backoff, if the nodes in the AON refrain from transmission (that is access with $\widehat{\tau}_A = 0$), the age of the AON only increases by the length of an idle slot. Since the benefit of idling surpasses that of contending aggressively, nodes in the AON occasionally choose to refrain from transmission irrespective of the relative length of collision slot.

3.6 The Coexistence Etiquette

The networks are selfish players and may find it beneficial to disobey the recommendations of the device. We enforce a coexistence etiquette which ensures that in the long run the networks either cooperate or compete forever. We have the net-

works adopt the grim trigger strategy [93] in case the other network doesn't follow the recommendation of the coordination device in a certain stage of the repeated game. Specifically, if in any stage, a network does not comply with the recommendation of the coordination device, the networks play their respective Nash equilibrium strategies (3.10) in each stage that follows.

The penalty of a network not following the coordination device in a stage is to have to compete in every stage thereafter. While this strategy is commonly understood to be a hardly plausible mode of cooperation and other strategies such as Tit-for-Tat strategy [93] in which players keep switching between cooperative and competitive mode are preferred more, we choose this strategy because it explores the theoretical feasibility of cooperation with arbitrarily patient players. Also, if even the strongest possible threat of perpetual competition posed under the grim trigger strategy cannot induce cooperation, then it is unlikely that players would cooperate under less severe strategies such as Tit-for-Tat.

To enable the etiquette, in addition to the recommendation of the device, we assume that the players at the beginning of any stage n have information about the actions that the players chose in stage $(n-1)$. Since the players may disobey the device, the action profile a_n is not restricted to that in (3.18). Let $\psi_n \in \{0,1\}$ be an indicator variable such that $\psi_n = 1$ if the networks obey the coordination device $\mathrm{P_R}$ in stage n, and $\psi_n = 0$ corresponds to them deviating. We set $\psi_n = 1$ when $\mathrm{R}_n = \mathbb{H}$ and action profile $a_n = (\mathcal{A}, \mathcal{B})$ or when $\mathrm{R}_n = \mathbb{T}$ and action profile $a_n = (\mathcal{B}, \mathcal{A})$. Else, $\psi_n = 0$.

If $\psi_{n-1} = 0$, networks play their respective Nash strategies (ϕ_A^*, ϕ_T^*) in stage n and all stages that follow.

3.6.1 Is cooperation self-enforceable?

We check if the cooperation strategy profile defined in (3.18) is self-enforceable when using grim trigger, that is, if the networks always comply with the recommendations of the coordination device and do not have any incentive to deviate. Nash Equilibrium [109] is often referred to as self-enforcing in any non-cooperative strategic game because once players expectations are coordinated on such behavior, players left to act on their own accord find that there is no incentive for them to deviate. In repeated games, such self-enforcing behavior after any history is true of a subgame-perfect equilibrium. Therefore, for the repeated game under study, we check whether the cooperation strategy profile is a SPE [93]. That is, whether either player would

benefit from deviating unilaterally from the recommendation of the randomization device at any stage of the game.

For the cooperation strategy profile, when using grim trigger, to be a SPE it has to remain a Nash Equilibrium in the repeated game that follows every history of play. While the repeated game under study has some initial age $\widetilde{\Delta}^{-}$ associated with it; it is otherwise the same as the repeated game starting at any point. Therefore, without loss of generality, we consider stage 1 and check whether networks always comply with the recommendations of the coordination device or if they have any incentive to deviate.

At the beginning of the stage the coordination device observes either $\mathbf{R_1} = \mathbb{H}$ or $\mathbf{R_1} = \mathbb{T}$. For both, we must consider the two deviations: (a) the AON adheres to the recommendation but the TON deviates and (b) the TON adheres but the AON deviates. We consider the resulting four possibilities in turn.

- $\mathbf{R_1} = \mathbb{H}$

  Suppose the networks follow the recommended action profile $(\mathcal{A}, \mathcal{B})$ in the stage 1. The resulting payoffs, respectively, of the AON and the TON, conditioned on $\mathbf{R_1} = \mathbb{H}$ and the action profile in stage 1, are given by

$$\mathrm{U}^{\mathrm{T}}_{\mathbb{C}}|_{\{\mathbb{H},(\mathcal{A},\mathcal{B})\}} = (1-\alpha)E\left[\sum_{n=2}^{\infty}\alpha^{n-1}u^{\mathrm{T}}_{\mathbb{C}}\right], \tag{3.20a}$$

$$\mathrm{U}^{\mathrm{A}}_{\mathbb{C}}|_{\{\mathbb{H},(\mathcal{A},\mathcal{B})\}} = -(1-\alpha)\left(E[\widetilde{\Delta}^{-}(2)] + E\left[\sum_{n=2}^{\infty}\alpha^{n-1}u^{\mathrm{A}}_{\mathbb{C}}\right]\right), \tag{3.20b}$$

$$\text{where } E[\widetilde{\Delta}^{-}(2)] = \widetilde{\Delta}^{-}(1)(1-\widehat{\tau}_A(1-\widehat{\tau}_A)^{(\mathrm{N_A}-1)}) + \sigma_{\mathrm{C}} + (1-\widehat{\tau}_A)^{\mathrm{N_A}}(\sigma_{\mathrm{I}}-\sigma_{\mathrm{C}}) + \mathrm{N_A}\widehat{\tau}_A(1-\widehat{\tau}_A)^{(\mathrm{N_A}-1)}(\sigma_{\mathrm{S}}-\sigma_{\mathrm{C}}).$$

  Since the TON backs-off its stage 1 throughput is 0.

  In case the AON unilaterally deviates, that is it backs-off, the age increases by the idle slot length. The action profile is $(\mathcal{B}, \mathcal{B})$. Given the grim trigger etiquette, stage 2 onward both networks play the MSNE. The discounted payoff obtained by the AON, denoted by $\mathrm{U}^{\mathrm{A}}_{\mathbb{N}\mathbb{C}}|_{\{\mathbb{H},(\boldsymbol{\mathcal{B}},\mathcal{B})\}}$, where the bold $\boldsymbol{\mathcal{B}}$ emphasizes the deviation, is given by (3.21a). On the other hand, if the TON unilaterally deviates, the resulting action profile is $(\mathcal{A}, \mathcal{A})$, and the TON gets an network throughput larger than 0 in stage 1. Given the grim trigger etiquette, its resulting discounted payoff

is given by (3.21b).

$$\mathrm{U}^{\mathrm{A}}_{\mathbb{N}\mathbb{C}}|_{\{\mathbb{H},(\boldsymbol{\mathcal{B}},\mathcal{B})\}} = -(1-\alpha)\left((\widetilde{\Delta}^{-}(1)+\sigma_{\mathrm{I}}) + E\left[\sum_{n=2}^{\infty}\alpha^{n-1}u^{\mathrm{A}}_{\mathbb{N}\mathbb{C}}\right]\right), \tag{3.21a}$$

$$\mathrm{U}^{\mathrm{T}}_{\mathbb{N}\mathbb{C}}|_{\{\mathbb{H},(\mathcal{A},\boldsymbol{\mathcal{A}})\}} = (1-\alpha)\left(\widehat{\tau}_T(1-\widehat{\tau}_T)^{(\mathrm{N_T}-1)}(1-\widehat{\tau}_A)^{\mathrm{N_A}}\sigma_{\mathrm{S}}r + E\left[\sum_{n=2}^{\infty}\alpha^{n-1}u^{\mathrm{T}}_{\mathbb{N}\mathbb{C}}\right]\right). \tag{3.21b}$$

The AON and the TON would want to deviate only if their resulting payoffs while competing were larger than when obeying the device. The equations (3.22a)-(3.22b) next capture the conditions under which both networks will always obey the coordination device.

$$\mathrm{U}^{\mathrm{A}}_{\mathbb{C}}|_{\{\mathbb{H},(\mathcal{A},\mathcal{B})\}} \geq \mathrm{U}^{\mathrm{A}}_{\mathbb{N}\mathbb{C}}|_{\{\mathbb{H},(\boldsymbol{\mathcal{B}},\mathcal{B})\}}, \tag{3.22a}$$

$$\mathrm{U}^{\mathrm{T}}_{\mathbb{C}}|_{\{\mathbb{H},(\mathcal{A},\mathcal{B})\}} \geq \mathrm{U}^{\mathrm{T}}_{\mathbb{N}\mathbb{C}}|_{\{\mathbb{H},(\mathcal{A},\boldsymbol{\mathcal{A}})\}}. \tag{3.22b}$$

- $\mathbf{R_1} = \mathbb{T}$

  The coordination device recommends the networks to play $(\mathcal{B},\mathcal{A})$. The resulting payoffs, respectively, of the AON and the TON, conditioned on the action profile in stage 1, are given by

$$\mathrm{U}^{\mathrm{T}}_{\mathbb{C}}|_{\{\mathbb{T},(\mathcal{B},\mathcal{A})\}} = (1-\alpha)\left(\widehat{\tau}_T(1-\widehat{\tau}_T)^{(\mathrm{N_T}-1)}\sigma_{\mathrm{S}}r + E\left[\sum_{n=2}^{\infty}\alpha^{n-1}u^{\mathrm{T}}_{\mathbb{C}}\right]\right), \tag{3.23a}$$

$$\mathrm{U}^{\mathrm{A}}_{\mathbb{C}}|_{\{\mathbb{T},(\mathcal{B},\mathcal{A})\}} = -(1-\alpha)\left(E[\widetilde{\Delta}^{-}(2)] + E\left[\sum_{n=2}^{\infty}\alpha^{n-1}u^{\mathrm{A}}_{\mathbb{C}}\right]\right), \tag{3.23b}$$

  where $E[\widetilde{\Delta}^{-}(2)] = \widetilde{\Delta}^{-}(1) + \sigma_{\mathrm{C}} + (1-\widehat{\tau}_A)^{\mathrm{N_A}}(\sigma_{\mathrm{I}}-\sigma_{\mathrm{C}}) + \mathrm{N_T}\widehat{\tau}_T(1-\widehat{\tau}_T)^{(\mathrm{N_T}-1)}(\sigma_{\mathrm{S}}-\sigma_{\mathrm{C}})$.

  Similarly to the earlier case when $\mathbf{R_1} = \mathbb{H}$, we can calculate the payoffs obtained by the AON and the TON, respectively, when they unilaterally deviate as

$$\mathrm{U}^{\mathrm{T}}_{\mathbb{N}\mathbb{C}}|_{\{\mathbb{T},(\mathcal{B},\boldsymbol{\mathcal{B}})\}} = (1-\alpha)E\left[\sum_{n=2}^{\infty}\alpha^{n-1}u^{\mathrm{T}}_{\mathbb{N}\mathbb{C}}\right], \tag{3.24a}$$

$$\mathrm{U}^{\mathrm{A}}_{\mathbb{N}\mathbb{C}}|_{\{\mathbb{T},(\boldsymbol{\mathcal{A}},\mathcal{A})\}} = -(1-\alpha)\left(E[\widetilde{\Delta}^{-}(2)] + E\left[\sum_{n=2}^{\infty}\alpha^{n-1}u^{\mathrm{A}}_{\mathbb{N}\mathbb{C}}\right]\right), \tag{3.24b}$$

$$\begin{aligned}\text{where } E[\widetilde{\Delta}^{-}(2)] = {} & \widetilde{\Delta}^{-}(1)(1-\widehat{\tau}_A(1-\widehat{\tau}_A)^{(\mathrm{N_A}-1)}(1-\widehat{\tau}_T)^{\mathrm{N_T}}) + \sigma_{\mathrm{C}} \\ & + (1-\widehat{\tau}_T)^{\mathrm{N_T}}(1-\widehat{\tau}_A)^{\mathrm{N_A}}(\sigma_{\mathrm{I}}-\sigma_{\mathrm{C}}) + \mathrm{N_A}\widehat{\tau}_A(1-\widehat{\tau}_A)^{\mathrm{N_A}-1}(1-\widehat{\tau}_T)^{\mathrm{N_T}} \\ & + \mathrm{N_T}\widehat{\tau}_T(1-\widehat{\tau}_T)^{(\mathrm{N_T}-1)}(1-\widehat{\tau}_A)^{\mathrm{N_A}}(\sigma_{\mathrm{S}}-\sigma_{\mathrm{C}}).\end{aligned}$$

The equations (3.25a)-(3.25b) capture the conditions under which both networks will always obey the coordination device.

$$\mathrm{U}^{\mathrm{A}}_{\mathbb{C}}|_{\{\mathbb{T},(\mathcal{B},\mathcal{A})\}} \geq \mathrm{U}^{\mathrm{A}}_{\mathbb{N}\mathbb{C}}|_{\{\mathbb{T},(\boldsymbol{\mathcal{A}},\mathcal{A})\}}, \tag{3.25a}$$

$$\mathrm{U}^{\mathrm{T}}_{\mathbb{C}}|_{\{\mathbb{T},(\mathcal{B},\mathcal{A})\}} \geq \mathrm{U}^{\mathrm{T}}_{\mathbb{N}\mathbb{C}}|_{\{\mathbb{T},(\mathcal{B},\boldsymbol{\mathcal{B}})\}}. \tag{3.25b}$$

We state the requirement for cooperation to be self-enforceable.

Statement 1. *Proof.* Cooperation is self-enforceable in the repeated game via grim trigger strategies if there exists $\overline{\alpha} \in (0,1)$, such that $\forall \alpha > \overline{\alpha}$, $\exists \mathrm{P_R} \in (0,1)$, such that the grim trigger strategy profile in (3.18) is a SPE. ■

The set of $(\overline{\alpha}, \mathrm{P_R})$ for which the Statement 1 is true can be obtained using the equilibrium incentive constraints specified by (3.22a)-(3.22b) and (3.25a)-(3.25b). We resort to computational analysis. In Section 3.7 we show that the existence of a non-empty set of $(\overline{\alpha}, \mathrm{P_R})$ is dependent on the size of the AON and the TON.

Observation 1. *Proof.* Cooperation is self-enforceable (Statement 1) for smaller networks. However, as the networks grow in size, competition becomes more favorable than cooperation, the SPE ceases to exist, and cooperation is not self-enforceable. ■

3.7 Evaluation Methodology and Results

We study two scenarios (a) when $\sigma_{\mathrm{S}} > \sigma_{\mathrm{C}}$ and (b) when $\sigma_{\mathrm{S}} \leq \sigma_{\mathrm{C}}$. In practice, the idle slot is much smaller than a collision or a successful transmission slot. We set $\sigma_{\mathrm{I}} = \beta << 1$. For the shown results, when $\sigma_{\mathrm{S}} > \sigma_{\mathrm{C}}$, we set $\sigma_{\mathrm{S}} = (1+\beta)$ and $\sigma_{\mathrm{C}} = 0.1(1+\beta)$. When evaluating $\sigma_{\mathrm{S}} < \sigma_{\mathrm{C}}$, we set $\sigma_{\mathrm{S}} = (1+\beta)$ and $\sigma_{\mathrm{C}} = 2(1+\beta)$. Lastly, we set $\sigma_{\mathrm{S}} = \sigma_{\mathrm{C}} = (1+\beta)$ when $\sigma_{\mathrm{S}} = \sigma_{\mathrm{C}}$. The results presented later use $\beta = 0.01$.**. To illustrate the impact of self-contention and competition, we simulated $\mathrm{N_A} \in \{1,2,5,10,50\}$ and $\mathrm{N_T} \in \{1,2,5,10,50\}$. To show when the networks cooperate, we simulated the discount factor $\alpha \in [0.01, 0.99]$ and the coordination device $\mathrm{P_R} \in [0.01, 0.99]$. We used Monte Carlo simulations to compute the average discounted payoff of the AON and the TON. Averages were calculated over $100,000$

**The selection of slot lengths is such that the ratio $(\sigma_{\mathrm{S}} - \sigma_{\mathrm{I}})/\sigma_{\mathrm{S}}$ for the simulation setup is approximately the same as that for 802.11ac [111] based WiFi devices and 802.11p [112] based vehicular network.

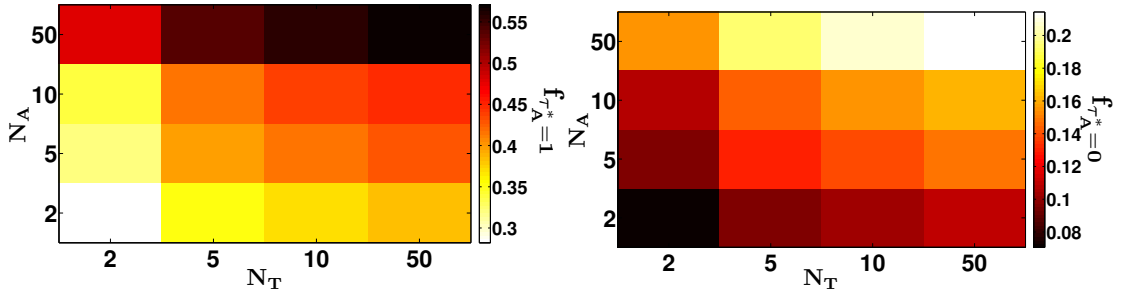

(a) Empirical frequency of $\tau_{\mathrm{A}}^* = 1$, $\mathbf{f}_{\tau_{\mathrm{A}}^*=\mathbf{1}}$ ($\sigma_{\mathrm{S}} > \sigma_{\mathrm{C}}$)

(b) Empirical frequency of $\tau_{\mathrm{A}}^* = 0$, $\mathbf{f}_{\tau_{\mathrm{A}}^*=\mathbf{0}}$ ($\sigma_{\mathrm{S}} = \sigma_{\mathrm{C}}$)

Figure 3.10: Average empirical frequency of occurrence of $\tau_{\mathrm{A}}^* = 1$ ($\mathbf{f}_{\tau_{\mathrm{A}}^*=\mathbf{1}}$) and $\tau_{\mathrm{A}}^* = 0$ ($\mathbf{f}_{\tau_{\mathrm{A}}^*=\mathbf{0}}$) for different scenarios computed over 100,000 independent runs with 1000 stages each when networks choose to play the MSNE in each stage. Figure 3.10a and Figure 3.10b correspond to when $\sigma_{\mathrm{S}} > \sigma_{\mathrm{C}}$ and $\sigma_{\mathrm{S}} = \sigma_{\mathrm{C}}$, respectively. The results correspond to $\sigma_{\mathrm{S}} = 1 + \beta$, $\sigma_{\mathrm{I}} = \beta$, $\sigma_{\mathrm{C}} = \{0.1\sigma_{\mathrm{S}}, \sigma_{\mathrm{S}}\}$ and $\beta = 0.01$..

independent runs each comprising of 1000 stages. We set the rate of transmission $r = 1$ bit/sec for each node in the WiFi network.

We begin by studying the impact of the length of collision slot σ_{C} on the average discounted payoff when (a) networks play the MSNE in each stage and compete for the medium (payoffs $\mathrm{U}_{\mathrm{T},\mathbb{NC}}$ and $\mathrm{U}_{\mathrm{A},\mathbb{NC}}$), and (b) networks obey the recommendation of the coordination device P_{R} in each stage and hence cooperate, (payoffs $\mathrm{U}_{\mathrm{T},\mathbb{C}}$ and $\mathrm{U}_{\mathrm{A},\mathbb{C}}$). We show that when networks compete, while nodes in the AON occasionally choose to refrain from transmitting during a stage when $\sigma_{\mathrm{S}} \leq \sigma_{\mathrm{C}}$, they choose to access the medium aggressively when $\sigma_{\mathrm{S}} > \sigma_{\mathrm{C}}$. Note that the nodes in the TON, however, access the shared spectrum independently of the ordering of the σ_{S} and σ_{C} (see (3.10b) and (3.11b)). Such behavior when competing impacts the desirability of cooperation over competition.

We show the region of cooperation, i.e., the range of α and P_{R} for which the inequalities (3.22a)-(3.22b) and (3.25a)-(3.25b) are satisfied and the repeated game has a SPE supported with the coordination device P_{R}. We discuss why cooperation isn't enforceable and the SPE ceases to exist in the repeated game, as the number of nodes in the networks increases.

Impact of σ_C on network payoffs in the repeated game with competition: Let $\mathbf{f}_{\tau_{\mathrm{A}}^*=\mathbf{1}}$ and $\mathbf{f}_{\tau_{\mathrm{A}}^*=\mathbf{0}}$ denote the average empirical frequency of occurrence of $\tau_{\mathrm{A}}^* = 1$, $\tau_{\mathrm{A}}^* = 0$, respectively. We computed these over the independent runs of the repeated game. Figure 3.10 shows these frequencies for different sizes of the AON and the TON when networks choose to play the MSNE in each stage, for the cases $\sigma_{\mathrm{S}} > \sigma_{\mathrm{C}}$

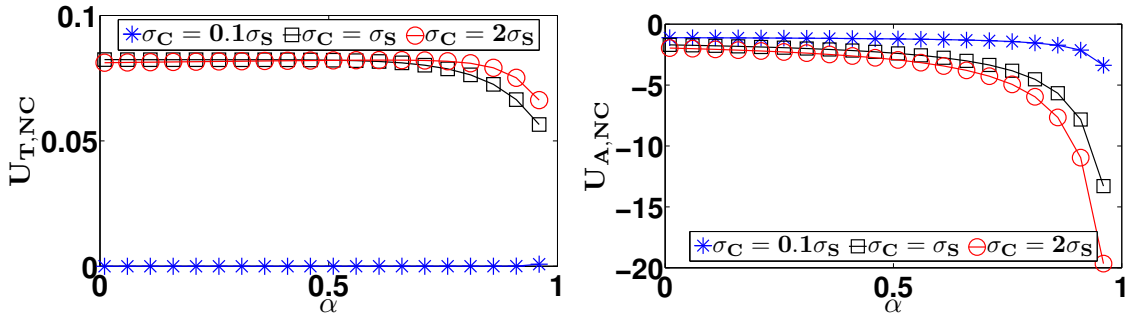

(a) TON average discounted payoff (b) AON average discounted payoff

Figure 3.11: Average discounted payoff of the TON and the AON for $N_T = N_A = 5$ when networks choose to play MSNE in each stage. We set $\sigma_S = 1 + \beta$, $\sigma_I = \beta$, $\sigma_C = \{0.1\sigma_S, \sigma_S, 2\sigma_S\}$ and $\beta = 0.01$.

and $\sigma_S = \sigma_C$. We skip $\sigma_S < \sigma_C$ as the observations are similar to $\sigma_S = \sigma_C$.

Figure 3.10a shows how $\mathbf{f}_{\tau_A^*=\mathbf{1}}$ varies as a function of the number of nodes in the AON and the TON for when $\sigma_S > \sigma_C$. Observe the increase in $\mathbf{f}_{\tau_A^*=\mathbf{1}}$ as N_A increases. This is explained by the resulting increase in the threshold age $N_A(\sigma_S - \sigma_C)$ (see (3.10a)). On the other hand, when $\sigma_S = \sigma_C$, the AON refrains from transmission more often as the number of nodes N_A in it increases. See Figure 3.10b that shows the increase in $\mathbf{f}_{\tau_A^*=\mathbf{0}}$.

The increase in $\mathbf{f}_{\tau_A^*=\mathbf{1}}$ with N_A, when $\sigma_S > \sigma_C$, increases the fraction of slots occupied by the AON. The resulting increased competition from the AON for the shared access adversely impacts the TON. In contrast, the increase in $\mathbf{f}_{\tau_A^*=\mathbf{0}}$ with N_A, when $\sigma_S \leq \sigma_C$, results in larger fraction of contention free slots for the TON and works in its favour. The impact of slot sizes on the average discounted payoff of the TON is summarized in Figure 3.11a, which shows this payoff for different selections of σ_C. In accordance with the above observations, the payoff increases with the length of the collision slot.

Further note that an increase in $\mathbf{f}_{\tau_A^*=\mathbf{1}}$ with N_A should result in the AON seeing collision slots more often. However, as shown in Figure 3.11b, despite this fact the average discounted payoff of the AON is larger when collision slots are smaller than the successful transmission slots. This is because when $\sigma_S > \sigma_C$ and the AON chooses to transmit aggressively leading to collision, the increase in age due to a collision slot is smaller than when the AON chooses not to transmit. The latter choice has the AON see a slot that is either successful (TON transmits successfully), a collision (more than one node in the TON transmits), or an idle slot, and for a longer σ_S, can be on an average longer than a collision slot.

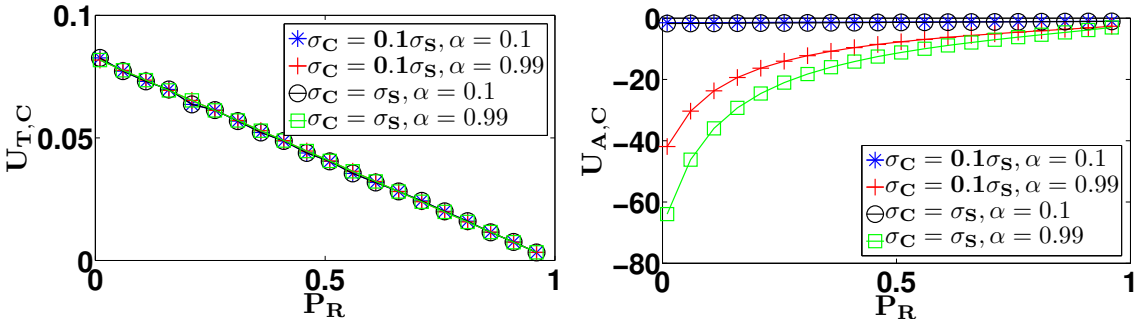

(a) (b)

Figure 3.12: Average discounted payoff of the TON and the AON for $N_T = N_A = 5$ when networks cooperate and follow the recommendation of the coordination device P_R in each stage. Shown for $\alpha = 0.1$, $\alpha = 0.99$, $\sigma_S = 1 + \beta$, $\sigma_I = \beta$ and $\beta = 0.01$.

Impact of σ_C on network payoffs in the repeated game with cooperation: Figure 3.12 shows the average discounted payoff of the TON and the AON when networks cooperate. As shown in Figure 3.12a, the payoff of the TON when networks obey the recommendation of the coordination device P_R, is the same, irrespective of the choice of length of collision slot σ_C. This is because the optimal strategy of the TON (see (3.13b)) is independent of σ_C.

Figure 3.12b shows the payoff of the AON as a function of P_R. The payoff increases with P_R. This is expected as a larger P_R implies that the AON gets to access the medium in a larger fraction of slots. Also seen in the figure is that a small collision slot (compare payoffs for $\sigma_C = 0.1\sigma_S$ and $\sigma_C = \sigma_S$) results in larger payoffs, especially at smaller values of $P_R \leq 0.5$. At any given value of P_R, an increase in σ_C for a given σ_S, increases the average length of slots occupied by the TON and thus the network age. At smaller P_R, a larger fraction of slots have the TON access, which makes the increase in age more significant.

Figure 3.13 shows the gains in payoff on choosing cooperation over competition for the AON and TON. While the TON prefers cooperation to competition for smaller collision slots, the AON prefers cooperation for larger collision slots. As seen in Figure 3.13a, when $\sigma_S > \sigma_C$, for all values of α and P_R, the payoff of the TON is higher when networks cooperate than when they compete. This is because, when $\sigma_S > \sigma_C$, nodes in the AON transmit aggressively (see Figure 3.10) when competing, making it less favorable for the TON. On the other hand, for larger collision slots, as seen in Figure 3.10 for $\sigma_C \geq \sigma_S$, the AON often refrains from transmission when competing. The resulting increase in slots free of contention from the AON makes competing favorable for the TON. Finally, observe in Figure 3.13a that the gains

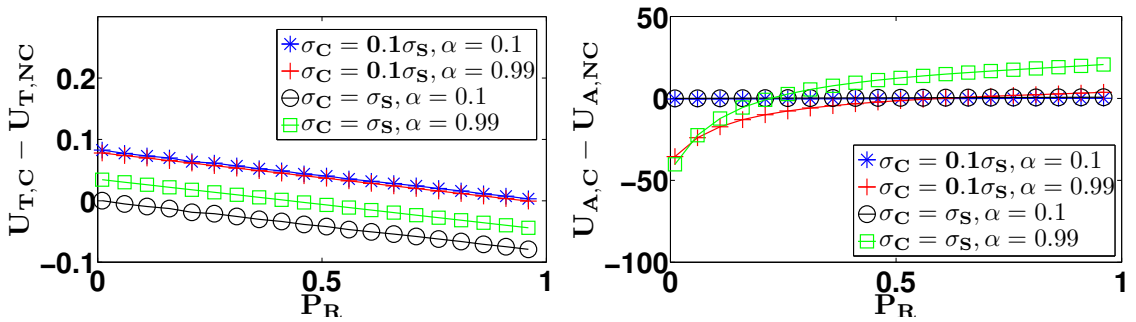

(a) (b)

Figure 3.13: Gain of cooperation over competition for the TON and the AON for $N_T = N_A = 5$. The results correspond to $\alpha = 0.1$, $\alpha = 0.99$, $\sigma_S = 1+\beta$, $\sigma_I = \beta$, $\sigma_C = \{0.1\sigma_S, \sigma_S\}$ and $\beta = 0.01$.

from cooperation reduce as P_R increases. As the fraction of slots available via the recommendation device decreases, the TON increasingly prefers competing over all slots.

Unlike the TON, as shown in Figure 3.13b, as σ_C increases, AON prefers cooperation. Also, the desirability of cooperation increases with P_R. As explained earlier, for $\sigma_C \geq \sigma_S$, when competing the AON refrains from transmitting in a stage in case the age at the beginning is small enough. Such a slot has the length of one of successful, collision or idle slots, and is determined by the TON. When cooperating such slots are always of length σ_I of an idle slot.

Lastly, as shown in Figure 3.13, the gains from cooperation for both the networks are larger for higher value of α indicating that cooperation is more beneficial when the player is farsighted, i.e., it cares about long run payoff. For instance, as shown in Figure 3.13a, when $\sigma_C \geq \sigma_S$, cooperation is more beneficial for the TON when $\alpha = 0.99$ as compared to when $\alpha = 0.01$. Similarly, as shown in Figure 3.13b, the benefits of cooperation for the AON increases with increase in α.

When is cooperation self-enforceable? The shaded region in Figures 3.14 and 3.15 show the values of α and P_R for which cooperation is self-enforceable, for when $\sigma_S = \sigma_C$ and $\sigma_S > \sigma_C$, respectively. We consider different selections of N_A and N_T. We are interested in the values of α and P_R that satisfy the inequalities (3.22a)-(3.22b) and (3.25a)-(3.25b). We observe that the range of α and P_R, shown by the shaded region, over which cooperation is self-enforceable reduces as the numbers of nodes in the networks increase. Next we discuss the cases $\sigma_S \leq \sigma_C$ and $\sigma_S > \sigma_C$ in detail.

Case I: When $\sigma_S \leq \sigma_C$: The shaded region in Figures 3.14a and 3.14b show the

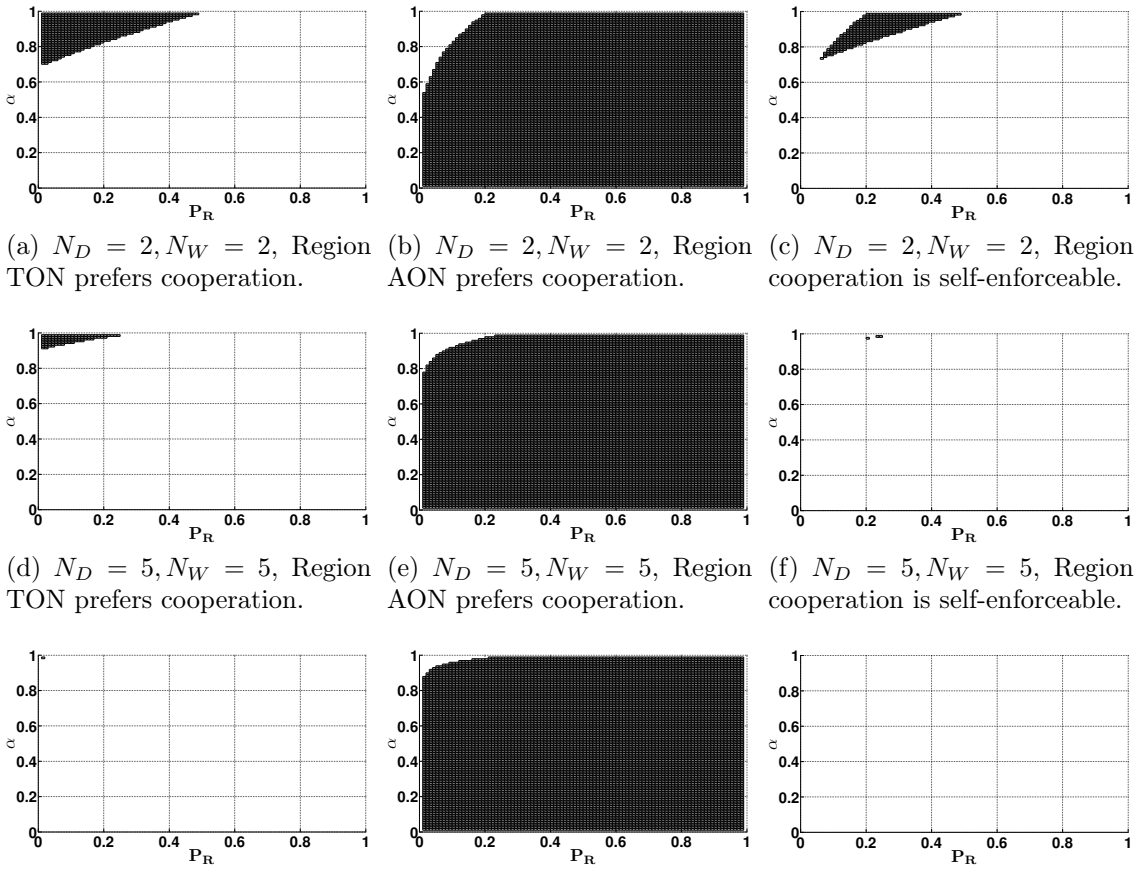

(a) $N_D = 2, N_W = 2$, Region TON prefers cooperation.

(b) $N_D = 2, N_W = 2$, Region AON prefers cooperation.

(c) $N_D = 2, N_W = 2$, Region cooperation is self-enforceable.

(d) $N_D = 5, N_W = 5$, Region TON prefers cooperation.

(e) $N_D = 5, N_W = 5$, Region AON prefers cooperation.

(f) $N_D = 5, N_W = 5$, Region cooperation is self-enforceable.

(g) $N_D = 10, N_W = 10$, Region TON prefers cooperation.

(h) $N_D = 10, N_W = 10$, Region AON prefers cooperation.

(i) $N_D = 10, N_W = 10$, Region cooperation is self-enforceable.

Figure 3.14: Range of α and $\mathrm{P_R}$ for different selections of $\mathrm{N_A}$ and $\mathrm{N_T}$ when $\sigma_\mathrm{C} = \sigma_\mathrm{S}$. The shaded region shows the range of α and $\mathrm{P_R}$ for which cooperation is self-enforceable. The ranges are qualitatively similar for $\sigma_\mathrm{C} > \sigma_\mathrm{S}$.

values of α and $\mathrm{P_R}$ for which the TON and the AON, respectively, prefer cooperation to competition. Both networks have two nodes each. The values in Figure 3.14a are the set of $(\alpha, \mathrm{P_R})$ that satisfy (3.22b) and (3.25b) and those in Figure 3.14b satisfy (3.22a) and (3.25a). As discussed earlier in the context of Figure 3.13, the AON prefers cooperation when $\sigma_\mathrm{S} \leq \sigma_\mathrm{C}$ while the TON prefers competition. This explains the larger shaded region of $(\alpha, \mathrm{P_R})$ in Figure 3.14b when compared to Figure 3.14a. Figure 3.14c shows the values $(\alpha, \mathrm{P_R})$ for which both the networks prefer cooperation. The resulting shaded region is an intersection of the shaded regions in Figures 3.14a and 3.14b. For the values in Figure 3.14c, all the Equations (3.22a), (3.22b), (3.25a), and (3.25b) are satisfied.

Similar to the figures described above, the shaded region in Figures 3.14d, 3.14e, and 3.14f show the regions of values, respectively, for which the TON prefers coop-

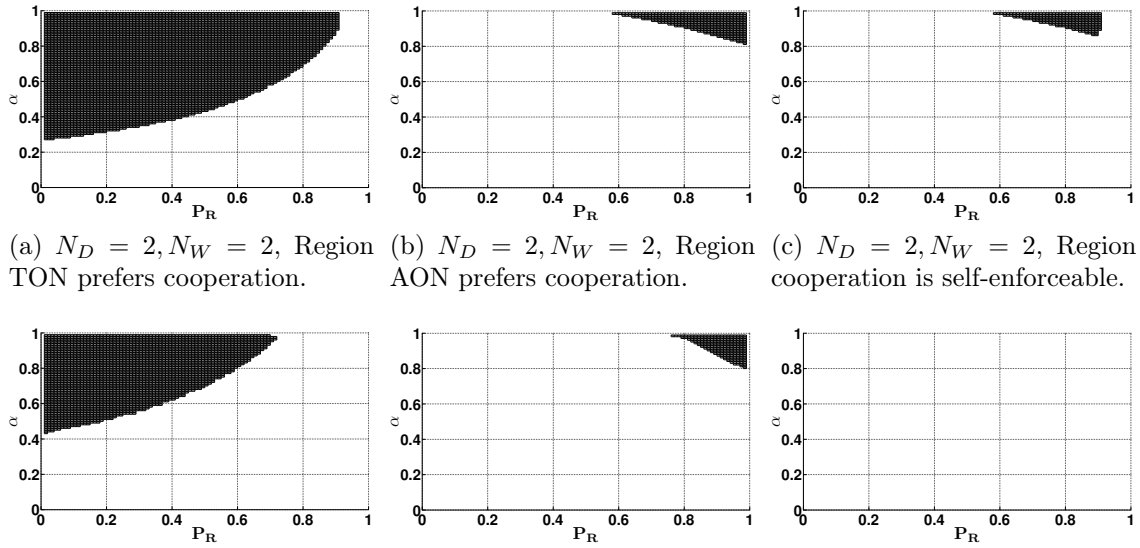

(a) $N_D = 2, N_W = 2$, Region TON prefers cooperation.

(b) $N_D = 2, N_W = 2$, Region AON prefers cooperation.

(c) $N_D = 2, N_W = 2$, Region cooperation is self-enforceable.

(d) $N_D = 10, N_W = 10$, Region TON prefers cooperation.

(e) $N_D = 10, N_W = 10$, Region AON prefers cooperation.

(f) $N_D = 10, N_W = 10$, Region cooperation is self-enforceable.

Figure 3.15: Range of α and $\mathrm{P_R}$ for different selections of $\mathrm{N_A}$ and $\mathrm{N_T}$ when $\sigma_\mathrm{S} > \sigma_\mathrm{C}$ ($\sigma_\mathrm{C} = 0.1\sigma_\mathrm{S}$). The shaded region shows the range of α and $\mathrm{P_R}$ for which cooperation is self-enforceable.

eration, the AON prefers cooperation, and both networks prefer cooperation. Each network now has five instead of two nodes. The larger number of nodes makes cooperation attractive for the AON over a larger range of α and $\mathrm{P_R}$ (compare Figures 3.14b and 3.14e). The range of values, however, shrinks for the TON. This is explained by the fact that as the number of AON nodes increases, as shown in Figure 3.10b, the frequency of $\tau_\mathrm{A}^* = 0$ increases, giving the TON greater contention free access when competing and making cooperation less favourable. The result is a smaller shaded region of values, shown in Figure 3.14f, over which cooperation is self-enforceable.

Similarly, the shaded region in Figures 3.14g, 3.14h, and 3.14i show the regions for when the networks have ten nodes each. As is clear, the region corresponding to AON further increases, while that corresponding to the TON almost disappears, and so does the region over which cooperation is self-enforceable.

Case II: When $\sigma_S > \sigma_C$: The shaded region in Figure 3.15 shows the region over which the two networks prefer cooperation and the resulting region of values $(\alpha, \mathrm{P_R})$ for which cooperation is self-enforceable. We show the regions for when both the networks have two and ten nodes each. In contrast to when $\sigma_\mathrm{S} \leq \sigma_\mathrm{C}$, we see that the region over which the AON prefers cooperation shrinks. Also the TON prefers cooperation over a range of values, which decreases as the number of nodes

increases. This is explained by the fact that the AON, as shown in Figure 3.10a, attempts access with probability 1 with higher frequency as networks grow in size, making competition better for the AON.

3.8 Conclusion

We formulated a repeated game to model coexistence between an AON and a TON. The AON desires a small age of updates while the TON desires a large throughput. The networks could either compete, that is play the MSNE in every stage of the repeated game, or cooperate by following recommendations in every stage from a randomized signalling device to access the spectrum in a non-interfering manner. The networks when cooperating employed the grim trigger strategy, which had both the networks play the MSNE in all stages following a stage in which a network disobeyed the device. This ensured that the networks would disobey the device only if they found competing to be more beneficial than cooperating in the long run.

Having modeled competition and cooperation, together with the grim trigger strategy, we investigated if cooperation between the networks was self-enforceable. For this we checked if and when the cooperation strategy profile was a subgame perfect equilibrium. We considered two distinct practical medium access settings (a) when $\sigma_{\mathrm{S}} \leq \sigma_{\mathrm{C}}$ and (b) when $\sigma_{\mathrm{S}} > \sigma_{\mathrm{C}}$. We showed that for both medium access settings while cooperation is self-enforceable when networks have a small number of nodes, networks prefer competing when they grow in size.

Chapter 4
Coexistence of Selfish Age Optimizing Nodes

4.1 Problem Overview and Motivation

The ubiquity of IoT devices has led to the emergence of applications that require these devices to sense and communicate information (status updates) to a monitoring facility, or share with other devices, in a timely manner. These applications include real-time monitoring for disaster management, environmental monitoring and surveillance [43, references therein], which require timely delivery of updates to a ground station, and vehicular networking for future autonomous operations where each vehicle broadcasts its status (e.g. position, velocity etc.) to enable applications like collision avoidance and platooning.

Given the many applications, it is essential to investigate spectrum sharing by nodes that would like freshness of information. We measure freshness using the age of information [45] metric. We consider N selfish nodes that share spectrum via a CSMA/CA (carrier sense multiple access with collision avoidance) based access mechanism. Each node in the network would like to minimize the age of its status at the other nodes.

We model the competition for the shared spectrum as a non-cooperative one-shot multiple access game parameterized by the age of every node and the medium access settings. This is motivated by the following consideration. The interaction for spectrum access is most realistically modeled as a repeated game [72] in which the ages of the nodes constitute the state of the system that endogenously evolve as a result of players' strategies over time [47]. Methodologically, however, it is important to understand the one-shot game and its equilibria first before delving

into a detailed analysis of the repeated game. Therefore, in this work, we restrict ourselves to a one-shot game that is played by the nodes in a CSMA/CA slot.

We assume that each node knows the ages of status updates at the beginning of the slot and can choose either to transmit during a slot or stay idle. We investigate the equilibrium strategies for two distinct medium access settings: (a) when a collision (which is when multiple transmissions overlap resulting in all being decoded in error) is shorter than the length of a successful (interference free) data transmission, and (b) when a collision may be at least as long as the length of a successful transmission. The former, for example, is the case when networks use the RTS/CTS based access mechanism of the 802.11 MAC [64], the latter can be exemplified by networks using the basic access mechanism [64] of the 802.11 MAC.

We find that medium access settings exert strong incentive effects on the nodes. We show that when the collision slot is smaller than the successful transmission slot, transmitting during a slot is a weakly dominant strategy. This result is independent of the initial ages. This, of course, leads to wastage of the shared spectrum and the age of updates of none of the nodes is reduced at the end of the slot. On the other hand, the access setting where collision is longer, no dominant strategy exists. In this case, we analytically derive the mixed strategy Nash equilibrium for when the ages at the beginning of the slot satisfy certain conditions.

Our work provides insights into how competing nodes that value timeliness would share the spectrum under different medium access settings. Specifically, our results indicate that under decentralized decision making by nodes, the access setting with longer successful transmissions is more vulnerable to collisions than the other.

The rest of the chapter is organized as follows. Section 4.2 discusses the related works followed by the network model in Section 4.3. The game is described in Section 4.4 and the equilibrium strategies are derived in Section 4.5. Results are discussed in Section 4.6. We conclude in Section 4.7.

4.2 Related Work

Unlike age, throughput as the payoff function in wireless networks has been extensively studied from the game theoretic point of view (see [49, 50, 53]). Age has been investigated for networks with multiple users sharing a slotted system in [65–70]. In [65] and [66] authors considered scheduled and random access mechanisms. In [67] authors studied a scheduling problem with respect to age and in [68] authors studied

a multi-source multi-hop wireless network with age as a performance metric. In [69] authors investigated age in a CSMA-based network and formulated an optimization problem to minimize the total average age of the network. In [70] authors considered the problem of minimizing the age over a random access channel and proposed distributed age-efficient transmission policies.

In [46, 47, 54, 55] authors studied games with age as the payoff function. In [54] and [55], authors studied an adversarial setting where one player aims to maintain the freshness of information updates while the other player aims to prevent this. In [46], we proposed a game theoretic approach to study the coexistence of DSRC and WiFi, where the DSRC network desires to minimize the average age of information and the WiFi network aims to maximize the average throughput. In [47], via the repeated game model we were able to shed better light on the interaction of age and throughput optimizing networks. Unlike these works, in this work we provide insights into how competing nodes that value timeliness of their information at others would share the spectrum using a CSMA/CA based medium access.

4.3 Network Model

Our network consists of N nodes, indexed $1, 2, \ldots, N$, which contend for access to a shared wireless medium. Each node uses a CSMA/CA based access mechanism. We assume that all nodes can sense each other's packet transmissions. This allows modeling the CSMA/CA mechanism as a slotted multiaccess system. A slot may either be (a) an idle slot in which no node transmits a packet, (b) a successful transmission slot in which exactly one node transmits an update packet that is decoded successfully by all other nodes, or (c) a collision slot in which more than one node transmits a packet and as a result none of the packets are successfully decoded. We assume a generate-at-will model [107, 108], wherein a node is able to generate a fresh update at will. The consequence of this assumption is that a node that transmits a packet always sends a freshly generated update (age 0 at the beginning of the transmission) in it. Each node would like to minimize the age of its status update packets at the other nodes in the network.

Let τ_i denote the probability with which node i attempts transmission in a slot.

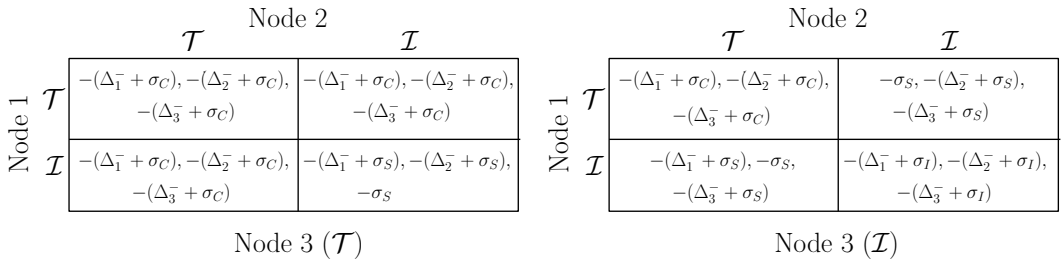

Figure 4.1: Payoff matrix with slot lengths and age values for the game G when 3 nodes contend for the medium. Nodes can choose between transmit ($\mathcal{T}$) and idle ($\mathcal{I}$).

Let $p_{\text{idle}}^{(s)}$ be the probability of an idle slot. We have

$$p_{\text{I}} = \prod_{i=1}^{\text{N}} (1 - \tau_i). \tag{4.1}$$

Let $p_{\text{S}}^{(i)}$ be the probability of a successful transmission by node i in a slot and let p_{S} be the probability of a successful transmission in a slot. We say that node i sees a busy slot if in the slot node i doesn't transmit and exactly one other node transmits. Let $p_{\text{B}}^{(i)}$ be the probability that a busy slot is seen by node i. Let p_{C} be the probability that a collision occurs in a slot. We have

$$\begin{aligned} p_{\text{S}}^{(i)} &= \tau_i \prod_{\substack{j=1 \\ j \neq i}}^{\text{N}} (1 - \tau_j), \;\; p_{\text{S}} = \sum_{i=1}^{\text{N}} p_{\text{S}}^{(i)}, \\ p_{\text{B}}^{(i)} &= \sum_{\substack{j=1 \\ j \neq i}}^{\text{N}} \tau_j \prod_{\substack{k=1 \\ k \neq j, k \neq i}}^{\text{N}} (1 - \tau_k) \text{ and } p_{\text{C}} = 1 - p_{\text{I}} - p_{\text{S}}. \end{aligned} \tag{4.2}$$

Let σ_I, σ_S and σ_C denote the lengths of an idle, successful, and collision slot, respectively. Next we define the age of a node's status updates at other nodes in terms of the above probabilities and slot lengths.

4.3.1 Age of a Node's Information

Let $u_i(t)$ be the timestamp of the most recent status update of a node i at other nodes $j \neq i$ at time t. The status update age of node i at any other node j at time t is the stochastic process $\Delta_i(t) = t - u_i(t)$ [45]. We assume that a status update packet that node i attempts to transmit in a slot contains an update that is fresh at the beginning of the slot.

Note that node i's age at the end of a slot is determined by its age at the beginning of the slot and the type of the slot. As a result, node i's age at any other node j either resets to σ_{S} if a successful transmission occurs or increases by σ_{I}, σ_{C} or σ_{S} at all other nodes, respectively, when an idle slot, collision slot or a busy slot occurs. Figure 3.4 shows an example sample path of the age $\Delta_i(t)$. In what follows we will drop the explicit mention of time t and let Δ_i^- and Δ_i, respectively, be the age of node i's update at the beginning and end of the slot.

The age Δ_i at the end of a slot is thus a random variable whose conditional PMF given Δ_i^- is as shown in (3.4). Using (3.4), we define the conditional expected age as shown in (3.5).

4.4 Game Model

We define a one-shot multiple access game to model the interaction between the nodes in a CSMA/CA slot. In every slot, nodes must compete for access with the goal of minimizing their age. We capture the interaction in a slot as a non-cooperative parameterized strategic one-shot multiple access game $G = (\mathcal{N}, (\mathcal{S}_k)_{k\in\mathcal{N}}, (u_k)_{k\in\mathcal{N}}, \mathbf{\Delta}^-)$, where $\mathcal{N}$ is the set of players, $\mathcal{S}_k$ is the set of strategies of player k, u_k is the payoff of player k and $\mathbf{\Delta}^-$ is the additional parameter input to the game G, which is the vector of ages of the nodes' updates (Δ_i^- for node i) at the beginning of the slot. We define the game G next.

- **Players:** The set of players $\mathcal{N} = \{1, 2, \ldots, \mathrm{N}\}$ is simply the set of all nodes in the network.

- **Strategy Space:** Let $\mathcal{T}$ denote transmit and $\mathcal{I}$ denote idle. The set of pure strategies for node i is $\mathcal{S}_i = \{\mathcal{T}, \mathcal{I}\}$. We allow nodes to play mixed strategies. Define $\mathbf{\Phi}_i$ as the set of all probability distributions over the set of strategies $\mathcal{S}_i$ of player i. A mixed strategy for player i is an element $\phi_i \in \mathbf{\Phi}_i$, where ϕ_i is a probability distribution over $\mathcal{S}_i$. We require $\phi_i(s_i) \geq 0$ for all $s_i \in \mathcal{S}_i$ and $\sum_{s_i\in\mathcal{S}_i} \phi_i(s_i) = 1$. In this work, since the strategy spaces are binary, a mixed strategy for node i is identified by specifying a probability $\tau_i \in [0, 1]$ with which i attempts transmission in a slot. As a result, the probability distribution corresponding to node i is $\phi_i = \{\phi_i(\mathcal{T}), \phi_i(\mathcal{I})\} = \{\tau_i, 1 - \tau_i\}$.

- **Payoffs:** We can calculate the probabilities (4.1)-(4.2) for each node in the network. The probabilities when substituted in (3.4) can be used to calculate the

average age in (3.5). For every node i, its expected payoff when its own transmission probability is τ_i and the vector of others' transmission probabilities is $\boldsymbol{\tau}_{-i}$ is given by

$$u_i(\tau_i, \boldsymbol{\tau}_{-i}) = -\widetilde{\Delta}_i(\tau_i, \boldsymbol{\tau}_{-i}). \tag{4.3}$$

where, $\widetilde{\Delta}_i(\tau_i, \boldsymbol{\tau}_{-i})$ is the average age in (3.5). Each node would like to maximize its payoff, which is the same as minimizing its expected age at the end of the stage.

4.5 Equilibrium Strategies

We will separately consider two common medium access settings found in CSMA/CA (a) $\sigma_{\mathrm{C}} < \sigma_{\mathrm{S}}$ and (b) $\sigma_{\mathrm{C}} \geq \sigma_{\mathrm{S}}$. The first setting is akin to RTS/CTS based medium access defined in the 802.11 MAC. The use of short RTS/CTS messages to reserve the medium before accessing it to send a larger data payload (status update) packet reduces the average length of a collision slot. The second setting is akin to the basic access mechanism defined in the 802.11 MAC and doesn't use RTS/CTS. All collisions are between packets carrying data payloads.

4.5.1 When $\sigma_{\mathbf{C}} \leq \sigma_{\mathbf{S}}$

Proposition 3 summarizes the strategy of choice for nodes in the network when the collision slots are shorter than or equal to successful transmission slots.

Proposition 3. *When $\sigma_C \leq \sigma_S$, for the one-shot multiple access game G, transmit ($\mathcal{T}$) is a weakly dominant strategy.*

Proof: As stated in [72], $s_i \in S_i$ is a weakly dominant strategy for player i, if for any possible combination of the other players' strategies, player i's payoff from s_i is weakly more than that from s_i'. That is, $u_i(s_i, s_{-i}) \geq u_i(s_i', s_{-i}), \forall s_{-i} \in S_{-i}$.

We verify that for every node i, pure strategy $\mathcal{T}$ weakly dominates the pure strategy $\mathcal{I}$. We fix a node i. Any vector of pure strategies $\boldsymbol{s}_{-i}$ played by nodes other than node i can be assigned to one of the following cases: (1) exactly one of the other nodes chooses to transmit while others stay idle or, (2) more than one of the other nodes chooses to transmit, or (3) all other nodes choose to stay idle. We now consider these cases in detail and illustrate each of them using the payoff matrix of a 3-player game shown in Figure 4.1.

Case 1*: Exactly one of the other nodes chooses to transmit ($\mathcal{T}$):* In this case, if node i chooses to transmit, a collision slot occurs and its age becomes $\Delta_i = \Delta_i^- + \sigma_{\mathrm{C}}$. On the other hand, if node i chooses to stay idle, it will see a busy slot and age at the end of the slot will be set to $\Delta_i = \Delta_i^- + \sigma_{\mathrm{S}}$. In this case, if $\sigma_{\mathrm{C}} < \sigma_{\mathrm{S}}$, node i will choose to transmit ($\mathcal{T}$) and if $\sigma_{\mathrm{C}} = \sigma_{\mathrm{S}}$ node i will be indifferent between idle and transmit. The above argument can be demonstrated using the payoff matrix of a 3-player game (see Figure 4.1). Assume node 2 chooses transmit (idle) and node 3 chooses idle (transmit). In this case, transmit is a weakly dominant strategy for node 1 if $u_1(\mathcal{T},\mathcal{T},\mathcal{I}) \geq u_1(\mathcal{I},\mathcal{T},\mathcal{I})$ and $u_1(\mathcal{T},\mathcal{I},\mathcal{T}) \geq u_1(\mathcal{I},\mathcal{I},\mathcal{T})$. As shown in Figure 4.1, $u_1(\mathcal{T},\mathcal{T},\mathcal{I}) = u_1(\mathcal{T},\mathcal{I},\mathcal{T}) = -(\Delta_1^- + \sigma_{\mathrm{C}})$ and $u_1(\mathcal{I},\mathcal{T},\mathcal{I}) = u_1(\mathcal{I},\mathcal{I},\mathcal{T}) = -(\Delta_1^- + \sigma_{\mathrm{S}})$. When $\sigma_{\mathrm{C}} < \sigma_{\mathrm{S}}$, $u_1(\mathcal{T},\mathcal{T},\mathcal{I}) > u_1(\mathcal{I},\mathcal{T},\mathcal{I})$ and $u_1(\mathcal{T},\mathcal{I},\mathcal{T}) > u_1(\mathcal{I},\mathcal{I},\mathcal{T})$, whereas, when $\sigma_{\mathrm{C}} = \sigma_{\mathrm{S}}$, $u_1(\mathcal{T},\mathcal{T},\mathcal{I}) = u_1(\mathcal{I},\mathcal{T},\mathcal{I})$ and $u_1(\mathcal{T},\mathcal{I},\mathcal{T}) = u_1(\mathcal{I},\mathcal{I},\mathcal{T})$.

Case 2*: More than one of the other nodes choose to transmit ($\mathcal{T}$):* In this case, collision will occur. Irrespective of the choice made by node i, $\Delta_i = \Delta_i^- + \sigma_{\mathrm{C}}$. Player i is indifferent between idle ($\mathcal{I}$) and transmit ($\mathcal{T}$) when $\sigma_{\mathrm{C}} \leq \sigma_{\mathrm{S}}$. This corresponds to the case in the 3-player game when node 2 and node 3 choose transmit and node 1 will prefer transmit ($\mathcal{T}$) if $u_1(\mathcal{T},\mathcal{T},\mathcal{T}) \geq u_1(\mathcal{I},\mathcal{T},\mathcal{T})$. As shown in Figure 4.1, $u_1(\mathcal{T},\mathcal{T},\mathcal{T}) = -(\Delta_1^- + \sigma_{\mathrm{C}})$ and $u_1(\mathcal{I},\mathcal{T},\mathcal{T}) = -(\Delta_1^- + \sigma_{\mathrm{C}})$. Clearly, $u_1(\mathcal{T},\mathcal{T},\mathcal{T}) = u_1(\mathcal{I},\mathcal{T},\mathcal{T})$ and node 1 is indifferent between transmit and idle.

Case 3*: All other nodes choose to stay idle ($\mathcal{I}$):* In this case, suppose node i along with other nodes chooses to stay idle. We have $\Delta_i = \Delta_i^- + \sigma_{\mathrm{I}}$. In case node i transmits, its status update will be successfully received and its age at all other nodes will reset to $\Delta_i = \sigma_{\mathrm{S}}$. Further note that the age of a node's status at other nodes at the beginning of the slot is at least as large as the length σ_{S} of a successful transmission slot. This is because σ_{S} is the time a fresh update must age before it is successfully received by another node. Thus $\Delta_i^- + \sigma_{\mathrm{I}} > \sigma_{\mathrm{S}}$ and the node will prefer to transmit. In the 3-player game, for this case, node 1 will prefer transmit if $u_1(\mathcal{T},\mathcal{I},\mathcal{I}) \geq u_1(\mathcal{I},\mathcal{I},\mathcal{I})$. We have $u_1(\mathcal{T},\mathcal{I},\mathcal{I}) = -\sigma_{\mathrm{S}}$ and $u_1(\mathcal{I},\mathcal{I},\mathcal{I}) = -(\Delta_1^- + \sigma_{\mathrm{I}})$. Thus, node 1 chooses transmit. ■

4.5.2 When $\sigma_{\mathbf{C}} > \sigma_{\mathbf{S}}$

For this medium access setting, no weakly dominant strategy exists and we look for mixed strategies.

Proposition 4. *For the one-shot multiple access game G, when $\sigma_C > \sigma_S$ no weakly*

Case	σ_{C}	Vector of Ages seen at the beginning of the stage, $\boldsymbol{\Delta}^{-}$	Mixed Strategy Nash Equilibrium, $\boldsymbol{\tau}^{*}$	Pure Strategy Nash Equilibrium
I	$0.1\sigma_{\mathrm{S}}$	$(\sigma_{\mathrm{S}},2\sigma_{\mathrm{S}},3\sigma_{\mathrm{S}})$	$(\mathbf{2.4877},\mathbf{-1.2782},0.3549)$	$(\mathcal{T},\mathcal{T},\mathcal{T}),(\mathcal{T},\mathcal{I},\mathcal{T}),(\mathcal{I},\mathcal{T},\mathcal{T}),(\mathcal{T},\mathcal{T},\mathcal{I})$
II	$0.1\sigma_{\mathrm{S}}$	$(\sigma_{\mathrm{S}},\sigma_{\mathrm{S}},\sigma_{\mathrm{S}})$	$(\mathbf{-0.0055},\mathbf{-0.0055},\mathbf{-0.0055})$	$(\mathcal{T},\mathcal{T},\mathcal{T}),(\mathcal{T},\mathcal{I},\mathcal{T}),(\mathcal{I},\mathcal{T},\mathcal{T}),(\mathcal{T},\mathcal{T},\mathcal{I})$
III	$2\sigma_{\mathrm{S}}$	$(\sigma_{\mathrm{S}},2\sigma_{\mathrm{S}},3\sigma_{\mathrm{S}})$	$(0.6008,0.3355,\mathbf{-0.9804})$	$(\mathcal{T},\mathcal{T},\mathcal{T}),(\mathcal{I},\mathcal{I},\mathcal{T}),(\mathcal{T},\mathcal{I},\mathcal{I}),(\mathcal{I},\mathcal{T},\mathcal{I})$
IV	$2\sigma_{\mathrm{S}}$	$(2\sigma_{\mathrm{S}},3\sigma_{\mathrm{S}},3\sigma_{\mathrm{S}})$	$(0.6008,0.3355,0.3355)$	$(\mathcal{T},\mathcal{T},\mathcal{T}),(\mathcal{I},\mathcal{I},\mathcal{T}),(\mathcal{T},\mathcal{I},\mathcal{I}),(\mathcal{I},\mathcal{T},\mathcal{I})$
V	$2\sigma_{\mathrm{S}}$	$(2\sigma_{\mathrm{S}},3\sigma_{\mathrm{S}},4\sigma_{\mathrm{S}})$	$(0.6672,0.5012,0.0049)$	$(\mathcal{T},\mathcal{T},\mathcal{T}),(\mathcal{I},\mathcal{I},\mathcal{T}),(\mathcal{T},\mathcal{I},\mathcal{I}),(\mathcal{I},\mathcal{T},\mathcal{I})$

Table 4.1: Mixed Strategy Nash Equilibrium $\boldsymbol{\tau}^{*}$ computed using (4.6) and the pure strategy Nash Equilibrium corresponding to different selections of $\mathrm{N}=3$, σ_{C} and $\boldsymbol{\Delta}$ computed by substituting the values of σ_{C} and $\boldsymbol{\Delta}$ in the payoff matrix shown in Figure 4.1. Other parameters used in the computation are $\sigma_{\mathrm{S}}=1.01$, $\sigma_{\mathrm{I}}=0.01$.

dominant strategy exists.

Proof: Similar to Proposition 3, we assume that in a slot, for different selections of strategies by other nodes in the network, node i may choose either to transmit ($\mathcal{T}$) or stay idle ($\mathcal{I}$), depending on which strategy gives a higher payoff. To find the strategy that is beneficial for node i, we consider the following cases: (1) exactly one of the other nodes chooses to transmit while others stay idle, or (2) all other nodes choose to stay idle, or (3) more than one of the other nodes chooses to transmit.

Case 1*: Exactly one of the other nodes chooses to transmit ($\mathcal{T}$):* In this case, if node i chooses to transmit, a collision slot occurs and its age becomes $\Delta_i=\Delta_i^{-}+\sigma_{\mathrm{C}}$. In contrast, if node i chooses to stay idle, it will see a busy slot and age at the end of the slot will be set to $\Delta_i=\Delta_i^{-}+\sigma_{\mathrm{S}}$. Since, $\sigma_{\mathrm{C}}>\sigma_{\mathrm{S}}$, node i will choose to stay idle ($\mathcal{I}$).

Case 2*: All other nodes choose to stay idle:* In this case if node i chooses to stay idle too, we have $\Delta_i=\Delta_i^{-}+\sigma_{\mathrm{I}}$ and if it chooses to transmit, its status update will be successfully received and its age at all other nodes will reset to $\Delta_i=\sigma_{\mathrm{S}}$. Since age of node i's status at other nodes at the beginning of the slot (Δ_i^{-}) is at least as large as σ_{S}, $\Delta_i^{-}+\sigma_{\mathrm{I}}>\sigma_{\mathrm{S}}$. Hence, node i will prefer to transmit ($\mathcal{T}$).

Case 1 and Case 2 shows that player's preferences are opposite, hence, the game has no weakly dominant strategy. ■

We consider mixed strategies and derive the Nash equilibrium when the initial ages of the nodes' updates lie within a certain assumed region. As stated in [109], every finite strategic-form game has a MSNE. For a strategic game G, a mixed-strategy profile $\phi^{*}=(\phi_1^{*},\phi_2^{*},\ldots,\phi_{\mathrm{N}}^{*})$ is a Nash equilibrium [109], if ϕ_i^{*} is the best

response of player i to his opponents' mixed strategy $\phi^*_{-i} \in \mathbf{\Phi}_{-i}$, for all $i \in \mathcal{N}$. We have

$$u_i(\phi^*_i, \phi^*_{-i}) \geq u_i(\phi_i, \phi^*_{-i}), \forall \phi_i \in \mathbf{\Phi}_i,$$

where $\phi^* \in \prod_{i=1}^{|\mathcal{N}|} \mathbf{\Phi}_i$ is the profile of mixed strategy. As stated earlier, the mixed strategy for player i is identified by the probability $\tau_i \in [0,1]$ with which node i attempts transmission in a slot. Let $\widetilde{\Delta}^- = (1/\mathrm{N}) \sum_{i=1}^{\mathrm{N}} \Delta_i^-$, which is the average of the ages of nodes' updates at the beginning of the slot.

Proposition 5. *If $\sigma_C > \sigma_S$ and*

$$\widetilde{\Delta}^- - \frac{(\mathrm{N}-1)\Delta_i^-}{\mathrm{N}} > \frac{\sigma_S - \sigma_I}{\mathrm{N}}, \ \forall i \in \mathcal{N}, \tag{4.4}$$

The MSNE is given by

$$\tau_i^* = \frac{\sigma_S - \sigma_I + (\mathrm{N}-1)\Delta_i^- - \mathrm{N}\widetilde{\Delta}^-}{\mathrm{N}\sigma_S - (\mathrm{N}-1)\sigma_C - \sigma_I + (\mathrm{N}-1)\Delta_i^- - \mathrm{N}\widetilde{\Delta}^-}, \ \forall i \in \mathcal{N}.$$

The condition (4.4) ensures that $\tau_i^* \in (0,1)$.

Proof: For node i to randomize, when other nodes play their mixed strategies τ^*_{-i}, both the pure strategies of transmit and idle must be best responses of i. Note that the choice of $\mathcal{T}$ and $\mathcal{I}$ are, respectively, equivalent to setting $\tau_i = 1$ and $\tau_i = 0$ in (4.3). We require $u_i(1, \tau^*_{-i}) = u_i(0, \tau^*_{-i})$. Using (4.3) we can write

$$u_i(1, \tau^*_{-i}) = -\left(1 - \prod_{j \neq i}^{\mathrm{N}} (1 - \tau_j^*)\right)(\Delta_i^- + \sigma_{\mathrm{C}}) - \prod_{j \neq i}^{\mathrm{N}} (1 - \tau_j^*)\sigma_{\mathrm{S}}, \tag{4.5a}$$

$$\begin{aligned} u_i(0, \tau^*_{-i}) = &-\left(1 - \prod_{j \neq i}^{\mathrm{N}} (1 - \tau_j^*) - \sum_{j \neq i}^{\mathrm{N}} \tau_j^* \prod_{k \neq j, k \neq i}^{\mathrm{N}} (1 - \tau_k^*)\right)(\Delta_i^- + \sigma_{\mathrm{C}}) \\ &- \prod_{j \neq i}^{\mathrm{N}} (1 - \tau_j^*)(\Delta_i^- + \sigma_{\mathrm{I}}) - \left(\sum_{j \neq i}^{\mathrm{N}} \tau_j^* \prod_{k \neq j, k \neq i}^{\mathrm{N}} (1 - \tau_k^*)\right)(\Delta_i^- + \sigma_{\mathrm{S}}). \end{aligned} \tag{4.5b}$$

Equation (4.5a) is explained by the fact that since node i chooses to transmit the slot is either a collision slot or a successful transmission slot. It is the former if one or more of the other nodes transmit. It is the latter in case none of the other nodes transmit. Similarly, Equation (4.5b) is explained by the fact that since i chooses to stay idle, the slot can be either idle, a collision slot, or a successful transmission

slot, as determined by the probabilistic choices made by the other nodes, which are governed by τ^*_{-i}.

Equating $u_i(1, \tau^*_{-i})$ and $u_i(0, \tau^*_{-i})$, for node i, we obtain

$$\sum_{j \neq i}^{\mathrm{N}} \frac{\tau_j}{1-\tau_j} = \frac{\sigma_{\mathrm{S}} - \sigma_{\mathrm{I}} - \Delta_i^-}{\sigma_{\mathrm{S}} - \sigma_{\mathrm{C}}}.$$

On solving the resulting system of N equations, we get the mixed equilibrium

$$\tau_i^* = \frac{\sigma_{\mathrm{S}} - \sigma_{\mathrm{I}} + (\mathrm{N}-1)\Delta_i^- - \mathrm{N}\widetilde{\Delta}^-}{\mathrm{N}\sigma_{\mathrm{S}} - (\mathrm{N}-1)\sigma_{\mathrm{C}} - \sigma_{\mathrm{I}} + (\mathrm{N}-1)\Delta_i^- - \mathrm{N}\widetilde{\Delta}^-}, \ \ \forall i \in \mathcal{N}. \tag{4.6}$$

Next, we must find the conditions that ensure that τ_i^* lies in the interval $(0, 1)$. We consider the following two cases:

Case I: When $[\sigma_{\mathrm{S}} - \sigma_{\mathrm{I}} + (\mathrm{N}-1)\Delta_i^- - \mathrm{N}\widetilde{\Delta}^-] > 0$ and $[\mathrm{N}\sigma_{\mathrm{S}} - (\mathrm{N}-1)\sigma_{\mathrm{C}} - \sigma_{\mathrm{I}} + (\mathrm{N}-1)\Delta_i^- - \mathrm{N}\widetilde{\Delta}^-] > 0$, for $\tau_i^* > 0$ we get:

$$\widetilde{\Delta}^- - \frac{\mathrm{N}-1}{\mathrm{N}}\Delta_i^- < \frac{\sigma_{\mathrm{S}} - \sigma_{\mathrm{I}}}{\mathrm{N}}, \tag{4.7a}$$

$$\widetilde{\Delta}^- - \frac{\mathrm{N}-1}{\mathrm{N}}\Delta_i^- < \frac{\sigma_{\mathrm{S}} - \sigma_{\mathrm{I}}}{\mathrm{N}} - \frac{(\mathrm{N}-1)(\sigma_{\mathrm{C}} - \sigma_{\mathrm{S}})}{\mathrm{N}}. \tag{4.7b}$$

For $\tau_i^* < 1$, we get $[\sigma_{\mathrm{S}} - \sigma_{\mathrm{I}} + (\mathrm{N}-1)\Delta_i^- - \mathrm{N}\widetilde{\Delta}^-] < [\mathrm{N}\sigma_{\mathrm{S}} - (\mathrm{N}-1)\sigma_{\mathrm{C}} - \sigma_{\mathrm{I}} + (\mathrm{N}-1)\Delta_i^- - \mathrm{N}\widetilde{\Delta}^-]$, which on simplification gives $\sigma_{\mathrm{S}} > \sigma_{\mathrm{C}}$. Note that in Proposition 3 we showed that when $\sigma_{\mathrm{S}} > \sigma_{\mathrm{C}}$, the one-shot game G has transmit $(\mathcal{T})$ as a weakly dominant strategy. As a result, we can discard this case, since for no selection of $\boldsymbol{\Delta}^-$, the inequalities in (4.7a) and (4.7b) will hold true.

Case II: When $[\sigma_{\mathrm{S}} - \sigma_{\mathrm{I}} + (\mathrm{N}-1)\Delta_i^- - \mathrm{N}\widetilde{\Delta}^-] < 0$ and $[\mathrm{N}\sigma_{\mathrm{S}} - (\mathrm{N}-1)\sigma_{\mathrm{C}} - \sigma_{\mathrm{I}} + (\mathrm{N}-1)\Delta_i^- - \mathrm{N}\widetilde{\Delta}^-] < 0$, for $\tau_i^* > 0$ we get:

$$\widetilde{\Delta}^- - \frac{\mathrm{N}-1}{\mathrm{N}}\Delta_i^- > \frac{\sigma_{\mathrm{S}} - \sigma_{\mathrm{I}}}{\mathrm{N}}, \tag{4.8a}$$

$$\widetilde{\Delta}^- - \frac{\mathrm{N}-1}{\mathrm{N}}\Delta_i^- > \frac{\sigma_{\mathrm{S}} - \sigma_{\mathrm{I}}}{\mathrm{N}} - \frac{(\mathrm{N}-1)(\sigma_{\mathrm{C}} - \sigma_{\mathrm{S}})}{\mathrm{N}}. \tag{4.8b}$$

For $\tau_i^* < 1$, we get $[\sigma_{\mathrm{S}} - \sigma_{\mathrm{I}} + (\mathrm{N}-1)\Delta_i^- - \mathrm{N}\widetilde{\Delta}^-] > [\mathrm{N}\sigma_{\mathrm{S}} - (\mathrm{N}-1)\sigma_{\mathrm{C}} - \sigma_{\mathrm{I}} + (\mathrm{N}-1)\Delta_i^- - \mathrm{N}\widetilde{\Delta}^-]$, which on simplification gives $\sigma_{\mathrm{S}} < \sigma_{\mathrm{C}}$. Equations (4.8a), (4.8b) give us the condition $\widetilde{\Delta}^- - \frac{\mathrm{N}-1}{\mathrm{N}}\Delta_i^- > \max\{\frac{\sigma_{\mathrm{S}} - \sigma_{\mathrm{I}}}{\mathrm{N}}, \frac{\sigma_{\mathrm{S}} - \sigma_{\mathrm{I}}}{\mathrm{N}} - \frac{(\mathrm{N}-1)(\sigma_{\mathrm{C}} - \sigma_{\mathrm{S}})}{\mathrm{N}}\}$, which implies $\widetilde{\Delta}^- - \frac{\mathrm{N}-1}{\mathrm{N}}\Delta_i^- > \frac{\sigma_{\mathrm{S}} - \sigma_{\mathrm{I}}}{\mathrm{N}}$.

■

Corollary 2. *The equilibrium strategy τ_i^* of node i is a monotonically decreasing function of Δ_i^- and a monotonically increasing function of Δ_j^-, where, $j \neq i$.*

Proof. Consider the following derivatives

$$\frac{\partial \tau_i^*}{\partial \Delta_i^-} = \frac{(\mathrm{N}-1)(\mathrm{N}-2)(\sigma_\mathrm{S}-\sigma_\mathrm{C})}{(\mathrm{N}\sigma_\mathrm{S}-(\mathrm{N}-1)\sigma_\mathrm{C}-\sigma_\mathrm{I}+(\mathrm{N}-1)\Delta_i^- - \mathrm{N}\widetilde{\Delta}^-)^2},$$
$$\frac{\partial \tau_i^*}{\partial \Delta_j^-} = \frac{(\mathrm{N}-1)(\sigma_\mathrm{C}-\sigma_\mathrm{S})}{(\mathrm{N}\sigma_\mathrm{S}-(\mathrm{N}-1)\sigma_\mathrm{C}-\sigma_\mathrm{I}+(\mathrm{N}-1)\Delta_i^- - \mathrm{N}\widetilde{\Delta}^-)^2}.$$

Clearly, when $\sigma_\mathrm{C} > \sigma_\mathrm{S}$, $\partial\tau_i/\partial\Delta_i^-$ is negative and $\partial\tau_i/\partial\Delta_j^-$ is positive. ■

Corollary 2 implies that as a node's age at the beginning of the slot increases, it becomes conservative and access the medium with smaller probability, while the other nodes in the network become aggressive and access the medium with higher probability. As we later show empirically, this reduces the probability of successful transmission for the node with large age while increasing it for the other nodes. As a result, the node with large age sees fewer successful transmissions and its age keeps increasing.

4.6 Empirical Evaluation

In this section, we empirically demonstrate Proposition 3, Proposition 5 and Corollary 2 using the 3-player one-shot game. Table 4.1 shows the scenarios when $\tau_i^* \notin (0,1)$ and when $\tau_i^* \in (0,1)$ for different selections of σ_C and $\boldsymbol{\Delta}$. Since idle slots are much smaller than both collision slots and successful transmission slots, we set $\sigma_\mathrm{I} = 0.01$ and $\sigma_\mathrm{S} = 1.01$. We compute the mixed strategy Nash equilibrium $\boldsymbol{\tau}^*$ for different scenarios using (4.6).

As shown in Table 4.1, when $\sigma_\mathrm{C} < \sigma_\mathrm{S}$ (see scenarios I-II), $\tau_i^* \notin (0,1)$. Note that this is in agreement with Proposition 3 which states that transmit is a weakly dominant strategy when $\sigma_\mathrm{C} < \sigma_\mathrm{S}$ and hence node would choose to transmit rather than randomize between pure strategies. When $\sigma_\mathrm{C} > \sigma_\mathrm{S}$, in scenario III, $\tau_i^* \notin (0,1)$, whereas, in scenarios IV-V, $\tau_i^* \in (0,1)$. In scenario III, while $\sigma_\mathrm{C} > \sigma_\mathrm{S}$, the inequality $\widetilde{\Delta}^- - \frac{(\mathrm{N}-1)\Delta_i^-}{\mathrm{N}} > \frac{\sigma_\mathrm{S}-\sigma_\mathrm{I}}{\mathrm{N}}$, $\forall i \in \mathcal{N}$, is not satisfied. In line with Proposition 5, since both inequalities are not satisfied, $\tau_i^* \notin (0,1)$. In contrast, in scenarios IV-V, since $\sigma_\mathrm{C} > \sigma_\mathrm{S}$ and the inequality $\widetilde{\Delta}^- - \frac{(\mathrm{N}-1)\Delta_i^-}{\mathrm{N}} > \frac{\sigma_\mathrm{S}-\sigma_\mathrm{I}}{\mathrm{N}}$ holds true $\forall i \in \mathcal{N}$, we get $\tau_i^* \in (0,1)$, $\forall i \in \mathcal{N}$.

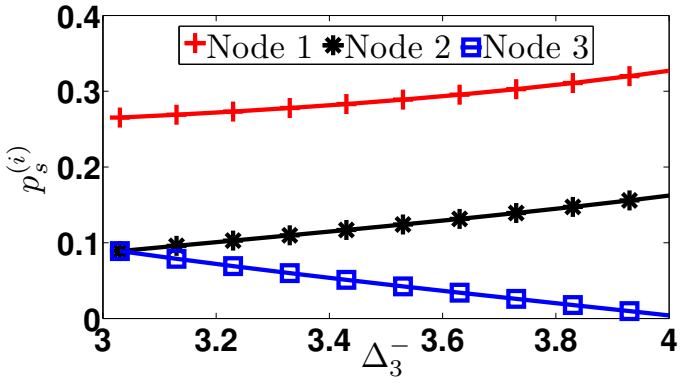

Figure 4.2: Probability of successful transmission of each node ($p_{\mathrm{S}}^{(i)}$) for different values of Δ_3^-, i.e., age of node 3 at the beginning of the slot, when $\Delta_1^- = 2\sigma_{\mathrm{S}}$ and $\Delta_2^- = 3\sigma_{\mathrm{S}}$.

The equilibrium strategy values in scenarios IV-V are in agreement with Corollary 2. As shown in Table 4.1, in scenario IV-V, we can see that as the age of node 3 at the beginning of the slot increases from $3\sigma_{\mathrm{S}}$ to $4\sigma_{\mathrm{S}}$ while the age of other nodes is the same, the node becomes conservative and its equilibrium strategy reduces from 0.3355 to 0.0049, whereas, node 1 and 2 become aggressive and their equilibrium strategy increases from 0.6008 to 0.6672 and 0.3355 to 0.5012, respectively. This reduces the probability of successful transmission for node 3, while that for other nodes increases. Figure 4.2 illustrates this for different selections of Δ_3^-. As a result, node 3 sees fewer successful tranmissions and its age keeps increasing.

Further, for each scenario we find the pure strategy Nash equilibrium by substituting the values of σ_{S}, σ_{I}, σ_{C} and $\boldsymbol{\Delta}^-$ in the payoff matrix shown in Figure 4.1. We see that for all selections of σ_{C}, multiple pure strategy Nash equilibria exist. While $(\mathcal{T},\mathcal{T},\mathcal{T})$ is a common equilibrium strategy for all selections of σ_{C}, we see that when $\sigma_{\mathrm{C}} < \sigma_{\mathrm{S}}$, the equilibrium strategy set comprises of $(\mathcal{T},\mathcal{I},\mathcal{T}),(\mathcal{I},\mathcal{T},\mathcal{T}),(\mathcal{T},\mathcal{T},\mathcal{I})$ indicating that nodes prefer transmit over idle. This is because when $\sigma_{\mathrm{C}} < \sigma_{\mathrm{S}}$, the age due to a collision ($\Delta_i = \Delta_i^- + \sigma_{\mathrm{C}}$) is less than that due to a busy slot ($\Delta_i = \Delta_i^- + \sigma_{\mathrm{S}}$). Similarly, when $\sigma_{\mathrm{C}} > \sigma_{\mathrm{S}}$, the equilibrium strategy set consists of $(\mathcal{I},\mathcal{I},\mathcal{T}),(\mathcal{T},\mathcal{I},\mathcal{I}),(\mathcal{I},\mathcal{T},\mathcal{I})$ indicating that nodes prefer idle over transmit, since the age due to a busy slot ($\Delta_i = \Delta_i^- + \sigma_{\mathrm{S}}$) would be less than that due to a collision ($\Delta_i = \Delta_i^- + \sigma_{\mathrm{C}}$).

4.7 Conclusion

We considered a network of selfish nodes that would like to minimize the age of their

updates at the other nodes. The nodes send their updates over a shared spectrum using a CSMA/CA based access mechanism. We modeled the resulting competition as a non-cooperative one-shot multiple access game and investigated equilibrium strategies for two distinct medium access settings (a) collisions are shorter than successful transmissions and (b) collisions are longer. We investigated competition in a CSMA/CA slot, where a node may choose to transmit or stay idle. We found that medium access settings exert strong incentive effects on the nodes and under decentralized decision making by the nodes, the access setting with longer successful transmissions is more vulnerable to collisions than the other. Specifically, we showed that when collisions are shorter, transmit is a weakly dominant strategy. This leads to all nodes transmitting in the CSMA/CA slot, therefore guaranteeing a collision. In contrast, when collisions are longer, no weakly dominant strategy exists. For the latter, under certain conditions on the ages at the beginning of the slot, we derived the mixed strategy Nash equilibrium.

Chapter 5
Discussion and Future Research Directions

In this work, we focussed on spectrum sharing amongst heterogeneous networks. While spectrum sharing caters to the data traffic growth, it introduces novel challenges that result from the networks having to coexist with each other. Coexistence could be challenging for several reasons, including disparity in spectrum access rights assigned to the networks by regulatory bodies and differences in technologies and utilities of the networks sharing the spectrum.

We began by investigating the coexistence of networks with disparate spectrum access rights. Specifically, we investigated the coexistence of White-Fi networks with licensed TV users in TV white spaces [21, 22]. We modeled the MAC throughput of a White-Fi network and proposed a heuristic algorithms to optimize it, given the spatial heterogeneity in channel availability and link quality. The algorithms assigned power, access probability, and channels to nodes in the network, under the constraint that reception at TV receivers is not impaired. We evaluated the efficacy of the proposed approach for city-wide White-Fi networks deployed over Denver and Columbus (respectively, low and high channel availability) in the USA, and compared with assignments cognizant of heterogeneity to a lesser degree, for example, akin to FCC regulations.

Next, we studied the coexistence of networks with different network objectives. We modeled the coexistence of an AON and a TON as a repeated game with networks as players [46–48]. The AON aimed to minimize the age of updates, and the TON sought to maximize throughput. The repeated games model allowed us to answer whether a simple coexistence etiquette that enables cooperation between an AON and a TON is self-enforceable. Specifically, we introduced a coordination device,

which is a randomized signaling device that allows the AON and the TON to access the spectrum in a non-interfering manner. The networks employed a grim trigger strategy when cooperating, which ensured that the networks would disobey the device only if competition were more beneficial than cooperation in the long run.

Further, we employed the proposed etiquette to two distinct practical medium access settings. One where collision slots are at least as large as slots that see a successful transmission, and the other where collision slots are smaller than successful transmission slots. For each access mechanism, via computational analysis, we showed that irrespective of the mechanism employed, as networks grow in size, cooperation cannot be sustained and is not self-enforceable.

Lastly, motivated by the distinct behavior of age optimizing network in our study of coexistence of age and throughput optimizing networks, we studied the coexistence of selfish nodes that share the spectrum using a CSMA/CA based access mechanism and have the same objective, that is, each node cares about timely delivery of its updates at other nodes in the network. We formulated a non-cooperative one-shot multiple access game with nodes as players, where each node values information freshness and would like to minimize the age of their updates at other nodes in the network [71]. We investigated nodes' equilibrium strategies in a CSMA/CA slot for the aforementioned medium access settings, i.e., when collisions are longer than successful transmissions and when they are shorter. For each setting, we provided insights into how competing nodes that value timeliness share the spectrum. We found that access settings exerted strong incentive effects and showed that under decentralized decision making by nodes, the access setting with longer successful transmissions is more vulnerable to collisions than the other.

5.1 Future Work

In this thesis, we proposed a simple game theoretic model that abstracts the coexistence of an AON and a TON, where, the TON obtains as payoff, at the end of a slot, the number of bits sent during the slot. As a result, a payoff of 0 is obtained at the end of an idle slot and also at the end of a collision slot. The payoff ignores the lengths of slots and wasted transmissions. In general, payoffs that distinguish between different slots and outcomes may be worth investigation. For example, the payoffs could incorporate the cost of transmission. In the future, we propose to investigate an extension of our model where network payoffs have transmission cost

included.

In addition to the above, we studied the coexistence of an AON and a TON under the implicit assumption that networks have equal access rights to the spectrum and defined the competitive mode of coexistence as one under which networks contend for the medium simultaneously [48]. However, as per the FCC ruling that opened up the $5.85 - 5.925$ GHz ITS band for unlicensed devices, the band's incumbents, i.e., the vehicular nodes, which value information timeliness, are the licensed primaries and the sharers, i.e., the WiFi devices, which desire high throughputs can be considered as the unlicensed secondaries with low priority. The resulting coexistence scenario is challenging because the primaries are highly mobile vehicular nodes that utilize spectrum in a dynamic manner in spatial and temporal dimensions. Motivated by this, in the future, we also propose to extend our work to study the coexistence of the networks where they have different access rights to the spectrum, i.e., the AON is the licensed primary and the TON is the unlicensed secondary network and protection of primaries from secondary interference is desired. We aim to model the interaction between the networks as a Stackelberg repeated game and study the stratified mode of coexistence, where the AON shares the spectrum with TON, networks access the medium sequentially, and only nodes in the network that accesses contend for the medium. Our objective is to compare competition with stratification to understand the corresponding gains and losses and determine the favorable coexistence mode.

Lastly, we investigated the coexistence of selfish nodes, each of which desires a small age of its updates at other nodes in the network and share the spectrum using a CSMA/CA based access mechanism. Specifically, we studied the one-shot game played by the nodes in a CSMA/CA slot [71]. However, realistically the interaction for spectrum access between selfish nodes is modeled as a repeated game. Hence, we propose to formulate a repeated game to study this coexistence scenario and, similar to [48], explore the possibility of cooperation between nodes in the network.

Chapter 6
Publications

- **S. Gopal**, S. K. Kaul, R. Chaturvedi and S. Roy, "Coexistence of Age and Throughput Optimizing Networks: A Spectrum Sharing Game," accepted for publication at IEEE/ACM Transactions on Networking 2021.
- **S. Gopal**, S. K. Kaul, R. Chaturvedi and S. Roy, "A Non-Cooperative Multiple Access Game for Timely Updates," Proc. 3rd IEEE INFOCOM Wkshop on Age of Information, Toronto, CA, July 2020.
- **S. Gopal**, S. K. Kaul and R. Chaturvedi, "Coexistence of Age and Throughput Optimizing Networks: A Game Theoretic Approach," 2019 IEEE 30th Annual International Symposium on Personal, Indoor and Mobile Radio Communications (PIMRC).
- **S. Gopal** and S. K. Kaul, "A game theoretic approach to DSRC and WiFi coexistence," IEEE INFOCOM 2018 - IEEE Conference on Computer Communications Workshops (INFOCOM WKSHPS), Honolulu, HI, 2018, pp. 565-570.
- **S. Gopal**, S. K. Kaul and S. Roy, "Optimizing City-Wide White-Fi Networks in TV White Spaces," in IEEE Transactions on Cognitive Communications and Networking, vol. 4, no. 4, pp. 749-763, Dec. 2018.
- **S. Gopal**, S. Kaul and S. Roy, "Optimizing Outdoor White-Fi Networks in TV White Spaces," in IEEE International Conference on Communications (ICC), 2016, pp. 2749-2755.

Appendix A
Solve for Access

We show how the problem of maximizing $T_m^{(s)}$ can be reduced to a minimization problem (2.16)-(2.17) in a single-variable $\tau_j^{(s)}$ of node j, where j is the node in cell m whose payload rate $R_{jj'}^{(s)}$ on channel s is the smallest amongst all nodes in the cell. We also show that the resulting problem (2.16)-(2.17) is convex in $\tau_j^{(s)}$.

The throughput of the i^{th} node in cell m on a channel s assigned to it is given as $T_{i,m}^{(s)} = \frac{p_{\text{succ,i}}^{(s)} L}{\sigma_{\text{avg}}^{(s)}}$. On simplifying $T_{i,m}^{(s)}$ we get

$$T_{i,m}^{(s)} = \left[\frac{1}{L} \left(\frac{p_{\text{I}}}{p_{\text{succ,i}}^{(s)}} \sigma + T_{\text{succ,i}} + \left(\sum_{\substack{j \in \mathcal{N}_m \\ j \neq i}} \frac{p_{\text{succ,j}}^{(s)}}{p_{\text{succ,i}}^{(s)}} T_{\text{succ,j}} \right) + \left(\frac{1}{p_{\text{succ,i}}^{(s)}} - \frac{p_{\text{I}}}{p_{\text{succ,i}}^{(s)}} - 1 - \sum_{\substack{j \in \mathcal{N}_m \\ j \neq i}} \frac{p_{\text{succ,j}}^{(s)}}{p_{\text{succ,i}}^{(s)}} \right) T_{\text{col}} \right) \right]^{-1},$$

where the probability $p_{\text{succ,i}}^{(s)}$ that a transmission by i is successful and the probability p_{I} that a slot is idle is given in (2.5). Using the time fairness constraint (2.10), we can write $p_{\text{succ,i}}^{(s)} R_{jj'}^{(s)} = p_{\text{succ,j}}^{(s)} R_{ii'}^{(s)}$, which gives

$$\tau_i^{(s)} = \frac{\tau_j^{(s)} R_{ii'}^{(s)}}{(1 - \tau_j^{(s)}) R_{jj'}^{(s)} + \tau_j^{(s)} R_{ii'}^{(s)}}. \tag{A.1}$$

By substituting $p_{\text{succ,i}}^{(s)}$ and p_{I} from (2.5) and $\tau_j^{(s)}$ from (A.1) we get

$$T_{i,m}^{(s)} = \left[f_1(P) + \frac{R_{jj'}^{(s)}}{L R_{ii'}^{(s)}} \left(\frac{1 - \tau_j^{(s)}}{\tau_j^{(s)}} \sigma + \left(\prod_{k \in \mathcal{N}_m} \left(\frac{R_{kk'}^{(s)}}{R_{jj'}^{(s)}} + \frac{1 - \tau_j^{(s)}}{\tau_j^{(s)}} \right) - \frac{1 - \tau_j^{(s)}}{\tau_j^{(s)}} - f_2(P) \right) T_{\text{col}} \right) \right]^{-1},$$

where, $f_1(P) = \frac{T_{\text{succ,i}}}{L} + \left(\sum_{\substack{j \in \mathcal{N}_m \\ j \neq i}} \frac{R^{(s)}_{jj'}}{LR^{(s)}_{ii'}} T_{\text{succ,j}} \right)$, $f_2(P) = \frac{R^{(s)}_{ii'}}{R^{(s)}_{jj'}} \left(1 + \sum_{\substack{j \in \mathcal{N}_m \\ j \neq i}} \frac{R^{(s)}_{jj'}}{R^{(s)}_{ii'}} \right)$. Observe that $f_1(P)$ and $f_2(P)$ are independent of $\tau_j^{(s)}$ and do not affect the optimal $\tau_j^{(s)}$. This allows us to reduce the throughput maximization problem to the problem (2.16)-(2.17).

Next we show that (2.16)-(2.17) is a convex optimization problem. Define $f(\tau_j^{(s)})$ to be the utility function (Equation (2.16)) in the problem (2.16)-(2.17). The function $f(\tau_j^{(s)})$ may be written as

$$f(\tau_j^{(s)}) = \sigma f_1(\tau_j^{(s)}) + T_{\text{col}} f_2(\tau_j^{(s)}), \tag{A.2}$$

where $f_1(\tau_j^{(s)}) = \frac{1-\tau_j^{(s)}}{\tau_j^{(s)}}$, $f_2(\tau_j^{(s)}) = \prod_{k \in \mathcal{N}_m} \left(\frac{R^{(s)}_{kk'}}{R^{(s)}_{jj'}} + \frac{1-\tau_j^{(s)}}{\tau_j^{(s)}} \right) - \frac{1-\tau_j^{(s)}}{\tau_j^{(s)}}$. $f_1(\tau_j^{(s)})$ is a non-increasing convex function on the interval $[0, 1]$. Next, we show that the function $f_2(\tau_j^{(s)})$ is also a convex function. For this, we rewrite $f_2(\tau_j^{(s)})$ as

$$f_2(\tau_j^{(s)}) = \frac{1}{\tau_j^{(s)}} \left(\prod_{\substack{k \in \mathcal{N}_m \\ k \neq j}} \left(\frac{R^{(s)}_{kk'}}{R^{(s)}_{jj'}} + \frac{1-\tau_j^{(s)}}{\tau_j^{(s)}} \right) - 1 \right) + 1,$$

and use the following fact [113, Chapter 3, Question 3.32].

Lemma 1. *If $f : \mathcal{R} \to \mathcal{R} : x \mapsto f(x)$ and $g : \mathcal{R} \to \mathcal{R} : x \mapsto g(x)$ are both convex, non-decreasing (or non-increasing) and positive, then $h : \mathcal{R} \to \mathcal{R} : x \mapsto h(x) = f(x)g(x)$ is also convex.*

Observe that $f_2(\tau_j^{(s)})$ consists of a product of $\frac{1}{\tau_j^{(s)}}$ and $\left(\prod_{\substack{k \in \mathcal{N}_m \\ k \neq j}} \left(\frac{R^{(s)}_{kk'}}{R^{(s)}_{jj'}} + \frac{1-\tau_j^{(s)}}{\tau_j^{(s)}} \right) - 1 \right)$. Both the functions are convex, non-increasing and positive functions on the interval $[0, 1]$. Hence, using Lemma 1, the product of these functions i.e. $f_2(\tau_j^{(s)})$ is also convex on the interval $[0, 1]$.

Therefore, $f(\tau_j^{(s)})$ in (A.2) is a non-negative weighted sum of convex functions i.e. $f_1(\tau_j^{(s)})$ and $f_2(\tau_j^{(s)})$, and hence a convex function [113]. Also note that the constraint set given by (2.17) is convex. Thus the problem (2.16)-(2.17) is a convex optimization problem.

Appendix B
Strategy of the AON and the TON

B.1 Mixed Strategy Nash Equilibrium (MSNE)

We define $\boldsymbol{\tau^*} = [\tau_{\mathrm{A}}^*, \tau_{\mathrm{T}}^*]$ as the parameter required to compute the mixed strategy Nash equilibrium of the one-shot game. We begin by finding the τ_{A}^* of the AON by solving the optimization problem

$$\begin{aligned} \textbf{OPT I:} \quad & \underset{\tau_{\mathrm{A}}}{\text{minimize}} \quad u_{\mathbb{NC}}^{\mathrm{A}} \\ & \text{subject to} \quad 0 \leq \tau_{\mathrm{A}} \leq 1. \end{aligned} \tag{B.1}$$

where, $u_{\mathbb{NC}}^{\mathrm{A}}$ is the payoff of the AON defined as

$$\begin{aligned} u_{\mathbb{NC}}^{\mathrm{A}} = &(1-\tau_{\mathrm{A}}(1-\tau_{\mathrm{A}})^{(\mathrm{N_A}-1)}(1-\tau_{\mathrm{T}})^{\mathrm{N_T}})\widetilde{\Delta}^{-} + (1-\tau_{\mathrm{A}})^{\mathrm{N_A}}(1-\tau_{\mathrm{T}})^{\mathrm{N_T}}(\sigma_{\mathrm{I}}-\sigma_{\mathrm{C}}) + \sigma_{\mathrm{C}} \\ &+ (\mathrm{N_A}\tau_{\mathrm{A}}(1-\tau_{\mathrm{A}})^{(\mathrm{N_A}-1)}(1-\tau_{\mathrm{T}})^{\mathrm{N_T}} + \mathrm{N_T}\tau_{\mathrm{T}}(1-\tau_{\mathrm{T}})^{(\mathrm{N_T}-1)}(1-\tau_{\mathrm{A}})^{\mathrm{N_A}})(\sigma_{\mathrm{S}}-\sigma_{\mathrm{C}}). \end{aligned}$$

The Lagrangian of the optimization problem (B.1) is

$$\mathcal{L}(\tau_{\mathrm{A}}, \mu) = u_{\mathbb{NC}}^{\mathrm{A}} - \mu_1\tau_{\mathrm{A}} + \mu_2(\tau_{\mathrm{A}} - 1).$$

where $\boldsymbol{\mu} = [\mu_1, \mu_2]^T$ is the Karush-Kuhn-Tucker (KKT) multiplier vector. The first derivative of the objective function in (B.1) is

$$\begin{aligned} {u_{\mathbb{NC}}^{\mathrm{A}}}' = &-\widetilde{\Delta}^{-}(1-\tau_{\mathrm{T}})^{\mathrm{N_T}}[(1-\tau_{\mathrm{A}})^{(\mathrm{N_A}-1)} - (\mathrm{N_A}-1)\tau_{\mathrm{A}}(1-\tau_{\mathrm{A}})^{(\mathrm{N_A}-2)}] \\ &+ (\sigma_{\mathrm{S}}-\sigma_{\mathrm{C}})[(1-\tau_{\mathrm{T}})^{\mathrm{N_T}}(\mathrm{N_A}(1-\tau_{\mathrm{A}})^{(\mathrm{N_A}-1)} - \mathrm{N_A}(\mathrm{N_A}-1)\tau_{\mathrm{A}}(1-\tau_{\mathrm{A}})^{(\mathrm{N_A}-2)}) \\ &- \mathrm{N_T}\tau_{\mathrm{T}}(1-\tau_{\mathrm{T}})^{(\mathrm{N_T}-1)}(1-\tau_{\mathrm{A}})^{\mathrm{N_A}-1}] - (\sigma_{\mathrm{I}}-\sigma_{\mathrm{C}})\mathrm{N_A}(1-\tau_{\mathrm{T}})^{\mathrm{N_T}}(1-\tau_{\mathrm{A}})^{(\mathrm{N_A}-1)}. \end{aligned}$$

The KKT conditions can be written as

$$u_{\mathbb{NC}}^{\mathrm{A}}{}' - \mu_1 + \mu_2 = 0, \tag{B.2a}$$
$$-\mu_1 \tau_{\mathrm{A}} = 0, \tag{B.2b}$$
$$\mu_2(\tau_{\mathrm{A}} - 1) = 0, \tag{B.2c}$$
$$-\tau_{\mathrm{A}} \leq 0, \tag{B.2d}$$
$$\tau_{\mathrm{A}} - 1 \leq 0, \tag{B.2e}$$
$$\boldsymbol{\mu} = [\mu_1, \mu_2]^T \geq 0. \tag{B.2f}$$

We consider three cases. In case (i), we consider $\mu_1 = \mu_2 = 0$. From the stationarity condition (B.2a), we get

$$\tau_{\mathrm{A}} = \frac{(1-\tau_{\mathrm{T}})(\widetilde{\Delta}^{-} - \mathrm{N_A}(\sigma_{\mathrm{S}} - \sigma_{\mathrm{I}})) + \mathrm{N_A N_T}\tau_{\mathrm{T}}(\sigma_{\mathrm{S}} - \sigma_{\mathrm{C}})}{\left(\begin{array}{r}(1-\tau_{\mathrm{T}})\mathrm{N_A}(\widetilde{\Delta}^{-} + (\sigma_{\mathrm{I}} - \sigma_{\mathrm{C}}) - \mathrm{N_A}(\sigma_{\mathrm{S}} - \sigma_{\mathrm{C}})) \\ + \mathrm{N_A N_T}\tau_{\mathrm{T}}(\sigma_{\mathrm{S}} - \sigma_{\mathrm{C}})\end{array}\right)}.$$

In case (ii) we consider $\mu_1 \geq 0, \mu_2 = 0$. Again, using (B.2a), we get $\mu_1 = u_{\mathbb{NC}}^{\mathrm{A}}{}'$. From (B.2f), we have $\mu_1 \geq 0$, therefore, $u_{\mathbb{NC}}^{\mathrm{A}}{}' \geq 0$. On solving this inequality on $u_{\mathbb{NC}}^{\mathrm{A}}{}'$ we get, $\widetilde{\Delta}^{-} \leq \Theta_{\mathrm{th},0}$, where $\Theta_{\mathrm{th},0} = \mathrm{N_A}(\sigma_{\mathrm{S}} - \sigma_{\mathrm{I}}) - \frac{\mathrm{N_A N_T}\tau_{\mathrm{T}}(\sigma_{\mathrm{S}} - \sigma_{\mathrm{C}})}{(1-\tau_{\mathrm{T}})}$.

Finally, in case (iii) we consider $\mu_1 = 0, \mu_2 \geq 0$. On solving (B.2a), we get $\widetilde{\Delta}^{-} \leq \Theta_{\mathrm{th},1}$, where $\Theta_{\mathrm{th},1} = \mathrm{N_A}(\sigma_{\mathrm{S}} - \sigma_{\mathrm{C}})$.

Therefore, the solution from the KKT condition is

$$\tau_{\mathrm{A}}^{*} = \begin{cases} \dfrac{(1-\tau_{\mathrm{T}}^{*})(\widetilde{\Delta}^{-} - \mathrm{N_A}(\sigma_{\mathrm{S}} - \sigma_{\mathrm{I}})) + \mathrm{N_A N_T}\tau_{\mathrm{T}}^{*}(\sigma_{\mathrm{S}} - \sigma_{\mathrm{C}})}{\left(\begin{array}{r}(1-\tau_{\mathrm{T}}^{*})\mathrm{N_A}(\widetilde{\Delta}^{-} + (\sigma_{\mathrm{I}} - \sigma_{\mathrm{C}}) - \mathrm{N_A}(\sigma_{\mathrm{S}} - \sigma_{\mathrm{C}})) \\ + \mathrm{N_A N_T}\tau_{\mathrm{T}}^{*}(\sigma_{\mathrm{S}} - \sigma_{\mathrm{C}})\end{array}\right)} & \widetilde{\Delta}^{-} > \Theta_{\mathrm{th}}, \\ 1 & \widetilde{\Delta}^{-} \leq \Theta_{\mathrm{th}} \ \&\ \Theta_{\mathrm{th}} = \Theta_{\mathrm{th},1}, \\ 0 & \widetilde{\Delta}^{-} \leq \Theta_{\mathrm{th}} \ \&\ \Theta_{\mathrm{th}} = \Theta_{\mathrm{th},0}. \end{cases} \tag{B.3}$$

where, $\Theta_{\mathrm{th}} = \max\{\Theta_{\mathrm{th},0}, \Theta_{\mathrm{th},1}\}$. Under the assumption that length of successful transmission is equal to the length of collision, i.e., $\sigma_{\mathrm{S}} = \sigma_{\mathrm{C}}$, (B.3) reduces to

$$\tau_{\mathrm{A}}^{*} = \begin{cases} \dfrac{\mathrm{N_A}(\sigma_{\mathrm{I}} - \sigma_{\mathrm{S}}) + \widetilde{\Delta}^{-}}{\mathrm{N_A}(\sigma_{\mathrm{I}} - \sigma_{\mathrm{C}} + \widetilde{\Delta}^{-})} & \widetilde{\Delta}^{-} > \mathrm{N_A}(\sigma_{\mathrm{S}} - \sigma_{\mathrm{I}}), \\ 0 & \text{otherwise .} \end{cases}$$

Similarly, we find τ_{T}^* for the TON by solving the optimization problem

$$\begin{aligned} \textbf{OPT II:} \quad & \underset{\tau_{\mathrm{T}}}{\text{minimize}} \quad -u_{\mathbb{NC}}^{\mathrm{T}} \\ & \text{subject to} \quad 0 \leq \tau_{\mathrm{T}} \leq 1. \end{aligned} \tag{B.4}$$

where, $u_{\mathbb{NC}}^{\mathrm{T}}$ is the payoff of the TON defined as

$$u_{\mathbb{NC}}^{\mathrm{T}} = \tau_{\mathrm{T}}(1-\tau_{\mathrm{T}})^{(\mathrm{N_T}-1)}(1-\tau_{\mathrm{A}})^{\mathrm{N_A}}\sigma_{\mathrm{S}}.$$

The Lagrangian of the optimization problem (B.4) is

$$\mathcal{L}(\tau_{\mathrm{T}}, \mu) = -u_{\mathbb{NC}}^{\mathrm{T}} - \mu_1\tau_{\mathrm{T}} + \mu_2(\tau_{\mathrm{T}} - 1).$$

where $\boldsymbol{\mu} = [\mu_1, \mu_2]^T$ is the KKT multiplier vector. The first derivative of $u_{\mathbb{NC}}^{\mathrm{T}}$ is

$$u_{\mathbb{NC}}^{\mathrm{T}}{}' = (1-\tau_{\mathrm{A}})^{\mathrm{N_A}}(1-\tau_{\mathrm{T}})^{(\mathrm{N_T}-1)}\sigma_{\mathrm{S}} - (\mathrm{N_T}-1)\tau_{\mathrm{T}}(1-\tau_{\mathrm{T}})^{(\mathrm{N_T}-2)}(1-\tau_{\mathrm{A}})^{\mathrm{N_A}}\sigma_{\mathrm{S}}.$$

The KKT conditions can be written as

$$-u_{\mathbb{NC}}^{\mathrm{T}}{}' - \mu_1 + \mu_2 = 0, \tag{B.5a}$$

$$-\mu_1\tau_{\mathrm{T}} = 0, \tag{B.5b}$$

$$\mu_2(\tau_{\mathrm{T}} - 1) = 0, \tag{B.5c}$$

$$-\tau_{\mathrm{T}} \leq 0, \tag{B.5d}$$

$$\tau_{\mathrm{T}} - 1 \leq 0, \tag{B.5e}$$

$$\boldsymbol{\mu} = [\mu_1, \mu_2]^T \geq 0. \tag{B.5f}$$

We consider three cases. In case (i), we consider $\mu_1 = \mu_2 = 0$. From the stationarity condition in (B.5a), we get $u_{\mathbb{NC}}^{\mathrm{T}}{}' = 0$. On solving (B.5a), we get $\tau_{\mathrm{T}}^* = 1/\mathrm{N_T}$. In case (ii) we consider $\mu_1 \geq 0, \mu_2 = 0$. Again, using (B.5a), we get $\mu_1 = -u_{\mathbb{NC}}^{\mathrm{T}}{}'$. From (B.5f), we have $\mu_1 \geq 0$, therefore, $u_{\mathbb{NC}}^{\mathrm{T}}{}' \leq 0$. On solving this inequality on $u_{\mathbb{NC}}^{\mathrm{T}}{}'$, we get $\tau_{\mathrm{T}}^* \geq 1/\mathrm{N_T}$. Finally, in case (iii) we consider $\mu_1 = 0, \mu_2 \geq 0$ and on solving (B.5a) we get $\mu_2 = u_{\mathbb{NC}}^{\mathrm{T}}{}'$. Since $\mu_2 \geq 0$ from (B.5f), we have $u_{\mathbb{NC}}^{\mathrm{T}}{}' \geq 0$. On solving this inequality, we get $\tau_{\mathrm{T}}^* \leq 1/\mathrm{N_T}$. Therefore, the solution from the KKT conditions is $\tau_{\mathrm{T}}^* = 1/\mathrm{N_T}$.

Note that any Mixed Strategy Nash Equilibrium (MSNE) $(\tau_{\mathrm{A}}^*, \tau_{\mathrm{T}}^*)$ is a solution of the optimization problems OPT I and OPT II. All solutions to the OPT I and OPT

II must satisfy the necessary KKT conditions. Since these conditions yield a unique solution $(\tau_{\mathrm{A}}^*, \tau_{\mathrm{T}}^*)$, this is the only MSNE.

B.2 Optimal Strategy under Cooperation

We define $\widehat{\boldsymbol{\tau}} = [\widehat{\tau}_A, \widehat{\tau}_T]$ as the optimal strategy of the one-shot game when networks cooperate. We begin by finding the $\widehat{\tau}_A$ of the AON by solving the optimization problem

$$\begin{aligned} \textbf{OPT I:} \quad & \underset{\widehat{\tau}_A}{\text{minimize}} \quad u_{\mathbb{C}}^{\mathrm{A}} \\ & \text{subject to} \quad 0 \leq \widehat{\tau}_A \leq 1. \end{aligned} \tag{B.6}$$

where, $u_{\mathbb{C}}^{\mathrm{A}}$ is the payoff of AON defined as

$$\begin{aligned} u_{\mathbb{C}}^{\mathrm{A}} = (1 - \mathrm{P_R}\tau_{\mathrm{A}}(1-\tau_{\mathrm{A}})^{(\mathrm{N_A}-1)})\widetilde{\Delta}^{-} + \sigma_{\mathrm{C}} + (\mathrm{P_R}(1-\tau_{\mathrm{A}})^{\mathrm{N_A}} + (1-\mathrm{P_R})(1-\tau_{\mathrm{T}})^{\mathrm{N_T}}) \\ (\sigma_{\mathrm{I}} - \sigma_{\mathrm{C}}) + ((1-\mathrm{P_R})\mathrm{N_T}\tau_{\mathrm{T}}(1-\tau_{\mathrm{T}})^{(\mathrm{N_T}-1)} + \mathrm{P_R}\mathrm{N_A}\tau_{\mathrm{A}}(1-\tau_{\mathrm{A}})^{(\mathrm{N_A}-1)})(\sigma_{\mathrm{S}} - \sigma_{\mathrm{C}}). \end{aligned}$$

The Lagrangian of the optimization problem (B.6) is

$$\mathcal{L}(\tau_{\mathrm{A}}, \mu) = u_{\mathbb{C}}^{\mathrm{A}} - \mu_1\tau_{\mathrm{A}} + \mu_2(\tau_{\mathrm{A}} - 1).$$

where $\boldsymbol{\mu} = [\mu_1, \mu_2]^T$ is the Karush-Kuhn-Tucker (KKT) multiplier vector. The first derivative of the objective function in (B.6) is

$$\begin{aligned} u_{\mathbb{C}}^{\mathrm{A}\prime} = -\mathrm{P_R}\widetilde{\Delta}^{-}[(1-\tau_{\mathrm{A}})^{(\mathrm{N_A}-1)} - (\mathrm{N_A}-1)\tau_{\mathrm{A}}(1-\tau_{\mathrm{A}})^{(\mathrm{N_A}-2)}] + (\sigma_{\mathrm{S}} - \sigma_{\mathrm{C}}) \\ \mathrm{P_R}\mathrm{N_A}[(1-\tau_{\mathrm{A}})^{\mathrm{N_A}-1} - (\mathrm{N_A}-1)\tau_{\mathrm{A}}(1-\tau_{\mathrm{A}})^{(\mathrm{N_A}-2)}] - (\sigma_{\mathrm{I}} - \sigma_{\mathrm{C}})\mathrm{P_R}\mathrm{N_A}(1-\tau_{\mathrm{A}})^{(\mathrm{N_A}-1)}. \end{aligned}$$

The KKT conditions can be written as

$$u_{\mathbb{C}}^{\mathrm{A}\prime} - \mu_1 + \mu_2 = 0, \tag{B.7a}$$

$$-\mu_1\tau_{\mathrm{A}} = 0, \tag{B.7b}$$

$$\mu_2(\tau_{\mathrm{A}} - 1) = 0, \tag{B.7c}$$

$$-\tau_{\mathrm{A}} \leq 0, \tag{B.7d}$$

$$\tau_{\mathrm{A}} - 1 \leq 0, \tag{B.7e}$$

$$\boldsymbol{\mu} = [\mu_1, \mu_2]^T \geq 0. \tag{B.7f}$$

We consider three cases. In case (i), we consider $\mu_1 = \mu_2 = 0$. From the stationarity condition (B.7a), we get

$$\tau_{\mathrm{A}} = \frac{\widetilde{\Delta}^{-} - \mathrm{N_A}(\sigma_{\mathrm{S}} - \sigma_{\mathrm{I}})}{\mathrm{N_A}(\widetilde{\Delta}^{-} + (\sigma_{\mathrm{I}} - \sigma_{\mathrm{C}}) - \mathrm{N_A}(\sigma_{\mathrm{S}} - \sigma_{\mathrm{C}}))}.$$

In case (ii) we consider $\mu_1 \geq 0, \mu_2 = 0$. Again, using (B.7a), we get $\mu_1 = u_{\mathbb{C}}^{\mathrm{A}\prime}$. From (B.7f), we have $\mu_1 \geq 0$, therefore, $u_{\mathbb{C}}^{\mathrm{A}\prime} \geq 0$. On solving this inequality on $u_{\mathbb{C}}^{\mathrm{A}\prime}$ we get, $\widetilde{\Delta}^{-} \leq \Theta_{\mathrm{th},0}$, where $\Theta_{\mathrm{th},0} = \mathrm{N_A}(\sigma_{\mathrm{S}} - \sigma_{\mathrm{I}})$.

Finally, in case (iii) we consider $\mu_1 = 0, \mu_2 \geq 0$. On solving (B.7a), we get $\widetilde{\Delta}^{-} \leq \Theta_{\mathrm{th},1}$, where $\Theta_{\mathrm{th},1} = \mathrm{N_A}(\sigma_{\mathrm{S}} - \sigma_{\mathrm{C}})$.

Therefore, the solution from the KKT condition is

$$\widehat{\tau}_A = \begin{cases} \dfrac{\widetilde{\Delta}^{-} - \mathrm{N_A}(\sigma_{\mathrm{S}} - \sigma_{\mathrm{I}})}{\mathrm{N_A}(\widetilde{\Delta}^{-} + (\sigma_{\mathrm{I}} - \sigma_{\mathrm{C}}) - \mathrm{N_A}(\sigma_{\mathrm{S}} - \sigma_{\mathrm{C}}))} & \widetilde{\Delta}^{-} > \Theta_{\mathrm{th}}, \\ 1 & \widetilde{\Delta}^{-} \leq \Theta_{\mathrm{th}} \ \& \ \Theta_{\mathrm{th}} = \Theta_{\mathrm{th},1}, \\ 0 & \widetilde{\Delta}^{-} \leq \Theta_{\mathrm{th}} \ \& \ \Theta_{\mathrm{th}} = \Theta_{\mathrm{th},0}. \end{cases} \tag{B.8}$$

where, $\Theta_{\mathrm{th}} = \max\{\Theta_{\mathrm{th},0}, \Theta_{\mathrm{th},1}\}$. Under the assumption that length of successful transmission is equal to the length of collision i.e. $\sigma_{\mathrm{S}} = \sigma_{\mathrm{C}}$, (B.8) reduces to

$$\widehat{\tau}_A = \begin{cases} \dfrac{\mathrm{N_A}(\sigma_{\mathrm{I}} - \sigma_{\mathrm{S}}) + \widetilde{\Delta}^{-}}{\mathrm{N_A}(\sigma_{\mathrm{I}} - \sigma_{\mathrm{C}} + \widetilde{\Delta}^{-})} & \widetilde{\Delta}^{-} > \mathrm{N_A}(\sigma_{\mathrm{S}} - \sigma_{\mathrm{I}}), \\ 0 & \text{otherwise .} \end{cases}$$

Similarly, we find $\widehat{\tau}_T$ for the TON by solving the optimization problem

$$\textbf{OPT II:} \quad \underset{\tau_{\mathrm{T}}}{\text{minimize}} \quad -u_{\mathbb{C}}^{\mathrm{T}} \qquad \text{subject to} \quad 0 \leq \tau_{\mathrm{T}} \leq 1. \tag{B.9}$$

where, $u_{\mathbb{C}}^{\mathrm{T}}$ is the payoff of TON defined as

$$u_{\mathbb{C}}^{\mathrm{T}} = (1 - \mathrm{P_R})\tau_{\mathrm{T}}(1 - \tau_{\mathrm{T}})^{(\mathrm{N_T}-1)}\sigma_{\mathrm{S}}.$$

The Lagrangian of the optimization problem (B.9) is

$$\mathcal{L}(\tau_{\mathrm{T}}, \mu) = -u_{\mathbb{C}}^{\mathrm{T}} - \mu_1\tau_{\mathrm{T}} + \mu_2(\tau_{\mathrm{T}} - 1).$$

where $\boldsymbol{\mu} = [\mu_1, \mu_2]^T$ is the KKT multiplier vector. The first derivative of $u_{\mathbb{C}}^{\mathrm{T}}$ is

$$u_{\mathbb{C}}^{\mathrm{T}\prime} = (1 - \mathrm{P_R})\sigma_{\mathrm{S}}[(1 - \tau_{\mathrm{T}})^{(\mathrm{N_T}-1)} - (\mathrm{N_T} - 1)\tau_{\mathrm{T}}(1 - \tau_{\mathrm{T}})^{(\mathrm{N_T}-2)}].$$

The KKT conditions can be written as

$$-u_{\mathbb{C}}^{\mathrm{T}\prime} - \mu_1 + \mu_2 = 0, \tag{B.10a}$$

$$-\mu_1\tau_{\mathrm{T}} = 0, \tag{B.10b}$$

$$\mu_2(\tau_{\mathrm{T}} - 1) = 0, \tag{B.10c}$$

$$-\tau_{\mathrm{T}} \leq 0, \tag{B.10d}$$

$$\tau_{\mathrm{T}} - 1 \leq 0, \tag{B.10e}$$

$$\boldsymbol{\mu} = [\mu_1, \mu_2]^T \geq 0. \tag{B.10f}$$

We consider three cases. In case (i), we consider $\mu_1 = \mu_2 = 0$. From the stationarity condition in (B.10a), we get $u_{\mathbb{C}}^{\mathrm{T}\prime} = 0$. On solving (B.10a), we get $\widehat{\tau}_T = 1/\mathrm{N_T}$. In case (ii) we consider $\mu_1 \geq 0, \mu_2 = 0$. Again, using (B.10a), we get $\mu_1 = -u_{\mathbb{C}}^{\mathrm{T}\prime}$. From (B.10f), we have $\mu_1 \geq 0$, therefore, $u_{\mathbb{C}}^{\mathrm{T}\prime} \leq 0$. On solving this inequality on $u_{\mathbb{C}}^{\mathrm{T}\prime}$, we get $\widehat{\tau}_T \geq 1/\mathrm{N_T}$. Finally, in case (iii) we consider $\mu_1 = 0, \mu_2 \geq 0$ and on solving (B.10a) we get $\mu_2 = u_{\mathbb{C}}^{\mathrm{T}\prime}$. Since $\mu_2 \geq 0$ (B.10f), we have $u_{\mathbb{C}}^{\mathrm{T}\prime} \geq 0$. On solving this inequality, we get $\widehat{\tau}_T \leq 1/\mathrm{N_T}$. Therefore, the solution from the KKT conditions is $\widehat{\tau}_T = 1/\mathrm{N_T}$.

Note that all solutions to the optimization problems, OPT I and OPT II, must satisfy the necessary KKT conditions and since these conditions yield a unique solution $(\widehat{\tau}_A, \widehat{\tau}_T)$, this is the unique global solution.

Bibliography

[1] T. Barnett, S. Jain, U. Andra, and T. Khurana, "Cisco visual networking index (vni), complete forecast update, 2017–2022," *Americas/EMEAR Cisco Knowledge Network (CKN) Presentation*, 2018.

[2] S. Gopal, "Tv whitespace data," https://sneihilg.github.io/TV-Database/, 2018.

[3] E. G. Larsson, O. Edfors, F. Tufvesson, and T. L. Marzetta, "Massive mimo for next generation wireless systems," *IEEE Communications Magazine*, vol. 52, no. 2, pp. 186–195, 2014.

[4] A. Faisal, H. Sarieddeen, H. Dahrouj, T. Y. Al-Naffouri, and M.-S. Alouini, "Ultra-massive mimo systems at terahertz bands: Prospects and challenges," *arXiv preprint arXiv:1902.11090*, 2019.

[5] L. Lu, G. Y. Li, A. L. Swindlehurst, A. Ashikhmin, and R. Zhang, "An overview of massive mimo: Benefits and challenges," *IEEE Journal of Selected Topics in Signal Processing*, vol. 8, no. 5, pp. 742–758, 2014.

[6] J. G. Andrews, S. Buzzi, W. Choi, S. V. Hanly, A. Lozano, A. C. Soong, and J. C. Zhang, "What will 5g be?" *IEEE Journal on Selected Areas in Communications*, vol. 32, no. 6, pp. 1065–1082, 2014.

[7] B. Romanous, N. Bitar, A. Imran, and H. Refai, "Network densification: Challenges and opportunities in enabling 5g," in *IEEE 20th International Workshop on Computer Aided Modelling and Design of Communication Links and Networks (CAMAD) 2015*. IEEE, 2015, pp. 129–134.

[8] J. G. Andrews, "Seven ways that hetnets are a cellular paradigm shift," *IEEE Communications Magazine*, vol. 51, no. 3, pp. 136–144, 2013.

[9] J. G. Andrews, H. Claussen, M. Dohler, S. Rangan, and M. C. Reed, "Femtocells: Past, present, and future," *IEEE Journal on Selected Areas in Communications*, vol. 30, no. 3, pp. 497–508, 2012.

[10] M. Bennis, M. Simsek, A. Czylwik, W. Saad, S. Valentin, and M. Debbah, "When cellular meets wifi in wireless small cell networks," *IEEE Communications Magazine*, vol. 51, no. 6, pp. 44–50, 2013.

[11] J. Lee, Y. Kim, H. Lee, B. L. Ng, D. Mazzarese, J. Liu, W. Xiao, and Y. Zhou, "Coordinated multipoint transmission and reception in lte-advanced systems," *IEEE Communications Magazine*, vol. 50, no. 11, pp. 44–50, 2012.

[12] O. Galinina, S. Andreev, M. Gerasimenko, Y. Koucheryavy, N. Himayat, S.-P. Yeh, and S. Talwar, "Capturing spatial randomness of heterogeneous cellular/wlan deployments with dynamic traffic," *IEEE Journal on Selected Areas in Communications*, vol. 32, no. 6, pp. 1083–1099, 2014.

[13] J. G. Andrews, S. Singh, Q. Ye, X. Lin, and H. S. Dhillon, "An overview of load balancing in hetnets: Old myths and open problems," *IEEE Wireless Communications*, vol. 21, no. 2, pp. 18–25, 2014.

[14] V. Chandrasekhar, J. G. Andrews, and A. Gatherer, "Femtocell networks: a survey," *IEEE Communications Magazine*, vol. 46, no. 9, pp. 59–67, 2008.

[15] X. Lin and H. Viswanathan, "Dynamic spectrum refarming with overlay for legacy devices," *IEEE Transactions on Wireless Communications*, vol. 12, no. 10, pp. 5282–5293, 2013.

[16] ——, "Dynamic spectrum refarming of gsm spectrum for lte small cells," in *2013 IEEE Globecom Workshops (GC Wkshps)*, 2013, pp. 690–695.

[17] S. Bhattarai, J.-M. J. Park, B. Gao, K. Bian, and W. Lehr, "An overview of dynamic spectrum sharing: Ongoing initiatives, challenges, and a roadmap for future research," *IEEE Transactions on Cognitive Communications and Networking*, vol. 2, no. 2, pp. 110–128, 2016.

[18] F. C. Commission, "Fcc-15-99a1_rcd," https://apps.fcc.gov/edocs_public/attachmatch/FCC-15-99A1_Rcd.pdf, adopted: August 6, 2015, Released: August 11, 2015.

[19] E. CEPT, "Technical and operational requirements for the possible operation of cognitive radio systems in the white spaces of the frequency band 470-790 mhz," *ECC report*, vol. 159, 2011.

[20] J. Liu, G. Naik, and J.-M. J. Park, "Coexistence of dsrc and wi-fi: Impact on the performance of vehicular safety applications," in *IEEE International Conference on Communications (ICC), 2017*. IEEE, 2017, pp. 1–6.

[21] S. Gopal, S. K. Kaul, and S. Roy, "Optimizing outdoor white-fi networks in tv white spaces," in *IEEE International Conference on Communications (ICC), 2016*. IEEE, 2016, pp. 1–6.

[22] ——, "Optimizing city-wide white-fi networks in tv white spaces," *IEEE Transactions on Cognitive Communications and Networking*, vol. 4, no. 4, pp. 749–763, 2018.

[23] K. Harrison, S. M. Mishra, and A. Sahai, "How much white-space capacity is there?" in *IEEE Symposium on New Frontiers in Dynamic Spectrum, 2010*. IEEE, 2010, pp. 1–10.

[24] F. Hessar and S. Roy, "Capacity considerations for secondary networks in tv white space," *IEEE Transactions on Mobile Computing*, vol. 14, no. 9, pp. 1780–1793, 2015.

[25] A. Achtzehn, M. Petrova, and P. Mähönen, "On the performance of cellular network deployments in tv whitespaces," in *IEEE International Conference on Communications (ICC), 2012*. IEEE, 2012, pp. 1789–1794.

[26] M. Deshmukh, F. B. Frederiksen, and R. Prasad, "A closed form estimate of tvws capacity under the impact of an aggregate interference," *Wireless Personal Communications*, vol. 82, no. 1, pp. 551–568, 2015.

[27] T. Dudda and T. Irnich, "Capacity of cellular networks deployed in tv white space," in *IEEE International Symposium on Dynamic Spectrum Access Networks (DYSPAN), 2012*. IEEE, 2012, pp. 254–265.

[28] R. Jäntti, J. Kerttula, K. Koufos, and K. Ruttik, "Aggregate interference with fcc and ecc white space usage rules: case study in finland," in *DySPAN*. IEEE, 2011.

[29] K. Harrison and A. Sahai, "Seeing the bigger picture: Context-aware regulations," in *IEEE International Symposium on Dynamic Spectrum Access Networks (DYSPAN), 2012*. IEEE, 2012, pp. 21–32.

[30] A. Rabbachin, G. Baldini, and T. Q. Quek, "Aggregate interference in white spaces," in *7th International Symposium on Wireless Communication Systems (ISWCS), 2010*. IEEE, 2010, pp. 751–755.

[31] A. Rabbachin, T. Q. Quek, and M. Z. Win, "Statistical modeling of cognitive network interference," in *IEEE Global Telecommunications Conference (GLOBECOM 2010), 2010*. IEEE, 2010, pp. 1–6.

[32] A. Rabbachin, T. Q. Quek, H. Shin, and M. Z. Win, "Cognitive network interference," *IEEE Journal on Selected Areas in Communications*, vol. 29, no. 2, pp. 480–493, 2011.

[33] A. Ghasemi and E. S. Sousa, "Interference aggregation in spectrum-sensing cognitive wireless networks," *IEEE Journal of Selected Topics in Signal Processing*, vol. 2, no. 1, pp. 41–56, 2008.

[34] M. Tercero, K. W. Sung, and J. Zander, "Aggregate interference from secondary users with heterogeneous density," in *IEEE 22nd International Symposium on Personal Indoor and Mobile Radio Communications (PIMRC), 2011*. IEEE, 2011, pp. 428–432.

[35] E. Obregon, L. Shi, J. Ferrer, and J. Zander, "A model for aggregate adjacent channel interference in tv white space," in *IEEE 73rd Vehicular Technology Conference (VTC Spring), 2011.* IEEE, 2011, pp. 1–5.

[36] Y. Yang, L. Shi, and J. Zander, "On the capacity of wi-fi system in tv white space with aggregate interference constraint," in *8th International Conference on Cognitive Radio Oriented Wireless Networks (CROWNCOM), 2013.* IEEE, 2013, pp. 123–128.

[37] K. Koufos, R. Jantti, and K. Ruttik, "Modeling of the secondary system's generated interference and studying of its impact on the secondary system design," *Radioengineering*, 2010.

[38] K. Koufos, K. Ruttik, and R. Jäntti, "Controlling the interference from multiple secondary systems at the tv cell border," in *IEEE 22nd International Symposium on Personal Indoor and Mobile Radio Communications (PIMRC), 2011.* IEEE, 2011, pp. 645–649.

[39] W.-Y. Lee and I. F. Akyildiz, "Joint spectrum and power allocation for inter-cell spectrum sharing in cognitive radio networks," in *3rd IEEE Symposium on New Frontiers in Dynamic Spectrum Access Networks, 2008. DySPAN 2008.* IEEE, 2008, pp. 1–12.

[40] A. T. Hoang, Y.-C. Liang, and M. H. Islam, "Power control and channel allocation in cognitive radio networks with primary users' cooperation," *IEEE Transactions on Mobile Computing*, vol. 9, no. 3, pp. 348–360, 2010.

[41] B. Jankuloska, V. Atanasovski, and L. Gavrilovska, "Combined power/channel allocation method for efficient spectrum sharing in tv white space scenario," in *Proceedings of the 4th International Conference on Cognitive Radio and Advanced Spectrum Management.* ACM, 2011, p. 59.

[42] A. T. Hoang and Y.-C. Liang, "Maximizing spectrum utilization of cognitive radio networks using channel allocation and power control," in *IEEE 64th Vehicular Technology Conference, 2006. VTC-2006 Fall. 2006.* IEEE, 2006, pp. 1–5.

[43] I. Bekmezci, O. K. Sahingoz, and Ş. Temel, "Flying ad-hoc networks (fanets): A survey," *Ad Hoc Networks*, vol. 11, no. 3, pp. 1254–1270, 2013.

[44] H. Hartenstein and L. Laberteaux, "A tutorial survey on vehicular ad hoc networks," *IEEE Communications Magazine*, vol. 46, no. 6, pp. 164–171, 2008.

[45] S. Kaul, R. Yates, and M. Gruteser, "Real-time status: How often should one update?" in *Proceedings IEEE INFOCOM, 2012.* IEEE, 2012, pp. 2731–2735.

[46] S. Gopal and S. K. Kaul, "A game theoretic approach to dsrc and wifi coexistence," in *IEEE INFOCOM 2018 - IEEE Conference on Computer Communications Workshops (INFOCOM WKSHPS)*, April 2018, pp. 565–570.

[47] S. Gopal, S. K. Kaul, and R. Chaturvedi, "Coexistence of age and throughput optimizing networks: A game theoretic approach," in *IEEE 30th Annual International Symposium on Personal, Indoor and Mobile Radio Communications (PIMRC) 2019*. IEEE, 2019, pp. 1–6.

[48] S. Gopal, S. K. Kaul, R. Chaturvedi, and S. Roy, "Coexistence of age and throughput optimizing networks: A spectrum sharing game," *arXiv preprint arXiv:1909.02863*, 2019.

[49] Y. Jin and G. Kesidis, "Equilibria of a noncooperative game for heterogeneous users of an aloha network," *IEEE Communications Letters*, vol. 6, no. 7, pp. 282–284, 2002.

[50] M. Cagalj, S. Ganeriwal, I. Aad, and J.-P. Hubaux, "On selfish behavior in csma/ca networks," in *Proceedings IEEE INFOCOM 2005. 24th Annual Joint Conference of the IEEE Computer and Communications Societies.*, vol. 4. IEEE, 2005, pp. 2513–2524.

[51] R. T. Ma, V. Misra, and D. Rubenstein, "Modeling and analysis of generalized slotted-aloha mac protocols in cooperative, competitive and adversarial environments," in *26th IEEE International Conference on Distributed Computing Systems (ICDCS'06)*. IEEE, 2006, pp. 62–62.

[52] H. Inaltekin and S. B. Wicker, "The analysis of nash equilibria of the one-shot random-access game for wireless networks and the behavior of selfish nodes," *IEEE/ACM Transactions on Networking (TON)*, vol. 16, no. 5, pp. 1094–1107, 2008.

[53] L. Chen, S. H. Low, and J. C. Doyle, "Random access game and medium access control design," *IEEE/ACM Transactions on Networking (TON)*, vol. 18, no. 4, pp. 1303–1316, 2010.

[54] G. D. Nguyen, S. Kompella, C. Kam, J. E. Wieselthier, and A. Ephremides, "Impact of hostile interference on information freshness: A game approach," in *15th International Symposium on Modeling and Optimization in Mobile, Ad Hoc, and Wireless Networks (WiOpt), 2017*. IEEE, 2017, pp. 1–7.

[55] Y. Xiao and Y. Sun, "A dynamic jamming game for real-time status updates," in *IEEE INFOCOM 2018-IEEE Conference on Computer Communications Workshops (INFOCOM WKSHPS)*. IEEE, 2018, pp. 354–360.

[56] A. Garnaev, W. Zhang, J. Zhong, and R. D. Yates, "Maintaining information freshness under jamming," in *IEEE INFOCOM 2019-IEEE Conference on Computer Communications Workshops (INFOCOM WKSHPS)*. IEEE, 2019, pp. 90–95.

[57] X. Gac, E. Akyol, and T. Başar, "On communication scheduling and remote estimation in the presence of an adversary as a nonzero-sum game," in *IEEE Conference on Decision and Control (CDC) 2018*. IEEE, 2018, pp. 2710–2715.

[58] G. D. Nguyen, S. Kompella, C. Kam, J. E. Wieselthier, and A. Ephremides, "Information freshness over an interference channel: A game theoretic view," in *IEEE INFOCOM 2018-IEEE Conference on Computer Communications*. IEEE, 2018, pp. 908–916.

[59] K. Saurav and R. Vaze, "Game of Ages," in *INFOCOM 2020 - IEEE Conference on Computer Communications Workshopss (INFOCOM WKSHPS)*, 2020.

[60] H. Zheng, K. Xiong, P. Fan, Z. Zhong, and K. B. Letaief, "Age-based utility maximization for wireless powered networks: A stackelberg game approach," in *IEEE Global Communications Conference (GLOBECOM) 2019*. IEEE, 2019, pp. 1–6.

[61] R. Etkin, A. Parekh, and D. Tse, "Spectrum sharing for unlicensed bands," *IEEE Journal on Selected Areas in Communications*, vol. 25, no. 3, 2007.

[62] Y. Wu, B. Wang, K. R. Liu, and T. C. Clancy, "Repeated open spectrum sharing game with cheat-proof strategies," *IEEE Transactions on Wireless Communications*, vol. 8, no. 4, pp. 1922–1933, 2009.

[63] B. Singh, K. Koufos, O. Tirkkonen, and R. Berry, "Co-primary inter-operator spectrum sharing over a limited spectrum pool using repeated games," in *IEEE International Conference on Communications (ICC), 2015*. IEEE, 2015, pp. 1494–1499.

[64] G. Bianchi, "Performance analysis of the ieee 802.11 distributed coordination function," *IEEE Journal on Selected Areas in Communications*, vol. 18, no. 3, pp. 535–547, 2000.

[65] S. K. Kaul and R. Yates, "Status updates over unreliable multiaccess channels," Jun. 2017, pp. 331–335.

[66] A. Kosta, N. Pappas, A. Ephremides, and V. Angelakis, "Age of information performance of multiaccess strategies with packet management," *Journal of Communications and Networks*, vol. 21, no. 3, pp. 244–255, 2019.

[67] Y.-P. Hsu, "Age of information: Whittle index for scheduling stochastic arrivals," in *Proc. IEEE Int'l. Symp. Info. Theory (ISIT)*, June 2018, pp. 2634–2638.

[68] S. Farazi, A. G. Klein, and D. R. Brown III, "Fundamental bounds on the age of information in multi-hop global status update networks," *Journal of Communications and Networks*, vol. 21, no. 3, pp. 268–279, 2019.

[69] A. Maatouk, S. Kriouile, M. Assaad, and A. Ephremides, "On the optimality of the Whittle's index policy for minimizing the age of information," *arXiv preprint arXiv:2001.03096*, 2020.

[70] X. Chen, K. Gatsis, H. Hassani, and S. S. Bidokhti, "Age of information in random access channels," *arXiv preprint arXiv:1912.01473*, 2019.

[71] S. Gopal, S. K. Kaul, R. Chaturvedi, and S. Roy, "A Non-Cooperative Multiple Access Game for Timely Updates," in *INFOCOM 2020 - IEEE Conference on Computer Communications Workshopss (INFOCOM WKSHPS)*, 2020.

[72] Z. Han, D. Niyato, W. Saad, T. Başar, and A. Hjørungnes, *Game Theory in Wireless and Communication Networks: Theory, Models, and Applications*. Cambridge University Press, 2011.

[73] F. C. Commission, "Cdbs database public files," https://www.fcc.gov/media/radio/cdbs-database-public-files, accessed: 2017-03-3.

[74] FCC, "Notice of proposed rule making and order: Facilitating opportunities for flexible, efficient, and reliable spectrum use employing cognitive radio technologies," *ET docket*, no. 03-108, p. 73, 2005.

[75] B. Radunovic, A. Proutiere, D. Gunawardena, and P. Key, "Exploiting channel diversity in white spaces," *Technical Report MSR-TR-2011–53*, 2011.

[76] F. Hessar and S. Roy, "Resource allocation techniques for cellular networks in tv white space spectrum," in *IEEE International Symposium on Dynamic Spectrum Access Networks (DYSPAN), 2014*. IEEE, 2014, pp. 72–81.

[77] L. T. Tan and L. B. Le, "Channel assignment for throughput maximization in cognitive radio networks," in *IEEE Wireless Communications and Networking Conference (WCNC), 2012*. IEEE, 2012, pp. 1427–1431.

[78] L. B. Le and E. Hossain, "Resource allocation for spectrum underlay in cognitive radio networks," *IEEE Transactions on Wireless communications*, vol. 7, no. 12, pp. 5306–5315, 2008.

[79] L. Shi, K. W. Sung, and J. Zander, "Secondary spectrum access in tv-bands with combined co-channel and adjacent channel interference constraints," in *IEEE International Symposium on Dynamic Spectrum Access Networks (DYSPAN), 2012*. IEEE, 2012, pp. 452–460.

[80] ——, "Controlling aggregate interference under adjacent channel interference constraint in tv white space," in *7th International ICST Conference on Cognitive Radio Oriented Wireless Networks and Communications (CROWNCOM), 2012*. IEEE, 2012, pp. 1–6.

[81] Y. Selén and J. Kronander, "Optimizing power limits for white space devices under a probability constraint on aggregated interference," in *IEEE International Symposium on Dynamic Spectrum Access Networks (DYSPAN), 2012*. IEEE, 2012, pp. 201–211.

[82] C.-H. Chen and C.-L. Wang, "Joint subcarrier and power allocation in multiuser ofdm-based cognitive radio systems," in *IEEE International Conference on Communications (ICC), 2010*. IEEE, 2010, pp. 1–5.

[83] V. Thumar, T. Nadkar, T. Gopavajhula, U. B. Desai, and S. N. Merchant, "Power allocation, bit loading and sub-carrier bandwidth sizing for ofdm-based cognitive radio," *EURASIP Journal on Wireless Communications and Networking*, vol. 2011, no. 1, pp. 1–24, 2011.

[84] A. Bhartia, M. Gowda, K. K. Chintalapudi, B. Radunovic, R. Ramjee, D. Chakrabarty, L. Qiu, and R. R. Chowdhury, "Wifi-xl: Extending wifi to wide areas in white spaces," *Microsoft Research TechReport TR-2014-132*, 2014.

[85] O. Ekici and A. Yongacoglu, "IEEE 802.11a Throughput Performance with Hidden Nodes," *IEEE Communications Letters*, vol. 12, no. 6, pp. 465–467, Jun. 2008.

[86] W. Wang and X. Liu, "List-coloring based channel allocation for open-spectrum wireless networks," in *IEEE Vehicular Technology Conference*, vol. 62, no. 1. IEEE; 1999, 2005, p. 690.

[87] M. R. Gary and D. S. Johnson, "Computers and intractability: A guide to the theory of np-completeness," 1979.

[88] C. Peng, H. Zheng, and B. Y. Zhao, "Utilization and fairness in spectrum assignment for opportunistic spectrum access," *Mobile Networks and Applications*, vol. 11, no. 4, pp. 555–576, 2006.

[89] fcc, "Tv service contour data points," https://www.fcc.gov/media/television/tv-service-contour-data-points, updated: 2016-12-26.

[90] W. S. D. A. Group, "Channel calculations for white spaces guidelines," http://spectrumbridge.com/wp-content/uploads/2014/08/Database-Calculation-Consistency-Specification.pdf, revision 1.29, 2013-06-03.

[91] R. Jain, D.-M. Chiu, and W. R. Hawe, *A quantitative measure of fairness and discrimination for resource allocation in shared computer system*. Eastern Research Laboratory, Digital Equipment Corporation Hudson, MA, 1984, vol. 38.

[92] A. B. Flores, R. E. Guerra, E. W. Knightly, P. Ecclesine, and S. Pandey, "Ieee 802.11 af: A standard for tv white space spectrum sharing," *IEEE Communications Magazine*, vol. 51, no. 10, pp. 92–100, 2013.

[93] G. J. Mailath and L. Samuelson, *Repeated games and reputations: long-run relationships*. Oxford university press, 2006.

[94] B. Cheng, H. Lu, A. Rostami, M. Gruteser, and J. B. Kenney, "Impact of 5.9 ghz spectrum sharing on dsrc performance," in *IEEE Vehicular Networking Conference (VNC), 2017*. IEEE, 2017, pp. 215–222.

[95] G. Naik, J. Liu, and J.-M. J. Park, "Coexistence of dedicated short range communications (dsrc) and wi-fi: Implications to wi-fi performance," in *Proc. IEEE INFOCOM*, 2017.

[96] I. Khan and J. Härri, "Can ieee 802.11 p and wi-fi coexist in the 5.9 ghz its band?" in *IEEE 18th International Symposium on A World of Wireless, Mobile and Multimedia Networks (WoWMoM), 2017*. IEEE, 2017, pp. 1–6.

[97] S. Kaul, M. Gruteser, V. Rai, and J. Kenney, "Minimizing age of information in vehicular networks," in *8th Annual IEEE Communications Society Conference on Sensor, Mesh and Ad Hoc Communications and Networks (SECON), 2011*. IEEE, 2011, pp. 350–358.

[98] Y. Sun, E. Uysal-Biyikoglu, R. D. Yates, C. E. Koksal, and N. B. Shroff, "Update or wait: How to keep your data fresh," *IEEE Transactions on Information Theory*, 2017.

[99] R. D. Yates and S. K. Kaul, "Status updates over unreliable multiaccess channels," in *IEEE International Symposium on Information Theory (ISIT), 2017*. IEEE, 2017, pp. 331–335.

[100] R. D. Yates, "Lazy is timely: Status updates by an energy harvesting source," in *IEEE International Symposium on Information Theory (ISIT), 2015*. IEEE, 2015, pp. 3008–3012.

[101] I. Kadota, A. Sinha, and E. Modiano, "Optimizing age of information in wireless networks with throughput constraints," in *IEEE INFOCOM 2018-IEEE Conference on Computer Communications*. IEEE, 2018, pp. 1844–1852.

[102] Z. Ning, P. Dong, X. Wang, X. Hu, L. Guo, B. Hu, Y. Guo, T. Qiu, and R. Kwok, "Mobile edge computing enabled 5g health monitoring for internet of medical things: A decentralized game theoretic approach," *IEEE Journal of Selected Areas of Communications*, pp. 1–16, 2020.

[103] S. Hao and L. Duan, "Economics of age of information management under network externalities," in *Proceedings of the Twentieth ACM International Symposium on Mobile Ad Hoc Networking and Computing*, 2019, pp. 131–140.

[104] M. Zhang, A. Arafa, J. Huang, and H. V. Poor, "How to price fresh data," *arXiv preprint arXiv:1904.06899*, 2019.

[105] X. Wang and L. Duan, "Dynamic pricing for controlling age of information," in *IEEE International Symposium on Information Theory (ISIT) 2019*. IEEE, 2019, pp. 962–966.

[106] Y. Yang, L. Shi, and J. Zander, "On the capacity of wi-fi system in tv white space with aggregate interference constraint," in *8th International Conference on Cognitive Radio Oriented Wireless Networks*. IEEE, 2013, pp. 123–128.

[107] I. Kadota, A. Sinha, E. Uysal-Biyikoglu, R. Singh, and E. Modiano, "Scheduling policies for minimizing age of information in broadcast wireless networks," *IEEE/ACM Transactions on Networking*, vol. 26, no. 6, pp. 2637–2650, 2018.

[108] B. T. Bacinoglu, E. T. Ceran, and E. Uysal-Biyikoglu, "Age of information under energy replenishment constraints," in *2015 Information Theory and Applications Workshop (ITA)*. IEEE, 2015, pp. 25–31.

[109] J. Nash, "Non-cooperative games," *Annals of mathematics*, pp. 286–295, 1951.

[110] D. P. Bertsekas, R. G. Gallager, and P. Humblet, *Data networks*. Prentice-hall Englewood Cliffs, NJ, 1987, vol. 2.

[111] G. Z. Khan, R. Gonzalez, and E.-C. Park, "A performance analysis of mac and phy layers in ieee 802.11 ac wireless network," in *18th International Conference on Advanced Communication Technology (ICACT) 2016*. IEEE, 2016, pp. 20–25.

[112] C. Han, M. Dianati, R. Tafazolli, R. Kernchen, and X. Shen, "Analytical study of the ieee 802.11 p mac sublayer in vehicular networks," *IEEE Transactions on Intelligent Transportation Systems*, vol. 13, no. 2, pp. 873–886, 2012.

[113] S. Boyd and L. Vandenberghe, *Convex optimization*. Cambridge University Press, 2004.